The effect op stress on the domain structures of iron whiskers

G. Lidgard

THE EFFECT OF STRESS ON THE DOMAIN STRUCTURES OF IRON WHISKERS

by

G. LIDGARD, B.Sc.

Presented in candidature for the degree of Doctor of Philosophy.

August, 1966.

ABSTRACT

Large iron whiskers were grown by the reduction of ferrous chloride and domain structures in unstrained and strained whiskers were investigated. Tensional stresses were applied along the whisker axis and the resulting domain patterns observed by means of the Bitter technique.

In the case of whiskers with axes in [100] directions and faces (001) cross-magnetised domains were observed to disappear upon the application of stress, either by the gradual reduction of their volume or by the sudden mutual annihilation of neighbouring domains. Calculations of the energy values for these sudden changes agree with the model postulated and visual observation of the movement confirmed the theory.

For whiskers with axes at an angle to the [100] direction and faces (001), calculations were carried out upon a number of different closure structure types to determine the equilibrium spacing for each pattern and these were then compared with observations to confirm the type of closure structure present. A method of estimating magnetostatic energy contributions for areas of free pole separated by neutral regions was developed.

Whiskers with axes [111] and faces (211) and (110) were also studied. Calculations showed that the main wall was a normal zig-zag wall. The main structure was observed to consist of six 90° domains and two different types of closure stucture were observed on alternate main domains. The effect

of stress on this structure was explained as being due to the change in energy of the complex wall structure in the two different closure structures.

CONTENTS

INTRODUCTION

1.1 Ferromagnetism

An important property of a ferromagnet is that its bulk intensity of magnetisation can be made large by relatively small applied magnetic fields. By the action of suitable magnetic fields it may either retain a significant intensity of magnetisation or be completely demagnetised in zero applied magnetic field.

The origin of ferromagnetism is the same as the origin of paramagnetism i.e. the magnetic moment of certain electrons of the material due to their orbital or spin momentum. In a para magnetic material the resultant magnetic moments of the atoms are randomly orientated to produce a zero resultant moment in in any direction in zero applied field. To produce alignment in the material and hence an intensity of magnetisation comparable with that exhibited by some ferromagnets an applied field of the order of 10^6 oersteds is necessary at room temper ature. In ferromagnets this degree of ordering of the individual magnetic moments occurs naturally with no applied field.

To explain the above effects Weiss (1907) postulated the existence of a strong internal molecular field which aligned the individual magnetic moments parallel. This ordering will be perfect at absolute zero but as the temperature is raised

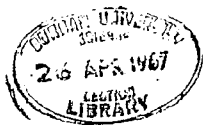

the disturbing effects of thermal vibrations countract this alignment and gradually reduce it until a critical temperature, called the Curie temperature, is reached at which the ordering breaks down and the material becomes paramagnetic. From the value of the Curie temperature of a material an estimate of the internal field can be made. This explains why ferromagnets can be easily magnetised but not why they are usually found with a nearly zero magnetisation. To account for this, Weiss also postulated the subdivision of the materials into domains. In each of these domains the magnetic moments are aligned parallel but the individual domains have magnetisation directions spread over a range of possible directions. The bulk intensity of magnetisation is then the vector sum of the individual domain magnetisations. The resultant magnetisation can therefore range from zero, when the domain magnetisations are distributed in all directions, to the maximum possible when the magnetisations of all the domains are aligned in one direction.

Weiss did not specify the origin of the alignment process but he showed that the value necessary for the effective internal field of 10^7 oersteds was beyond the limit for normal magnetic interactions. Heisenberg (1928) provided an explanation for the origin of this field by showing that there is, according to quantum theory, an electrostatic term arising from the overlap of the orbital wave function which gives the necessary

force by the mechanism of exchange interaction and leads to an effective spin$^{\frac{1}{2}}$ - spin coupling. It can be shown that the exchange energy between two atoms i,j is given by

$$E_{ex} = -2 J_{ij} S_i \cdot S_j \qquad (1.1)$$

where S_i is the spin of atom i, and J is the exchange integral. If J is positive the minimum energy configuration is with the two spins parallel, so that ferromagnetic behaviour will occur. The magnetic behaviour has been shown in the transition metals to be mainly due to the spinof the electrons, the orbital motion being almost quenched. The particular electrons responsible for the magnetisation are those in the unfilled 3d band of the transition metals rather than the valence electrons.(Van Vleck.1952)Thus for a substance to be ferromagnetic there must be some overlap of these unfilled inner shells of adjacent atoms and this is most likely to occur if a substance with an unfilled inner shell of large radius forms a crystal of small interatomic spacing. It has also been suggested that the interaction is due to some of the 3d electrons moving through the crystal and hence providing interactions between the various atoms. A discussion of these theories is given by Herring(1960). The molecular fields in ferromagnets are so large that the effect of external magnetic fields on the magnitude of the spontaneous magnetisation can be neglected for temperatures well below their Curie temperature.

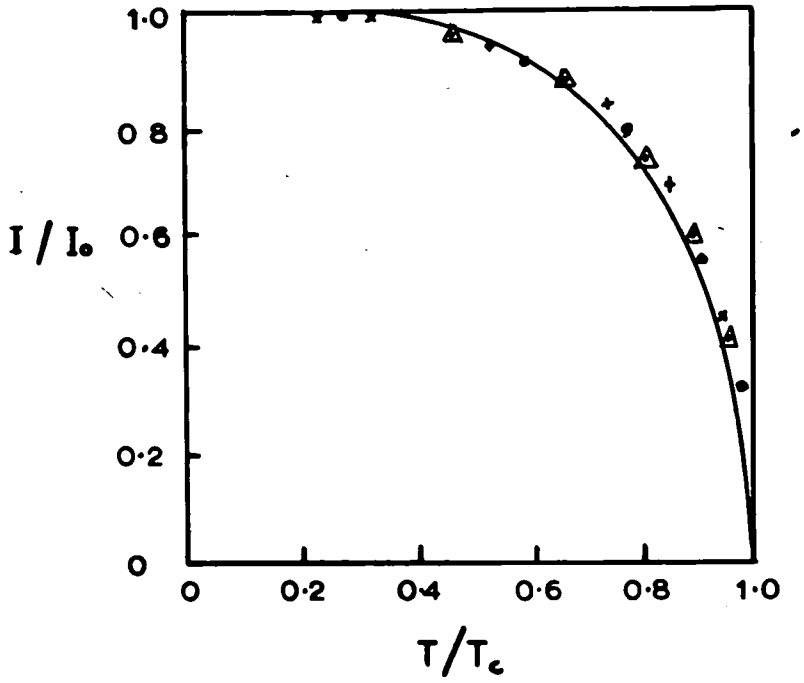

Saturation intensity of magnetization as a function of temperature for

x Iron

△ Nickel

• Cobalt

FIG. I.I

The spontaneous magnetisation is temperature dependent due to the thermal vibrations as described above and it varies from material to material. However if the variation is plotted against temperature in reduced units as in fig.1.1, then a general curve which is approximately correct for all ferro magnets is obtained.

The second of the Weiss postulates is the subdivision of the material into domains with differing directions of magne tisations. There are in the magnetised material certain crystal directions, known as "easy" directions, in which the intrinsic magnetisation settles under the influence of magnetocrystalline anisotropy. The domain directions of magnetisation are therefore limited to these easy directions and are separated by relatively narrow regions known as domain walls. On application of a magnetic field to such a subdivided material the domains magnetised nearest to the applied field direction grow at the expense of the others, initially by reversible, then by irreversible boundary motion, and finally by the rotation of the magnetisation direction into the field direction. Such processes as these can be used to explain the magnetisation curves of materials.

The first observation of domains was by Bitter(1931) using a colloid to make the boundary walls visible. This work only observed bomains on a strained surface bearing no relationship

to the bulk domain structure. In 1935 Landau and Lifshitz proposed theoretical domain structures using a geometrical technique. They considered the domain structure to be a system of minimum energy and considered the various energy contributions in detail. This method computes the energy states of a system and obtains a minimum. Such theoretical work however must always be in some doubt (Brown 1957) as there are always the possibilities that either a model of lower energy could be produced by greater ingenuity or the model arrived at is separated from the previous state by an energy barrier so that the expected transition is impossible. In arriving at the energy of a system the factors to be taken into account are wall area, magnetostriction, stress (applied or internal), and magneto-static energy. The constituent energy contributions will be dealt with in the following section.

1.2 Energy Contributions

1.2.1 Exchange Energy

Summing equation 1.1 over all values i,j gives

$$E_{ex} = -2JS^2 \sum_{i>j} \cos \phi_{ij} \qquad 1.2$$

where ϕ_{ij} is the angle between the spin vectors. In a domain ϕ_{ij} is zero giving the minimum value for the exchange energy. However in the transition regions of the walls there is an excess of exchange energy since neighbouring atoms no longer

have their moments aligned parallel. In subsequent calculations it will be assumed that the exchange energy in the domains is the zero level so that only the excess in the walls need be considered. To obtain a value for this we need to know the value of $2JS^2$, or more often the energy density A given by $A \pm \frac{2JS^2}{a}$ where a is the lattice constant. J was evaluated for iron by Kittel (1949) obtaining a value of 205k where k is Boltzmann's constant.

1.2.2 Anisotropy Energy

If the magnetisation curves for a ferromagnet are studied as a function of the crystal orientation, it is found that the applied field necessary to produce saturation varies and has a minimum in a certain crystal direction. This direction is known as the easy or preferred direction and additional energy must be supplied to rotate the magnetisation direction away from this direction. This energy is known as magnetocrystalline anisotropy energy. The easy directions are [100] in iron, [111] in nickel, and [0001] in cobalt.

The value of this additional energy can be expressed as a function of the direction cosines $[\alpha_1, \alpha_2, \alpha_3]$ of the magnetisation direction relative to the crystal axes. For cubic crystals like iron and nickel, symmetry requirements allow all but the even powers of α to drop out and the expression for the anisotropy

becomes:

$$E_{an} = K_0 + K_1(\alpha_1^2\alpha_2^2 + \alpha_2^2\alpha_3^2 + \alpha_3^2\alpha_1^2) + K_2\alpha_1^2\alpha_2^2\alpha_3^2 + \cdots \qquad 1.3$$

where K_0, K_1, K_2, are constants depending on the material. Higher powers can be neglected as the constants become very small. The values for these anisotropy constants for pure iron are $K_1 = 4.2 \times 10^5$ ergs/cm.^{3} and $K_2 = 1.5 \times 10^5$ergs/cm.^{3} at room temperature.

1.2.3 Magnetoelastic Energy

When a crystal undergoes mechanical strain there is an additional energy term due to the interaction between the magnetisation and the mechanical strain. This is known as the magnetoelastic energy and is zero for an unstrained lattice. It is the inverse of the magnetostriction, the change in length upon magnetising a ferromagnet.

Becker and Doring (1939) developed the formal theory for magnetostriction by mimimising the total energy of a crystal i.e. the anisotropy energy, the magnetostrictive energy, and the stress energy. Thus if a state of constant stress is considered, the change in length in a direction specified by direction cosines $[\beta_1\beta_2\beta_3]$ with the magnetisation specified by $[\alpha_1\alpha_2\alpha_3]$ is:

$$\frac{\delta L}{L} = h_1\left(\alpha_1^2\beta_1^2 + \alpha_2^2\beta_2^2 + \alpha_3^2\beta_3^2 - \frac{1}{3}\right) + h_2\left(2\alpha_1\alpha_2\beta_1\beta_2 + 2\alpha_2\alpha_3\beta_2\beta_3 + 2\alpha_3\alpha_1\beta_3\beta_1\right) + \cdots \qquad 1.4$$

where h_1 and h_2 are constants depending on the material. In general higher terms are necessary in this equation but for iron they can be ignored. It is more usual to express the constant

h_1 and h_2 in terms of the longitudinal magnetostriction coefficents λ_{100} and λ_{111}, the fractional changes in length measured along the magnetisation directions with the magnetisation in the [100] and [111] directions respectively. We have:

$$\frac{2}{3} h_1 = \lambda_{100} \quad ; \quad \frac{2}{3} h_2 = \lambda_{111} \qquad 1.5$$

In a similar manner the magnetoelastic energy can be calculated. This is done by considering the contribution to the free energy arising from the magnetostrictive distortion when the body is in a stress field. If the stress is defined by a stress tensor Π_{ik} and the strain by a strain tensor A_{ik}, then the magnetoelastic energy is given by:

$$E_\sigma = \sum_{i,k=1}^{3} \Pi_{ik} \cdot A_{ik} \qquad 1.6$$

A_{ik} can be expressed as a power series of $[\alpha_1\alpha_2\alpha_3]$ the magnetisation direction cosines. Discounting terms above second order and including the magnetostriction coefficients gives:

$$E_\sigma = -\frac{3}{2}\lambda_{100}\left(\Pi_{11}\alpha_1^2 + \Pi_{22}\alpha_2^2 + \Pi_{33}\alpha_3^2\right) - 3\lambda_{111}\left(\alpha_1\alpha_2\Pi_{12} + \alpha_2\alpha_3\Pi_{23} + \alpha_3\alpha_1\Pi_{31}\right) \qquad 1.7$$

In the following sections the type of stress used is a pure tension of σ dynes/sq.cm. If this has direction cosines $[\gamma_1\gamma_2\gamma_3]$ then

$\Pi_{ik} = \sigma\gamma_i\gamma_k$ and 1.7 becomes

$$E_\sigma = -\frac{3}{2}\sigma\left[\lambda_{100}\left(\alpha_1^2\gamma_1^2 + \alpha_2^2\gamma_2^2 + \alpha_3\gamma_3^2\right) + 2\lambda_{111}\left(\alpha_1\alpha_2\gamma_1\gamma_2 + \alpha_2\alpha_3\gamma_2\gamma_3 + \alpha_3\alpha_1\gamma_3\gamma_1\right)\right] \qquad 1.8$$

If the magnetisation is in an easy direction we have for iron:

$\alpha_i = \pm 1 ; \alpha_j = \alpha_k = 0$ and so

$$E_\sigma = -\frac{3}{2}\sigma\lambda_{100}\cos^2\Theta \qquad 1.9$$

where Θ is the angle between the magnetisation and the

tension directions. Also if the magnetisation is isotropic then

$$E_\sigma = -\frac{3}{2}\sigma\lambda \qquad 1.10$$

whatever the direction of magnetisation.

1.2.4 Magnetostatic Energy

This energy term is the energy of a magnetic vector in its own field. The energy is given by:

$$E_{m.s.} = -\frac{1}{2}\int \mathbf{I}.\mathbf{H}\, dv \qquad 1.11$$

where I is the magnetisation and H is the field arising from the magnetisation, the integration being over the total volume of the specimen. One of the most important cases in domain theory has been worked out by Kittel (1949). This case is when the structure consists of parallel strips of alternate polarity. In the case of the magnetisation normal to the surface and strips of width D, the result is

$$E_{ms} = 0.852 I_s^2 D \text{ /unit surface area.} \qquad 1.12$$

If the magnetisation vector makes an angle δ with the surface, then the pole density is given by $I\sin\delta$ and then

$$E_{ms} = 0.852\, I_s^2 D \sin^2\delta \qquad 1.13$$

It has been shown (Shockley 1948) that in the surface, the magnetisation can move slightley from the easy direction giving an effective permeability μ^x. In the stress free case this is given by

$$\mu^x = 1 + \frac{2\pi I_s^2}{K_1} \qquad 1.14$$

for a (100) surface of a cubic system. This affects the

magnetostatic energy and gives a correction factor to the value of equation 1.13 of $\frac{2}{1+\mu^2}$, so that the final expression for the magnetostatic energy is:

$$E_{ms} = \frac{2}{1+\mu^2} \cdot 0.952\, I_s^2 b \sin^2\delta$$
$$= \frac{1.7}{1+\mu^2} I_s^2 b \sin^2\delta \qquad 1.15$$

1.2.5 Total Energy

The energy terms described in the preceeding sections are present in a given domain structure, and to determine whether a particular structure is stable, the individual energy terms must be determined. The different terms appear from different parts of the domain structure. The exchange energy and anisotropy energy appear only in the domain boundaries where neighbouring atoms do not have their magnetic moments parallel or in easy directions. The energy associated with domain walls (Bloch walls) will be considered in the next section. Magnetoelastic energy occurs in all of the domains themselves and is given by equation 1.8. The closure domains of a structure, or any small domains magnetised at right angles to the main domain direction have a magnetostrictive contribution to their energy because they have their magnetostrictive change in length perpendicular to the main domain magnetostriction. This produces a strain in the material giving an energy which is magnetoelastic in origin of

$$E = \frac{1}{2} C_{11} \lambda_{100}^2 \qquad 1.16$$

where c_{11} is an elastic constant.

To distinguish between this energy term and the term due to applied or internal stress, in the rest of this work it will be referred to as magnetostrictive energy. The final energy contribution is the magnetostatic energy arising from the surface distribution of magnetisation.

1.3 Bloch Walls

If a ferromagnet is not saturated but consists of an arrangement of domains, between the individual domains a transition region where the direction of magnetisation changes between one easy direction and another. This transition is known as a domain wall and in bulk ferromagnets is a Bloch wall in which the rotation occurs in the plane of the wall. In thin films, below a certain critical thickness this type of wall is unfavourable and a Néel wall forms. This has the rotation occuring normal to the plane of the wall. For the work on iron whiskers the walls are Bloch walls and these only will be described here.

To have the minimum possible wall energy, Néel (1944a) has shown that the component of magnetisation normal to the wall must be continuous from one side of the wall through to the other side. If this is not so, free polarity will be produced at the wall and a large amount of magnetostatic energy is involved. For example, if the wall makes an angle θ with the zero pole position, the resulting energy will be $2\pi I_s^2 \sin^2\theta$.

In the case of iron this is approximately $2\times10^{7}\sin\theta$ ergs/cc. To meet this condition we can have two main types of boundary in iron, a 180° boundary between antiparallel domains with its normal in a (100) plane, and a 90° boundary between perpendicularly magnetised domains with its normal in a (110) plane.

The energy terms involved in the transition region are anisotropy and exchange energy. The former term would give a minimum for the change occuring over one lattice site and the latter would give a minimum for the change occuring over an infinite number of lattice sites, so that these terms counteract each other to produce an equilibrium wall width when the total energy is a minimum. This occurs when the two energy terms have equal values, hence the wall energy is given by:

$$\gamma = 2\int E_{ex}\,dx = 2\int E_{an}\,dx \qquad 1.17$$

Detailed calculations of wallenergy and wall width have been made by Lilley(1950), dealing with walls with normals in the [100], [110], and [111] directions. The results for wall energy are given below in units of γ_0 the energy perunit area of a 90° wallwith its normal in a [100] direction.

Values of Wall Energy per Unit Area γ in Units of γ_o for Iron

Type of Boundary / Normal Direction	[100]	[110]	[111]
90°	1.000	1.727	1.185
180°	2.000	2.760	

A general expression for the energy of a 90° wall in terms of the orientation of its normal has been determined by a number of workers, Chikazumi and Suzuki(1955), Graham(1957), and Kaczér and Gemperle(1959). The energy of the wall, expressed as a function of ψ, the angle between the wall normal and the [100] direction is, from Kaczér and Gemperle:

$$\frac{\gamma}{\gamma_o} = 1.7274 - 1.2289\cos\psi + 0.5015\cos^2\psi \qquad 1.18$$

The value of γ_o has been determined by a number of workers and is given by Stewart(1954 page 99) as

$$\gamma_o = \frac{a}{2}\sqrt{\frac{2}{3}AK_1} \qquad 1.19$$

neglecting K_2 which, in the case of iron, alters the value by a few percent, A being the exchange energy density as given in section 1.2.1. Using the value of J determined by Kittel(1949) gives A as 2.0×10^6ergs/cc. and γ_o as 0.9ergs/cm^2. for iron. Néel(1949b) using a different method obtains a value for γ_o of 0.7ergs/cm^2. in iron.

1.4 Domain Structures

In iron there are six easy directions of magnetisation along the cube edge directions determined by the anisotropy

energy. The domain structures present therefore consist of domains magnetised along these directions. The basic structure consists of main 180^{o} domains magnetised antiparallel along one of the cube edge directions. At the surface of the specimen there are closure structures present to reduce the magneto-energy of the system. The form these closure structures take and any distortion of the main domains depends on the surface orientation of the specimen. The closure domains vary from simple triangular prisms in the case of (100) surfaces, to highly complex arrangements of interpenetrating domains when the surface is not a simple crystallographic plane. In the case of iron whiskers similar variations from very simple to very complex closure structures have been observed.

1.5 Observation of Domains

The two techniques most used to observe the intersection of domain walls with the surface of an opaque material are the Bitter technique and the Kerr magneto-optical effect.

In the Bitter technique a colloidal suspension of magnetite is placed on the surface of the specimen. The particles are then attracted to regions of strong magnetic field on the surface and show these up as dark lines. If the surface is sufficiently wellprepared these stray fields are mostly present at the intersection of Bloch walls with the surface, so that subsequent observation of the surface through a microscope shows up the domain boundaries in the surface as dark lines. If the surface

has small scratches normal to the magnetisation direction then these also collect the magnetite particles and enable the magnetisation direction to be determined. This technique has the disadvantage that after a short time the colloid, which is usually acidic, attacks the surface and stains it so that further observations are impossible. To overcome this different types of colloid have been devoped with Celacol (sodium carboxymethyl cellulose) as the suspending solution. Craik(1956) using this technique with a celacol based colliod allowed the film to dry on the specimen, removed it from the surface and observed the pattern under an electron microscope. Another disadvantage of the Bitter technique is that on materials with low anisotropy and hence wide domain walls, the stray fields are too low to attract the magnetite particles so that it is impossible to obtain patterns on these materials.

In the Kerr magneto-optical effect, the rotation of the plane of polarisation of a plane polarised beam of light upon reflection from a magnetised surface is used. The direction of rotation depends on the direction of magnetisation in the surface so that adjacent domains magnetised in different directions produce rotations differing in either sign and/or magnitude. If the surface is subsequently viewed through an analyser arranged at the extinction angle for one particular rotation i.e. one particular surface magnetisation direction,

then differently magnetised domains will show up as regions of differing intensities. This method therefore has the advantage that it renders visible domains rather than domain boundaries, as in the powder pattern technique. Unfortunately the amount of rotation is small, the maximum being only about 5' for iron at the most favourable angle of incidence. Also the system uses crossed polariser and analyser so that the light intensities are low. Nevertheless it is being used now quite extensively both for steady state and moving domain patterns, it being especially suitable for the latter as there is no delay before the new pattern is formed, as occurs using the Bitter pattern technique while the colloid particles re-arrange themselves. In the case of bulk specimens, where the surfaces have to be prepared by electropolishing, small irregularities are still present, comparable in size to the domains under investigation, and these produce a large amount of surface noise. In fact observation through crossed Nicols is a technique used to observe surface structure. To overcome this Fowler and Fryer(1954) superimposed the positive photograph of the saturated specimen upon the negative of the state of interest. By this means they were able to remove the surface structure effects. For bulk materials therefore this method is rather tedious. However in the case of whiskers and thin films the surfaces obtained during the production of the

specimens are good mirror-like surfaces with few irregularities so that the surface domain patterns can be viewed directly. The contrast between domains using this technique is not very good but it can be increased by 'blooming' the surface with layers of transparent dielectric as first described by Kranz(1956) A discussion of this technique and also domain observations in general is given by Prutton(1964), and a general survey is also given by Craik and Tebble(1961),(1965).

1.6 Previous Work on the Effect of Stress on Domain Structures

Though little work has been done on the stress effects on domain structures in whiskers, there has been quite a considerable study of the case of bulk materials, notably by Dijkstra and Martius(1953), Kirenskii, Dylgerov, and Savchenko(1957), Bozorth, Williams, and Shockley(1949), mainly in a qualitative way, and by Corner and Mason(1963,1964) in a quantative way.

In the case of iron whiskers, DeBlois and Graham(1957) applied axial pressure to [100] whiskers and observed a zig-zag wall running down the whisker edge. This was explained by Kaczér and Gemperle(1959) as being due to the positive magnetostriction of iron turning the magnetisation perpendicular to the whisker axis. In this structure the walls become 90° walls and it has been shown that this particular type of 90° wall has a minimum energy state consisting of sections of zig-zag wall(Chikazumi and Suzuki 1955). DeBlois and Graham also applied stress by bending their whiskers. This produced a serrated

or zig–zag 90^{o} wall running along the length of the whiskers. In the zig–zag alternate parts were not observed on the powder patterns. An explanation of this structure was also given by Kaczér and Gemperle in terms of a complex internal structure to the wall with the apparantly missing portion being due to two 90^{o} walls meeting in the surface. They also calculated the effective wall energy of this composite wall and obtained a value of $4.15\gamma_{o}$.

1.7 Object of Investigations

The absence of any systematic work on stress effects on iron whiskers, coupled with the previous investigations carried out by Corner and Mason on the stress effects on bulk silicon iron led to the start of this work. Whiskers have distinct advantages over bulk material in that they grow with smooth shiny surfaces requiring no treatment before domain patterns can be observed, and they are also largely internal stress free, producing no distortion of the results from unknown internal stresses. In general they grow with their axes as simple crystallographic directions and their faces also are usually simple cystallographic planes. They are small in size ranging from a few microns to about a millimetre across at maximum, so that there are only a few domains in their width. This means that their internal structure should be fairly easy to determine, compared to bulk crystals where the stucture

determination is little more than an enlightened guess.

These considerations therefore led to the following work being carried out in an attempt to produce a reasonable survey of the effects of stress on iron whisker domain stuctures.

Experimental Techniques

2.1 Production of specimens

For the effect of stress to be studied large iron whiskers were needed, a width of 100microns being necessary to ensure that there is more than one domain across the width of the specimens, and a length of 2 – 3 cms. to facilitate handling and bonding of the crystals. In addition to the size requirements, the whiskers must be single crystals with surfaces which are smooth simple crystal planes to make the observation of domains possible.

Iron whiskers are produced by the reduction of ferrous chloride in a stream of hydrogen at a temperature in the range 700–750^{o}C (Brenner 1956). Previously the technique had been used with only a few grammes of ferrous chloride to produce small whiskers. The method was modified following a paper by Wayman(1961) to produce whiskers of the required size by using a scaled up version, i.e. large quantities of ferrous chloride in a large diameter furnace. The furnace was based on a design of Morganite Electroheat Ltd. for a $4\frac{1}{2}$" internal diameter furnace tube and a hot zone 24" in length. The furnace was designed so as to be suitable for the growth of these and other crystals too and to reach temperatures of 1500^{o}C using six Crusilite elements, but for the growth of the iron whiskers it was found that only four elements gave the most

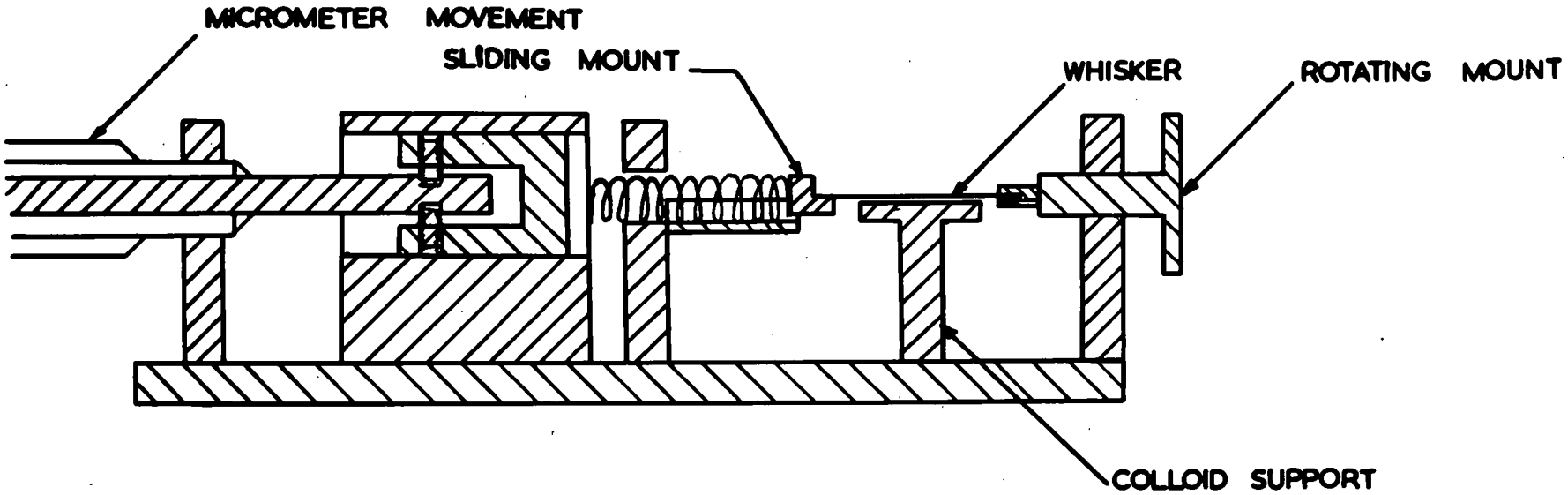

FIG 2·4 APPARATUS FOR APPLYING TENSILE STRESS TO WHISKERS

satisfactory conditions using a maximum power of five kilowatts. The temperature control was by a West Instruments Stepless controller. This uses a chromel/alumel thermocouple as the temperature sensing element and a saturable reactor as the power control device giving a continuously variable power output up to the maximum 5Kwatts.(figure 2.1)

About 250 grammes of reagent grade of ferrous chloride were used at a time, these being placed in an iron boat in the centre of the Vitreosil furnace tube. The boat was made of 16 s.w.g. steel sheet rolled to a semicircular cross-section with steel plate end pieces brazed on. The furnace was heated up to the reaction temperature of 740°C with a slow stream of nitrogen passing through to flush out the system and to prevent the ferrous chloride being reduced before the required temperature was reached. This took about two hours. When the reaction temperature was reached, the nitrogen was replaced with hydrogen flowing through the system at the rate of five litres per minute. The reaction took about four hours to complete after which the hydrogen was replaced by a slow stream of oxygen free nitrogen. This was passed through while the furnace was cooling down to prevent oxidation of the whisker faces. The gases were passed over phosphorous pentoxide to dry them before they passed into the furnace tube. After leaving the furnace tube the exhaust fumes passed through a

water trap to absorb hydrochloric acid gas and provide an isolation between the atmosphere and the hydrogen in the furnace. The flow rates were monitored by a thermistor on the inlet side of the furnace connected in one arm of a bridge network. The bridge was balanced for zero gas flow and the change of resistance of the thermistor when the gas was flowing caused an unbalance. The change in resistance depends on the rate of flow of the gas so the out of balance current across the bridge was used as an indication of the flow rate. The circuit is shown in fig.2.2 and an out of balance current of 50μa corresponded to the required flow rate of hydrogen, the gas flow being adjusted to give this value. The thermistor was mounted in the centre of a length of 1" internal diameter pipe with the ends coned down to prevent turbulent flow at an angle of 10° to pipes of $\frac{1}{4}$" I.D. and $\frac{1}{2}$" I.D. at the inlet and outlet respectively.

2.2 Selection of Specimens

Using this method iron whiskers of the required size were grown and a typical boat of crystals is shown in fig.2.3. From such a collection suitable specimens were then obtained.

By simple visual inspection the majority of the whiskers were rejected because of either irregular growth and poor surfaces, or sudden changes in their direction and side growth

reducing their useful size. The few that remained from this preliminary inspection were then examined further under a microscope(magnification 100x), which enabled specimens with growth steps or twins to be discarded.

2.3 Observation of Domains

For the observation of the domain structures, investigations were carried out into the use of the Kerr magnetooptical effect. By this method the actual domains show up as light and dark areas since the direction of rotation depends on the direction of the magnetisation in the reflecting surface. In certain cases therefore this method can provide additional information to that given by the colloid technique since the latter method can meet situations where domain boundaries do not show up, i.e. where two boundaries of opposite sense meet in the surface to give zero net effect and hence no colloid deposit. If the surface under observation is irregular then the Kerr effect will not show up the domain structure due to the scattering of the light destroying the contrast between adjacent domains. In these circumstances the colloid technique will often still give results. The Kerr effect on iron whiskers was studied using an optical bench arrangement but it was found that the light intensity available for photography was very low compared with the colloid technique and hence much longer exposures

FIG. 2.3

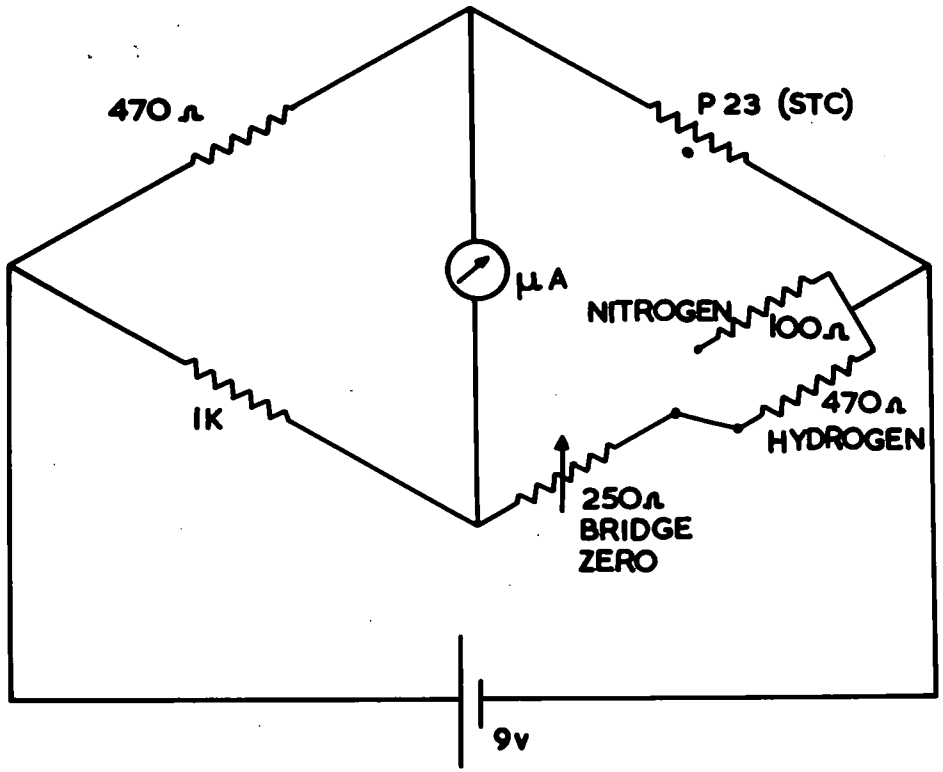

FIG. 2·2 BRIDGE CIRCUIT FOR GAS FLOW RATE INDICATOR

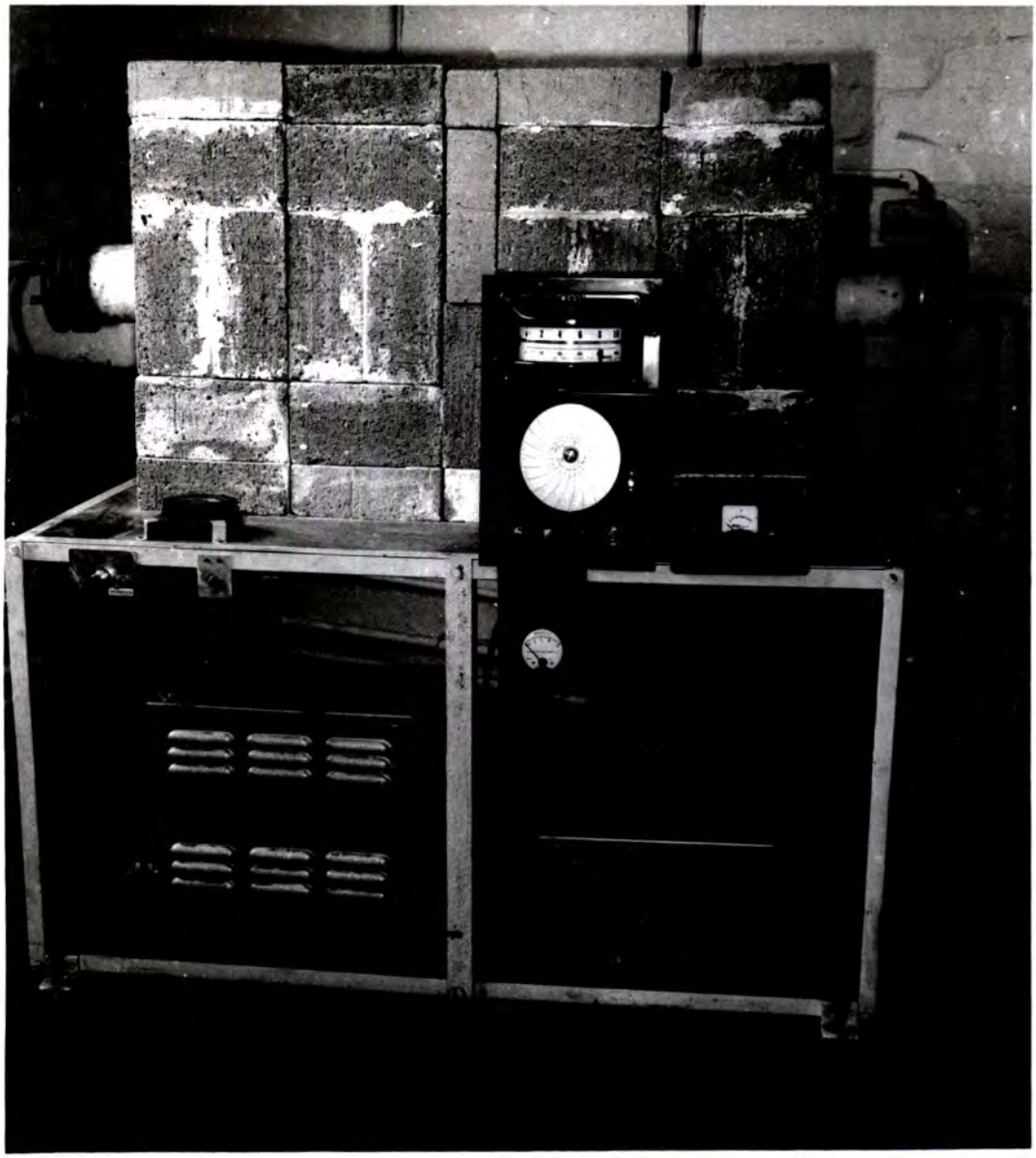

FIG. 2.1

were necessary. In addition, it was estimated that the time neededto convert the Kerr effect apparatus to use on a microscope in conjunction with the apparatus for applying stress to the whiskers would be too long for it to give any contribution to this investigation, so that despite its potential usefulness it was not continued with, and the magnetic colloid technique used for the rest of the investigation.

The magnetic colloid used was prepared by the standard method of Elmore(1938), except that it was made to a concentration four times greater than Elmore gave, as this was found to give clearer Bitter patterns on the whiskers than the standard concentration.

2.4 Apparatus and Observation of Domain Patterns

The apparatus used to apply stress to the whiskers is shown in fig.2.4. It was mounted under an optical microscope in place of the stage on slides so that it could be moved in any direction relative to the microscope body. The right-hand end was free to rotate about the centre line of the apparatus and also slide in and out a short distance. The centre of this piece was bored out and one end of the whisker bonded into it. The position of the whisker was adjusted so that a good surface was seen through the microscope and then the surface was immersed just below the surface of a pool of magnetic colloid on a glass slide, rendering the domain boundaries visible. After this the whisker position was further adjusted

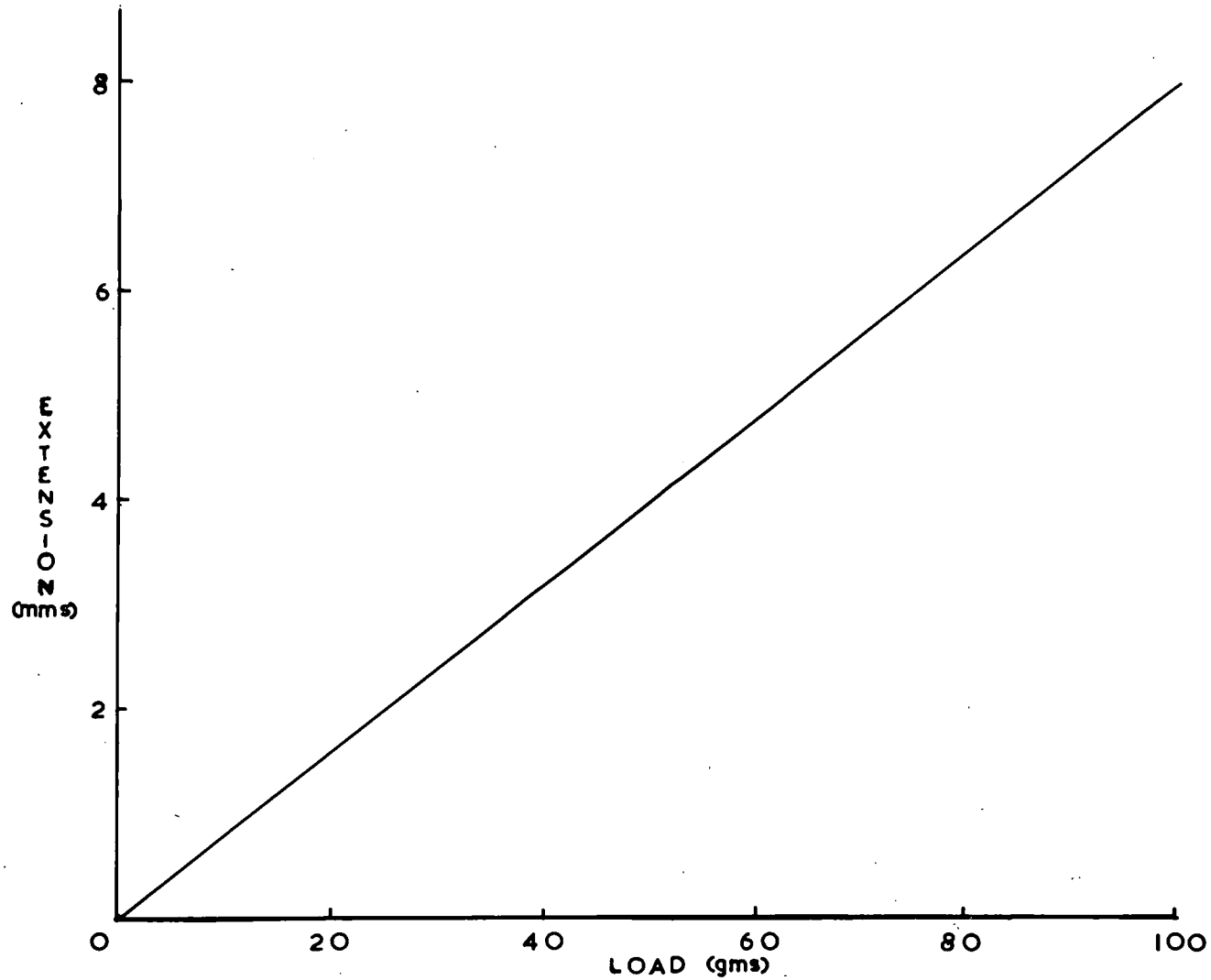

FIG2·5 CALIBRATION OF SPRING IN STRESS APPARATUS

either by horizontal movement to another part of the same face, or by rotation to a different whisker face in order to obtain the best domain pattern and the mount then clamped. Some of the selected whiskers did not give a visible domain pattern and so these were discarded at this stage. The ones that did show a pattern were then bonded to the left hand end of the apparatus. This was a piece of $\frac{1}{4}$" diameter brass rod, the end of which had the top half removed, the end of the whisker being bonded onto this flat region. The brass rod was attached to a spring, the other end of which was attached to, and moved back by, a micrometer movement. The spring and brass rod moved in a channel to support their weight and prevent bending of the whisker. The channel also provided a guide to keep the tension acting along the centre line of the apparatus. A calibration of tension against extension is shown in fig. 2.5. The bonding of the whiskers to the apparatus was done using diphenyl carbazide. This is a substance obtained in powder form that melts at 172^{o}C and re-solidifies to form a glass-like material around the whisker. On solidifying it is strain free so there are no initial strains in the whisker due to the mounting, as occur with a number of bonding materials.

When a suitable whisker had been fixed in the apparatus, the domain pattern was photographed using Pan F 35mm film in a Pentax camera mounted on top of the microscope. The microscope had a 5x objective and a 20x eyepiece and the camera used with

its lens removed in the Pentax microscope adaptor.

A tensile stress was then applied along the whisker axis by extending the spring a known amount using the micrometer, and the corresponding pattern photographed. The stress was increased in small steps and, after each, time allowed for the colloid to settle on the new pattern before it was photographed. While the stress was being changed, the pattern was observed using the reflex viewing of the camera. If any sudden transitions occured in the pattern, the stress was kept at the value corresponding to the change and the new pattern photographed. In addition to observing the change in the pattern as the stress was increased, photographs were also taken while the stress was being released, unless, as sometimes happened, the whisker broke or slipped out of the bonding material. The domain pattern photographs were then printed in the normal way and measurements made directly on the prints.

After a whisker had been used it was disconnected at the left-hand end and its size determined. This was done under the microscope using a 10x eyepiece and the 5x objective, the eyepiece having a scale that had previously been calibrated using a ruled slide marked in hundredths of a millimetre. Then from the calibration of the spring and the cross-sectional area, the tension in the whiskers for each pattern could be calculated.

2.5 Orientation of Whisker

The orientation of the whisker was next carried out. For some of the whiskers this was unnecessary as the domain pattern observed was characteristic of a particular face and orientation. For the rest, forward reflection X-ray photographs were taken and compared with standard ones given by Majima and Togino(1927) to determine the crystal orientation. The whiskers were then re-orientated on the X-ray machine according to the results from the photographs until one characteristic of a [100] direction was obtained. This was done because a number of different orientations of the crystal relative to the X-ray beam give similar photographs, and it was sometimes difficult to determine just which was the correct one.

CHAPTER THREE

WHISKERS WITH SURFACES (001), AND AXIS [100] OR A SMALL ANGLE TO THE [100] DIRECTION

3.1 Axis Exactly [100] Direction

This orientation leads to the simplest possible domain patterns, and as the whiskers usually grow with this orientation, the characteristic patterns are often seen and a large amount of work has been carried out on them. The patterns usually consist of two domains along the length of the whisker with one 180^{o} wall between them and a simple closure structure at the ends. (Coleman and Scott 1957) This simple structure can be modified by the addition of domains magnetised across the width of the whisker i.e. at right angles to the main domains. (Coleman and Scott 1957, Isin and Coleman 1965) These cross magnetised domains can be single rectangular ones as shown in the references above, or they can form patterns of their own as seen in plate 3.1.

The patterns seen in plate 3.1 are simply the running together of a number of cross magnetised domains, the resultant system being in essence only a more complex pattern of the type mentioned above, i.e. the structure is the same all through the thickness of the whisker, the pattern seen on the whisker face directly below being exactly the same as that on the top face. This was observed during the mounting of the whisker, the face selected and subsequently photographed being the one

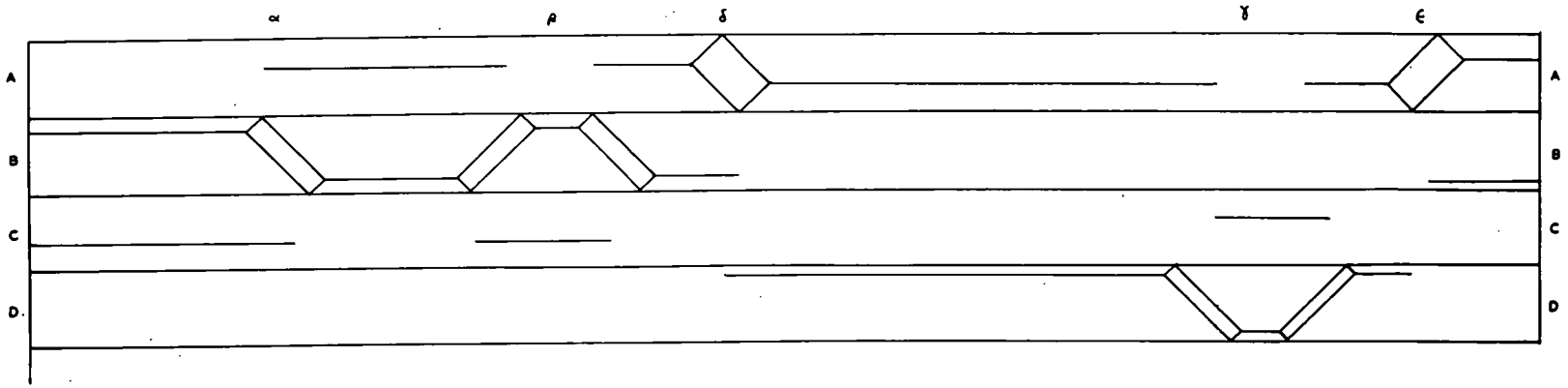

FIG 3.1a Surface patterns on the faces of the whisker shown in Plate 3.2

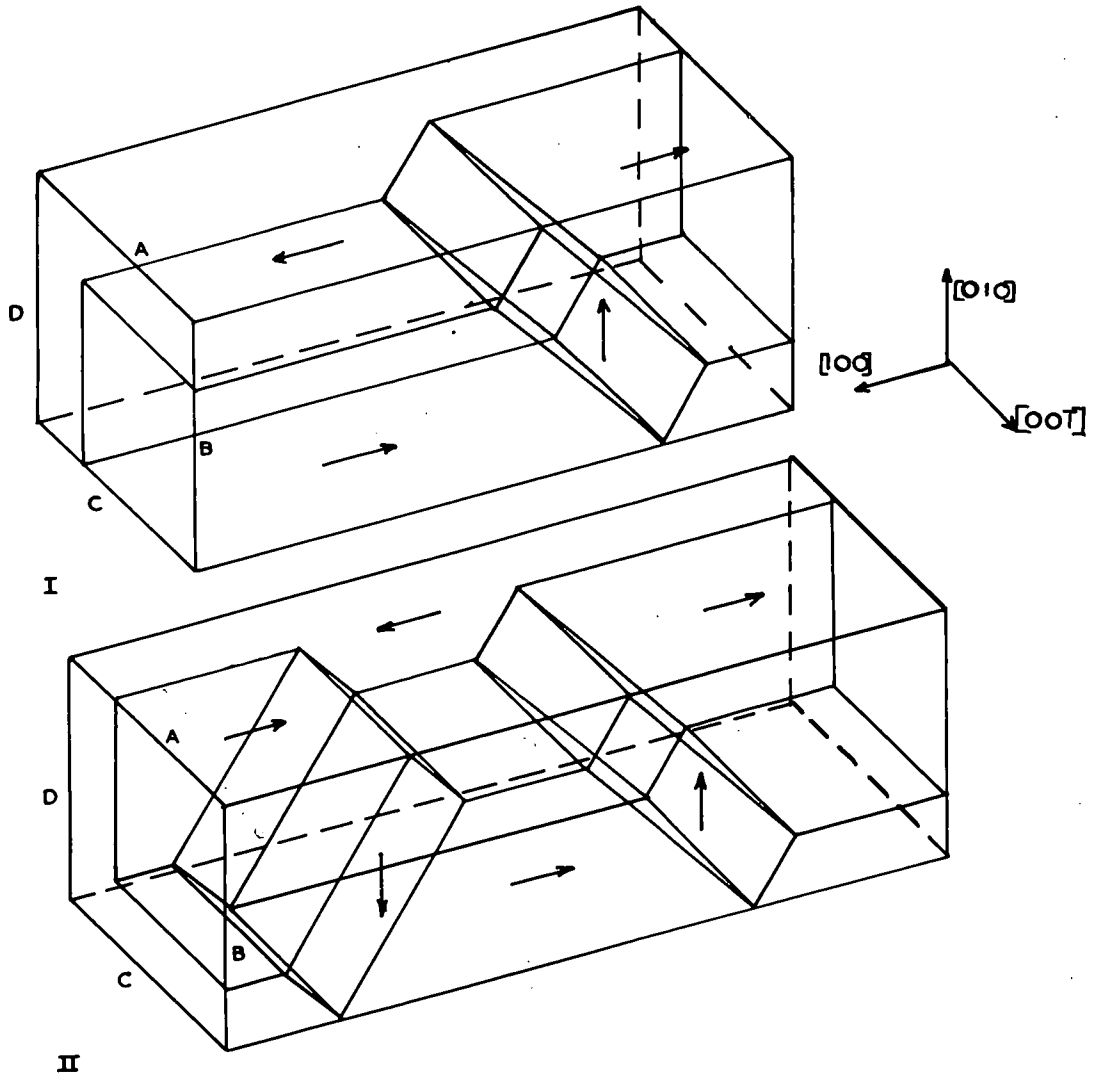

FIG 3·1b Internal domain patterns for structure shown in fig 3·1a.

Type I appears at α, δ, ϵ in fig 3·1a and II at β and γ.

that gave the clearest domain pattern.

A different type of structure to the one above is shown in plate 3.2 with a diagramatic representation of the structure in fig. 3.1. In this system the patterns observed on all the whisker faces are different and instead of the cross magnetised domains being continuous throughout the thickness of the whisker, they only occupy about two thirds of the width and no corresponding patterns are observed on opposite whisker faces. Nevertheless the effect of stress on this type of structure should be similar to that observed for the other patterns.

Other more complex structures are shown in plate 3.3. In this whisker the basic magnetisation consists of two domains magnetised along the whisker axis with two 180^{o} walls betwwen them similar to those in the whiskers described above. At two points along the whisker the positions of these walls change. The changes involve the appearance of the main 180^{o} walls in different segments of the whisker passing from one side of the cross magnetised structure to the other. These changes in orientation involve complex domain structures magnetised normal to the whisker axis and are illustrated in fig. 3.2. The change at the left hand end of the photographs of plate 3.3 involve 'V' line structures on two of the faces similar to those shown by DeBlois and Graham (1958). At the common face of the two cross magnetised domains there is a short piece of

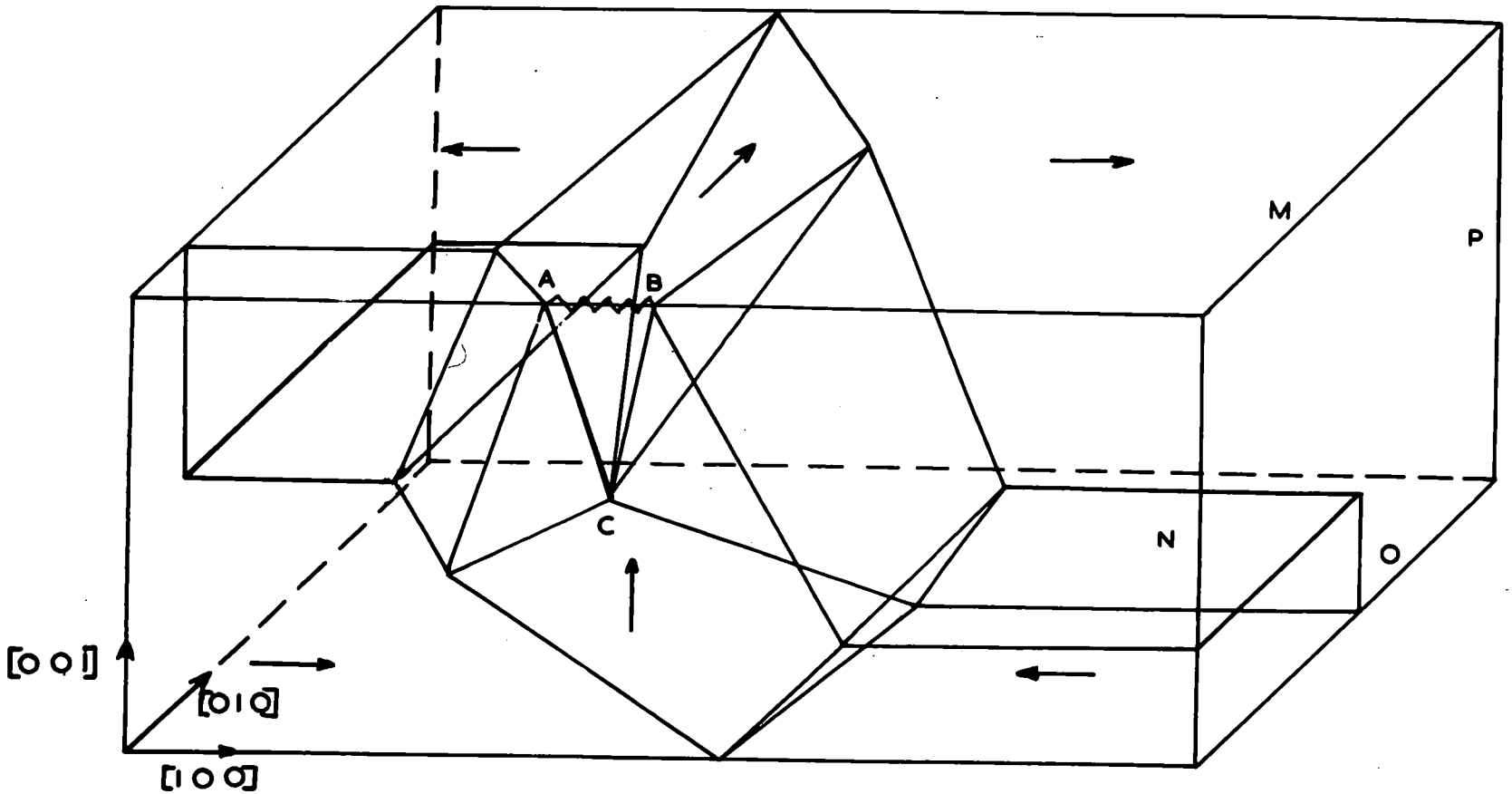

FIG 3·2a Internal structure for domain patterns shown at left hand end of plate 3·3

Wall AB C is a zig-zag wall

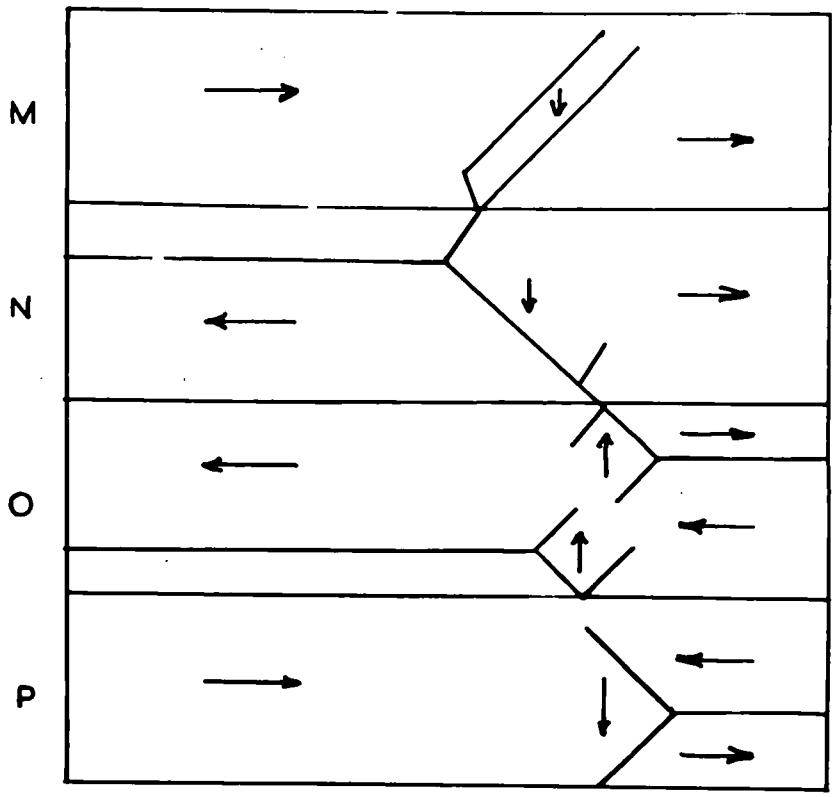

FIG 3·2b Surface domain patterns on whisker surfaces at right hand end of whisker shown in plate 3·3.

Magnetisation shows discontinuities where walls are apparantly absent indicating additional internal structure

zig–zag wall which shows up at the corner of the whisker. The apparently open sides of the domains on the two adjacent surfaces separated by the zig–zag wall are in fact closed by 90^{o} walls which intersect with other 90^{o} walls in the surface. This gives a much reduced field gradient at the surface and hence colloid does not collect in large enough amounts to be plainly visible. The change at the right hand end of plate 3.3 is more complex still and in the explanation in fig. 3.2 only the surface directions of magnetisation of the structure are shown as it was not possible to obtain a complete internal domain structure to fit the observed patterns. The internal domain structure from the bottom apparantly uncompleted square domain on the front surface is similar to that from the top one and it is proposed that these structures also have the 'V' line configuration on the adjacent whisker faces. The apparent absence of some of the domain bondaries on the surface is again due to the intersection of two walls in the surface giving a reduced colloid deposit.

The whiskers shown in both plate 3.2 and 3.3 were too short to be mounted in the apparatus described in chapter two for the application of stress, so that only the zero stress patterns are available. However it is expected that the structures seen in these two whiskers under a tensile stress would be similar to that of other structures on similarly orientated whiskers

i.e. the domains magnetised along, or nearest to, the stress direction should grow at the expense of the others.

The simplest pattern with only two domains magnetised parallel to the whisker axis has the lowest energy of all, the other systems being in positions of energy minima, but having a larger energy value in absolute terms than the simple pattern. These other structures therefore will change over to the simplest structure if a disturbance is produced, either by the application of a suitable magnetic field or the application of stress to the system to overcome the energy minimum between the two states. These changes can take place either as a series of abrupt steps involving the sudden disappearance of complete domains, or as a gradual process as the cross magnetised domains slowly decrease in volume, or as a combination of both of these methods.

3.1.1 The Effect of a Tensile Stress along the [100] Direction

In general the effect of a tensile stress along the axis of a whisker is to make the easy directions of magnetisation nearest to the axis energetically more favourable than the others. Because of this the usual end result of applying such a stress on a [100] whisker is to produce the simplest domain pattern referred to in the previous section. In practice however the value of the stress that has to be applied to overcome the energy maximum between the two domain systems can be very

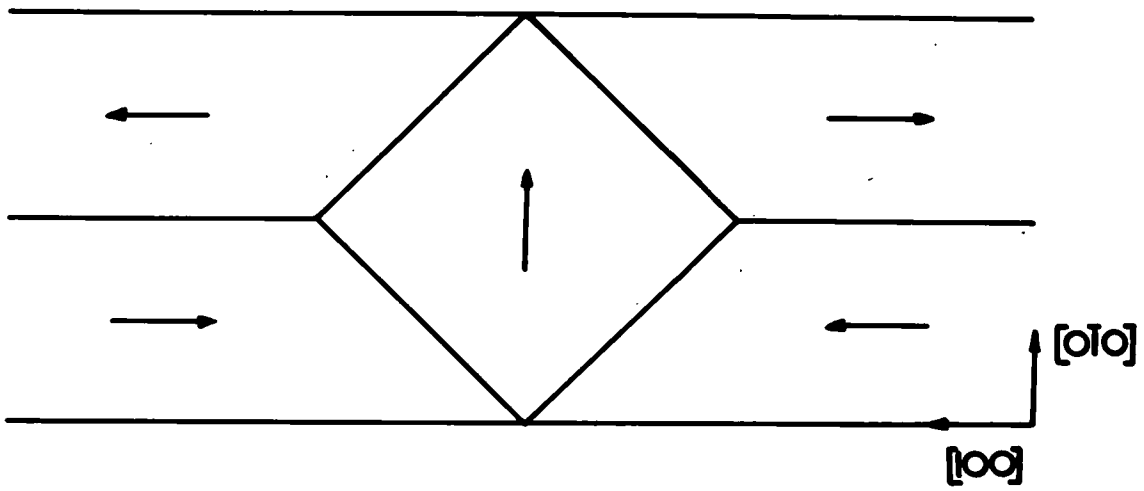

FIG 3·3 DOMAIN STRUCTURE WITH SINGLE CROSS MAGNETISED DOMAIN

large and above the yield point of the whisker so that the changeover cannot in fact be produced by this method.

An example of this is shown in plate 3.4. The domain structure present consisted of antiparallel domains magnetised along the length of the whisker with only one cross magnetised domain, apart from the closure domains at the ends. A schematic drawing is shown in fig. 3.3. Whem a tensile stress was applied to this whisker there was no visible change in the pattern observed up to a stress of 10Kgms/sq.mm, the maximum that could be attained with the apparatus. In this system with only one cross magnetised domain there is not an equivalent domain magnetised in the opposite direction with which annihilation could occur. From the results which follow in later sections it appears that in this type of domain structure changes occur by the moving together and mutual destruction of two neighbouring and oppositely magnetised cross domains. Thus, in this case, where there is only one cross magnetised domain, there is nothing with which it can interact and be destroyed. If it simply disappeared, then, as can be seen from the magnetisation directions in fig 3.3, it would leave two oppositely magnetised domains meeting in a single 180° wall with their normal components of magnetisation in direct opposition on both sides of the wall and hence have a very unfavourable system energetically The effect of stress therefore on this system is to leave it unchanged despite the making of the cross magnetised domain

a less favoured direction of magnetisation.

In contrast to this are the effects seen in plate 3.1 and plate 3.5. The whiskers seen in these two plates have domains magnetised antiparallel along the whisker axis with complex arrangements of domains magnetised across the whisker at certain points, there being only the one such arrangement shown in the plates in the appropriate whisker. The effect of applying a tensile stress along the whisker axis can be seen in the photographs. The volumesof the cross magnetised domains are gradually reduced as their energy relative to the main domains increases. This reduction in volume follows the increase in stress in a qualitative way until the cross magnetised domains virtually disappear, when there is a sudden change in the pattern as the main domains rearrange themselves on the disappearance of the cross domains. Due to the irregular nature of the patterns, especially in plate 3.5, it is impossible to obtain a quantitative agreement between the stress applied and the resulting pattern.

Also appearing in plate 3.5 is a section of zig-zag or serrated wall. A small length of this gradually appears at one end of the whisker as the stress is increased, becoming more clearly defined as the stress rises. On release of the stress, this type ofpattern disappeared completely. DeBlois and Graham(1958) have observed a similar type of wall to this

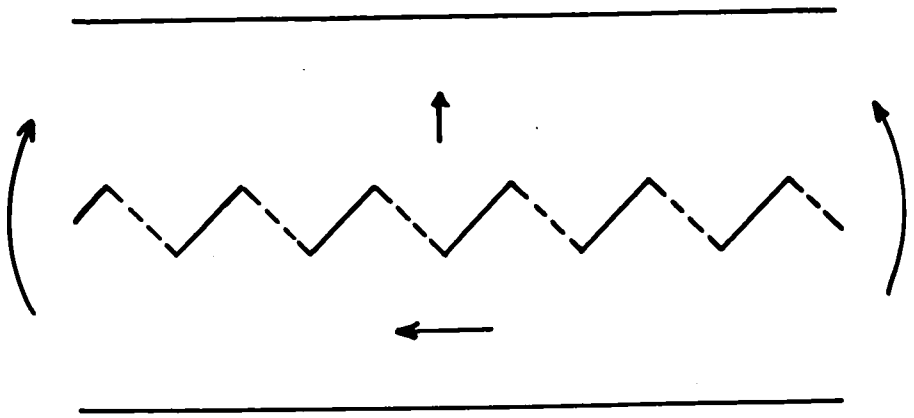

a) The domain structure on the surface of a [100] whisker strained by bending

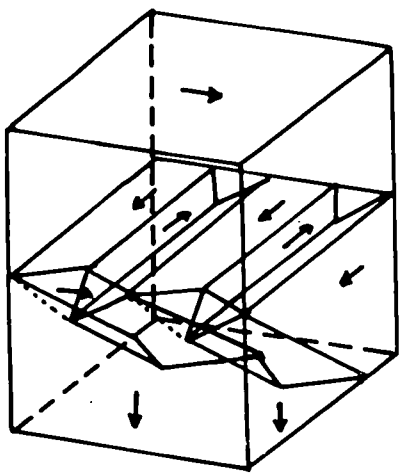

b) The internal structure of the zig-zag wall in a) above (Kaczér and Gemperle 1959)

FIG 3·4

on a whisker by bending it. This gives a compressive stress at one edge and a tensile stress at the other. A subsequent explanation of this wall configuration was given by Kaczer and Gemperle(1959) in terms of magnetisation perpendicular to the whisker axis where there is compression, along the whisker where there is a tension, and a complex closure structure between. These are illustrated in fig 3.4. The origin of the zig–zag wall in plate 3.5 therefore is probably due to slight bending of the whisker, either from misalignment in the mounting of the whisker, or the straightening out of a small growth kink in the whisker at that point. This latter mechanism was seen to apply to another specimen with an obvious kink at one point, which, on subsequent staightening out under tension, caused a similar zig–zag wall to appear.

In addition to these short lengths of zig–zag walls due to local accidental bending of the whiskers, full length zig–zag walls similar to those shown by DeBlois and Graham were produced by bending the whiskers. Apart from the observation of this type of structure no further work was done as the complex domain structure at the wall is difficult to analyse mathematically

3.2 Axis at a Small Angle δ to [100] Direction

In this orientation we have to consider the magnetostatic energy of the system. The presence of this modifies the domain stuctures and the way the system reacts to the application of

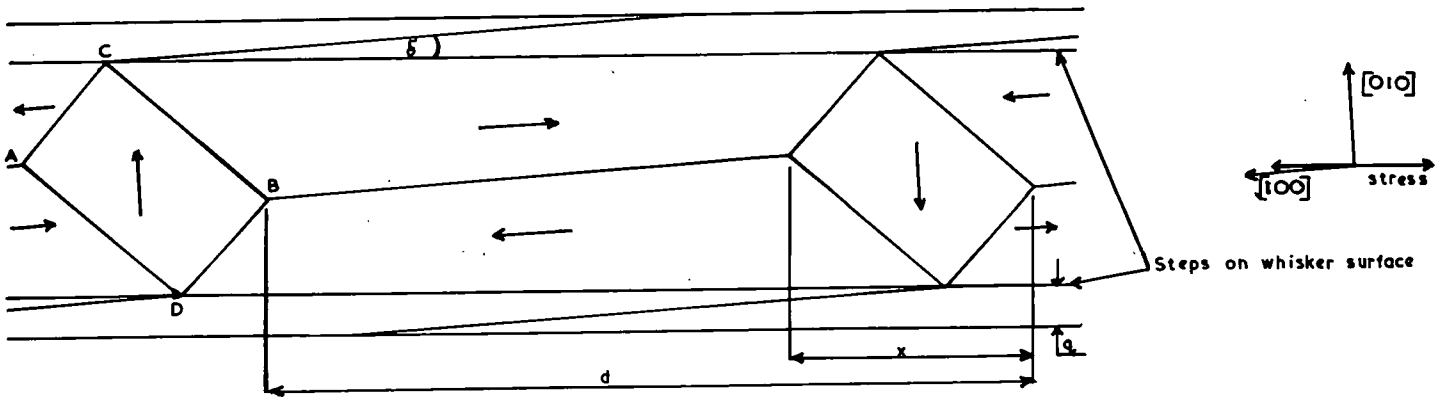

FIG 3·5 Initial pattern on [100] surface.

Perimeter AB CD = 4a. Thickness of whisker is t

stress. As in the previous section, the simplest pattern consists of antiparallel domains magnetised in [100] directions. This gives domains at an angle to the whisker axis and with no closure structures present, a high value for the magnetostatic and hence the total energy of the structure. The result is a domain pattern with a very narrow spacing between domain boundaries. The pattern is shown in fig 3.6 and is the structure all whiskers with a small value for λ tend to upon application of a tensile stress.

The total energy can be reduced considerably by the introduction of small diamond domains magnetised in [010] directions, i.e. across the whisker. This effect has been observed on a number of whiskers and the effect of stress on the structure studied. One particular whisker gave the simplest case of this structure and will be considered in detail. It is illustrated in plate 3.6. On this whisker small steps occured along the edges of the whisker and the cross domains seemed to be pinned at them,i.e. they did not reach right to the whisker sides. A simplified diagram is shown in fig 3.5. Other specimens showed similar features but with complications arising from the cross magnetised domains not beingsingle rectangles, double and treble triangles occuring quite frequently. The following discussion therefore refers only to the simple structure of fig 3.5.

3.2.1 Initial Structure

This is the zero stress state and so the energy terms involved are wall energy, magnetostatic energy, and the magnetostrictive energy of the cross magnetised domains relative to the other domains.

Refering to fig 3.5, the total wall energy for one complete pattern is $\gamma_{90}\, 4at + \frac{(d-x)}{\cos\theta} t\, \gamma_{180} + \frac{2qt}{\sin\theta}\gamma_{180}$ 3.1

Assuming that γ_{90}, the energy of a 90° wall is half γ_{180}, the energy of a 180° wall, the wall energy per unit length is given by

$$\frac{\gamma_{180}}{d} t\left[2a + \frac{2q}{\sin\theta} + \frac{(d-x)}{\cos\theta}\right] = \frac{W}{d} \qquad 3.2$$

The magnetostatic energy per unit area of the whisker side is

$$\frac{2}{1+\mu^*} \cdot 0.852\, I_s^2\, d \sin^2\theta \qquad 3.3$$

where $\mu^* = 1 + \frac{2\pi I_s^2}{K} = 44.2$ for iron.

Taking account of both sides of the whisker gives the magnetostatic energy per unit length as

$$\frac{2}{1+\mu^*} \cdot 1.7\, I_s^2\, d\, t \sin^2\theta = S d \qquad 3.4$$

For the cross magnetised domains, their magnetostrictive energy per unit volume is

$$\frac{1}{2}\lambda_{100}^2 c_{11}$$

Thus the magnetostrictive energy per unit length is

$$\frac{1}{2}\lambda_{100}^2 c_{11} \frac{V}{d} = \frac{M}{d} \qquad 3.5$$

where $V = a^2 t$ is the volume of one of the cross magnetised domains, a being one quarter of the perimeter of one of the cross domains since δ is small.

Then:

Total energy per unit length = $\frac{W}{d} + sd + \frac{M}{d}$ 3.6

To obtain the equilibrium spacing, d_o, for this structure, we have to minimise equation 3.6 with respect to d.

We then have

$$d_o = \left\{ \frac{(1+\mu^2)\left[\gamma_{180}\left(2a + \frac{2q}{\sin\delta} - \frac{x}{\cos\delta}\right) + \lambda_{100}^2 c_{11} a^2\right]}{3 \cdot 4 I_s^2 \sin^2\delta} \right\}^{1/2} \qquad 3.7$$

For the whisker under consideration the following values were obtained:

$a = 0.01$cms, $q = 0.975 \times 10^{-3}$cms, $\gamma_{180} = 1.8$dyn.cms^{-2}, $\lambda_{100} = 19.5 \times 10^{-6}$, $c_{11} = 2.41 \times 10^{12}$ergcms^{-3}, $I_s = 1.7 \times 10^{3}$e.m.u., $x \simeq \sqrt{2}a$ for δ small, $\delta = 1.5°$

Inserting these values in equation 3.7 we obtain a value of $d_o = 3.5 \times 10^{-2}$cms. The measured value of d_o from the whisker photographs is 3.3×10^{-2}cms. so that the agreement between theory and experiment is quite good. Any disagreement may be due to the cross domains not being completely regular, giving uneven areas of free pole along the whisker sides, and also to the presence of steps on the surface at the edges altering the wall and magnetostatic energy terms slightly.

3.2.2 The Effect of Stress on the Domain Structure

When tension is applied to the whisker there is an additional energy term to consider i.e. the magnetoelastic energy due to

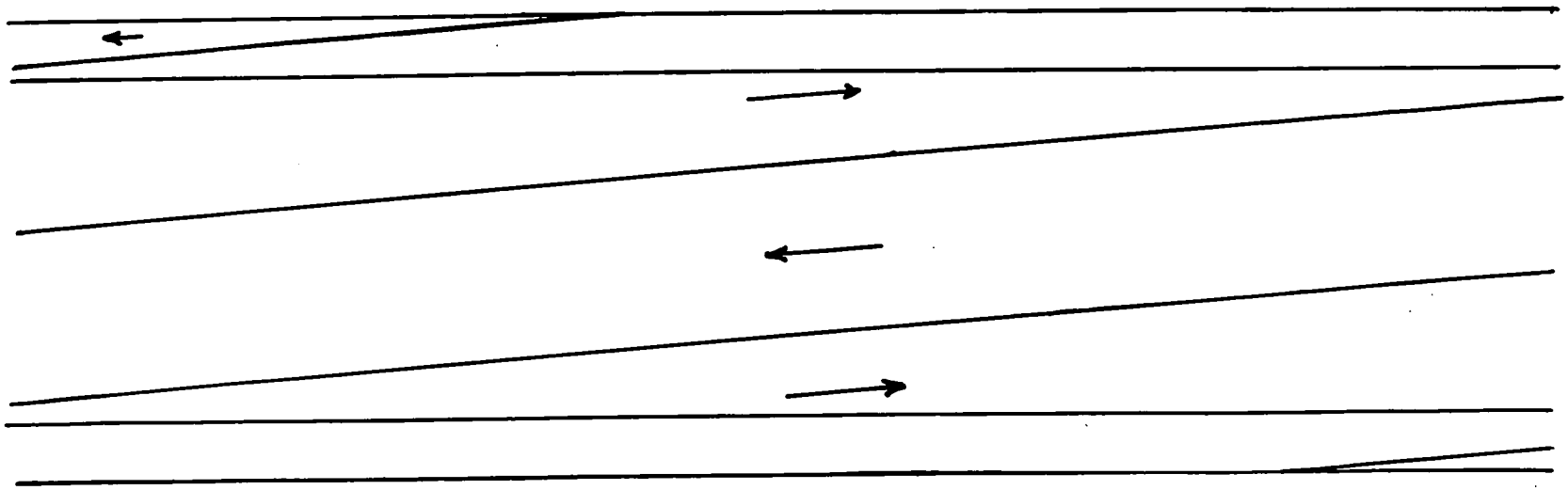

FIG 3·6 Simplified final pattern

the applied stress. This gives an additional contribution per unit volume to the energy of the cross magnetised domains of $\frac{3}{2}\lambda_{100}\sigma$ where σ is the applied stress in dynes cms^{-2}. Thus the energy of the system can be altered by the application of stress and changes, from one state to another of lower energy at that stress value, normally prevented by an energy maximum, can be brought about.

In the system dealt with in this section the sequence of events as a tensile stress was applied to the whisker along its axis is shown in plate 3.6. The initial structure remains unchanged until a stress of 5×10^{7} dynes cm^{-2} was applied. At this value alternate adjacent pairs of cross magnetised domains moved together and anihilated each other so that the pattern spacing was doubled. As the stress was further increased the remaining cross domains altered their shape somewhat and the separation changed slightly. At a stress of 15×10^{7} dynes cm^{-2} another sudden change occured. All the cross magnetised domains disappeared and an apparantly simple set of domains magnetised in the easy direction close to the whisker axis was formed. This pattern is shown schematically in fig 3.6. The tension was further increased and then released slowly down to zero with no other changes occuring. If the energy of this final state is compared with the energy of the initial structure, both at zero applied stress, it is found that the energy of

the final pattern is greater than that of the initial structure. It is however in an energy minimum state and is consequently stable, and a return to the initial structure is prevented by the absence of any suitable magnetised regions from which cross magnetised domains could nucleate.

The anihilation mechanism for the cross magnetised domains seems to be, as stated above, the coming together of two oppositely magnetised cross domains, rather than the simple disappearance of the domains. Evidence for this comes from the photographs shown in plate 3.7. In these, which relate to a different whisker from the one under consideration here, the changes occur in a similar manner and the motion of the cross magnetised domain at the left of the photographs can be clearly seen. The subsequent motion was toorapid to photograph but this first step gives evidence for the mechanism that can be seen to occur.

3.2.2.1 Energy Values for the First Pattern Change

In the following the energies of the system are calculated both before and after the change. At the changeover stress the energy of the initial and stress induced structure should be equal.

The spacing of the pattern increases from d_o to d_1, where $d_o = 3.3 \times 10^{-2}$ cm and $d_1 = 6.5 \times 10^{-2}$ cm, as measured on the photographs. The thickness of the whisker is t which is 6×10^{-3} cm.

The increase in magnetostatic energy per unit length is

$$\frac{2}{1+\mu'} \cdot 1{\cdot}7 I_s^2 \sin^2\delta (d_1 - d_0) t \qquad 3.8$$

$$= 2860 \times 10^{-5} \text{erg/cm}$$

The other energy terms all decrease after the changeover. The decrease in wall energy per unit length is

$$\gamma_{100} t \left(2a + \frac{2y}{\sin\delta} - \frac{x}{\cos\delta}\right)\left(\frac{1}{d_0} - \frac{1}{d_1}\right) \qquad 3.9$$

$$= 1630 \times 10^{-5} \text{erg/cm}$$

The decrease in magnetostrictive energy per unit length is

$$\frac{1}{2} \lambda_{100}^2 c_{11} V \left(\frac{1}{d_0} - \frac{1}{d_1}\right) \qquad 3.10$$

$$= 400 \times 10^{-5} \text{erg/cm}$$

The decrease in magnetoelestic energy per unit length is

$$\frac{3}{2} \lambda_{100} \sigma V \left(\frac{1}{d_0} - \frac{1}{d_1}\right) \qquad 3.11$$

$$= 1220 \times 10^{-5} \text{erg/cm}$$

Total decrease in energy per unit length is 3250×10^{-5} erg/cm.

At the changeover the increase in magnetostatic energy should equal the sum of the reduction in the other energy terms due to the disappearance of half of the cross magnetised domains, and it can be seen that the agreement between these is approximately correct, the increase being 12% lower than the decrease. This discrepancy is probably due to the additional energy needed to start the domains moving and provide any extra energy that may be needed during the annihilation process

while the domains are moving to change the domain pattern to the new equilibrium state.

3.2.2.2 Energy Values for the Second Pattern Change

As the stress was increased further pattern changes were expected to take place. The general form of the pattern remained the same but the actual size and shape of the cross magnetised domains changed. This can be seen in plate 3.6. This change altered the actual domain spacing along the length of the whisker, but as can be seen from the photographs this change was small compared with the actual pattern spacing, and so together with the change in the size of the cross domains, it will be discounted in the following approximate calculation. The effect of these changes will be considered at the end of the section.

At a stress of 15×10^{7} dynes/cm^2 the cross magnetised domains disappeared and left a stucure as shown in fig 3.6, the spacing of the domain walls along the axis of the whisker now being $d_2 = 32 \times 10^{-2}$ cm.

The increase in magnetostatic energy per unit length is

$$\frac{2}{1+\mu^*} 1.7 I_s^2 \sin^2\delta (d_2 - d_1) t \qquad 3.12$$

$$= 22800 \times 10^{-5} \text{ ergs/cm}$$

The decrease in wall energy per unit length is

$$\left[\frac{\gamma_{180} t}{d_1}\left(2a + \frac{2g}{\sin\delta} - \frac{x}{\cos\delta}\right) + \frac{\gamma_{180} t}{\cos\delta}\right] - \left[\frac{\gamma_{180} \omega t}{d_2 \sin\delta}\right] \qquad 3.13$$

$$= 420 \times 10^{-5} \text{ ergs/cm}$$

The magnetostrictive and magetoelastic energy of the cross domains completely disappears.

The decrease of magnetostrictive energy per unit length is

$$\frac{1}{2}\lambda_{100}^2 c_{11} \frac{V}{d_1} \qquad 3.14$$

$$= 420 \times 10^{-5} \text{ergs/cm}$$

The decrease in magnetoelastic energy per unit length is

$$\frac{3}{2}\lambda_{100}\sigma \frac{V}{d_1} \qquad 3.15$$

$$= 3990 \times 10^{-5} \text{ergs/cm}$$

The total decrease in energy per unit length is 4830×10^{-5}ergs/cm.

Comparing this with the increase in magnetostatic energy that occurs does not give any real agreement. The energy after the change should be equal to or less than the energy before the change. In this case however there is apparantly a large increase in energy after the change. Consideration of the actual pattern changes up to the sudden disappearance of the cross domains even further increases the energy gain. This occurs because the cross domains have in fact been reduced in volume before the change and hence the reduction in their wall, magnetostrictive and magnetoelastic energies is less than that calculated above. Similarly the slightly reduced pattern spacing before the change reduces the value of d_1 in equation 3.12 and so increases the change in magnetostatic energy.

This pattern change therefore is not as simple as the first one. As the energy changes for the first pattern change are in good agreement, it seems likely that the calculations for the domain structure before the second change are reasonable. The difficulty must therefore lie with the assumption that the final pattern is as simple as it is shown in fig 3.6. Further evidence for this is seen if the equilibrium spacing for the final pattern of fig 3.6 is calculated assuming it consists only of a set of domains almost parallel with the whisker axis, as the above calculations assume.

In fig 3.6 the area of one domain wall is $\frac{\omega t}{\sin\delta}$. If d is the separation along the whisker edge between two walls, and the walls are 180° walls, then the wall energy per unit length of the whisker is $\frac{\gamma_{180}\,\omega t}{d\sin\delta}$

The only other energy is the magnetostatic energy and is given by equation 3.4. Then minimising the total energy with respect to d gives the equilibrium spacing of

$$d_3 = \left[\frac{\gamma_{180}\,\omega\,(1+\mu^2)}{3\cdot 4\,I_s^2\sin^3\delta}\right]^{1/2} \qquad 3.16$$

Inserting values in this for the whisker under consideration gives $d_3 = 8.5\times10^{-2}$cm compared with the observed value of 32×10^{-2} cm. for this spacing. This discrepancy is far outside the experimental error and so the simple model is not good enough.

On the photographs of the final domain structure, the domain walls appear to be denser in some parts than in others.

This is probably due to the walls being alternately left hand and right hand Bloch walls. The presence of small stray fields at the surface of the whisker polarizes the colloid slightly and it is then preferentially deposited on either left or right hand walls, depending on the field direction, leading to the dashed structure seen in the photographs. Calculations on this type of wall structure have been performed by Shtrikman and Treves(1960) and Bhide and Shenoy(1963). The latter workers obtain a value for the energy of this type of alternating wall approximately twice that for a simple Bloch wall. If this valuemis now used in equation 3.16 we obtain a value for the equilibrium spacing of the pattern of 12×10^{-2} cm. This however is still a factor of 2.5 different from the observed value.

Unfortunately it was not possible to observe the pattern on the whisker sides so no evidence is available for the structure present on these surfaces. It would appear from the preceeding work that some kind of closure structure must be present on the whisker sides in order to reduce the total energy of the system. One type of stucture that has been observed by previous workers using bulk material consists of daggers of reverse magnetisation at the surface reducing the magnetostatic energy. The equilibrium spacing for the pattern occurs when the wall energy and the magnetostatic energy are equal, so if regions of reverse polarity were

present these would have the effect of reducing the magneto-static energy and hence the wall energy per unit length at equilibrium. Also the introduction of an additional area of domain wall around the daggers necessarily reduces further the energy available to form the main boundaries. Thus the presence of these daggers of reverse polarity should increase the spacing of the domain structure considerably. Unfortunately calculations on these structures are not possible unless the structure is known accurately and lack of any information about the patterns on the whisker sides prevents anything other than the qualitative explanation given above.

CHAPTER FOUR

WHISKERS WITH SURFACES (001) AND AXIS AT A LARGE ANGLE TO THE [100] DIRECTION

4.1 Possible Domain Structures with Different Types of Closure Structures

There are a number of possible types of domain stucture that can exist in this orientation with main domains magnetised at an angle across the whisker, each type having a different kind of closure structure at the whisker edges. Each type of domain pattern has an energy minimum at a different domain separation, and it should be possible to predict this minimum energy spacing and hence distinguish between the different structures. The various types of structure considered in this section have main domains magnetised at an angle to the whisker axis and:

a) no closure structure,

b) single closure domains magnetised in [010] directions,

c) echelon closure structure with magnetisation in [100] and [010] directions,

d) single closure domain magnetised in [001] directions.

4.2 Calculations of Domain Energy with Different Types of Closure Structure

4.2.1 No closure Structure

In this type of pattern the main domains reach to the edge of the whisker as seen in fig 4.1. The energy considerations

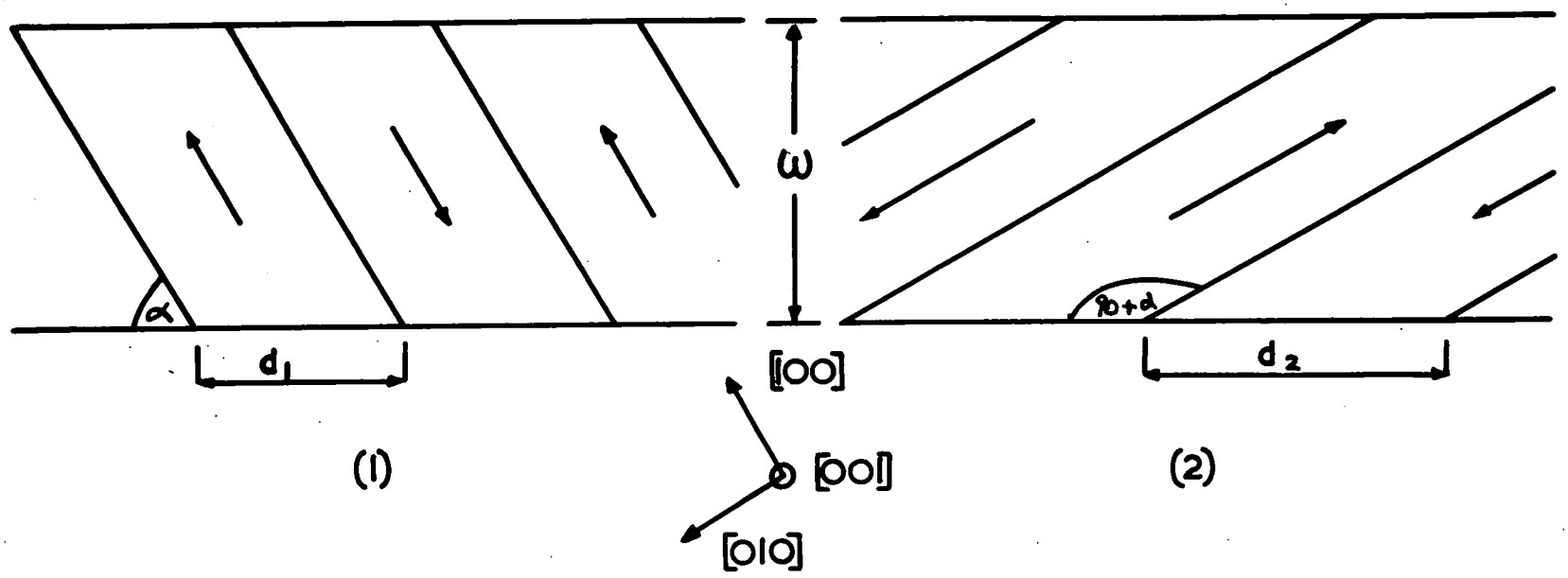

FIG 4·1 SIMPLE DOMAIN STRUCTURE WITH NO CLOSURE STRUCTURE

involved here are wall, magnetostatic, and magnetoelastic energy, and these are given by:

Wall energy per unit length $\dfrac{\gamma_{180}\,\omega t}{d\sin\theta}$ 4.1

Magnetostatic energy per unit length

$$\frac{2}{1+\mu^*}\,1{\cdot}7\,I_s^2\sin^2\theta\,dt \qquad 4.2$$

Magnetoelastic energy per unit length

$$-\frac{3}{2}\sigma\omega t\lambda_{100}\cos^2\alpha \quad \text{for (1) in fig 4.1}$$
$$-\frac{3}{2}\sigma\omega t\lambda_{100}\sin^2\alpha \quad \text{for (2) in fig 4.1} \qquad 4.3$$

Total energy per unit length

$$\frac{\gamma_{180}\,\omega t}{d\sin\theta}+\frac{2}{1+\mu^*}\,1{\cdot}7\,I_s^2\sin^2\theta\,dt-\frac{3}{2}\sigma\omega t\lambda_{100}\begin{vmatrix}\cos^2\alpha & \text{for (1)}\\ \sin^2\alpha & \text{for (2)}\end{vmatrix} \qquad 4.4$$

Differentiating with respect to d and equating to zero at $\sigma = 0$ to find d_o, the zero stress spacing, gives

$$d_o=\left(\frac{\gamma_{180}(1+\mu^*)\omega}{3{\cdot}4\,I_s^2\sin^3\theta}\right)^{1/2}=c\left(\frac{\omega}{\sin^3\theta}\right)^{1/2} \qquad 4.5$$

$$\text{where}\quad c=\left(\frac{\gamma_{180}(1+\mu^*)}{3{\cdot}4\,I_s^2}\right)^{1/2}$$

substituting $\alpha=\theta$ for (1) and $90+\alpha=\theta$ for (2) gives:

$$d_o=c\left(\frac{\omega}{\sin^3\alpha}\right)^{1/2}\text{for (1) and}\quad d_o=c\left(\frac{\omega}{\cos^3\alpha}\right)^{1/2}\text{for (2)} \qquad 4.6$$

Because for $\alpha = 45^\circ$ the two patterns are equivalent, the spacing should be the same for both cases at this angle, and the above theory predicts this. For other values of α

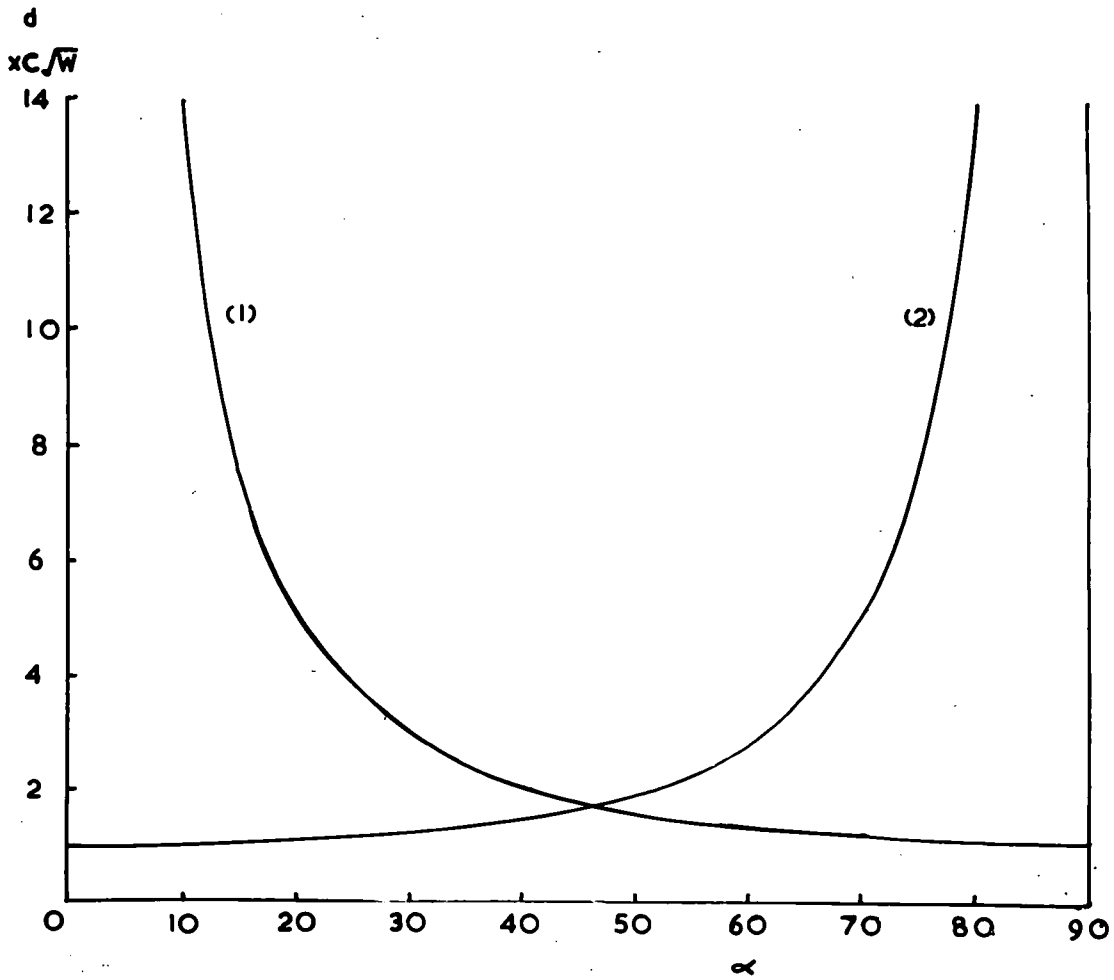

FIG 4.2a Minimum energy spacing as a function of orientation for simple domain structure at zero stress

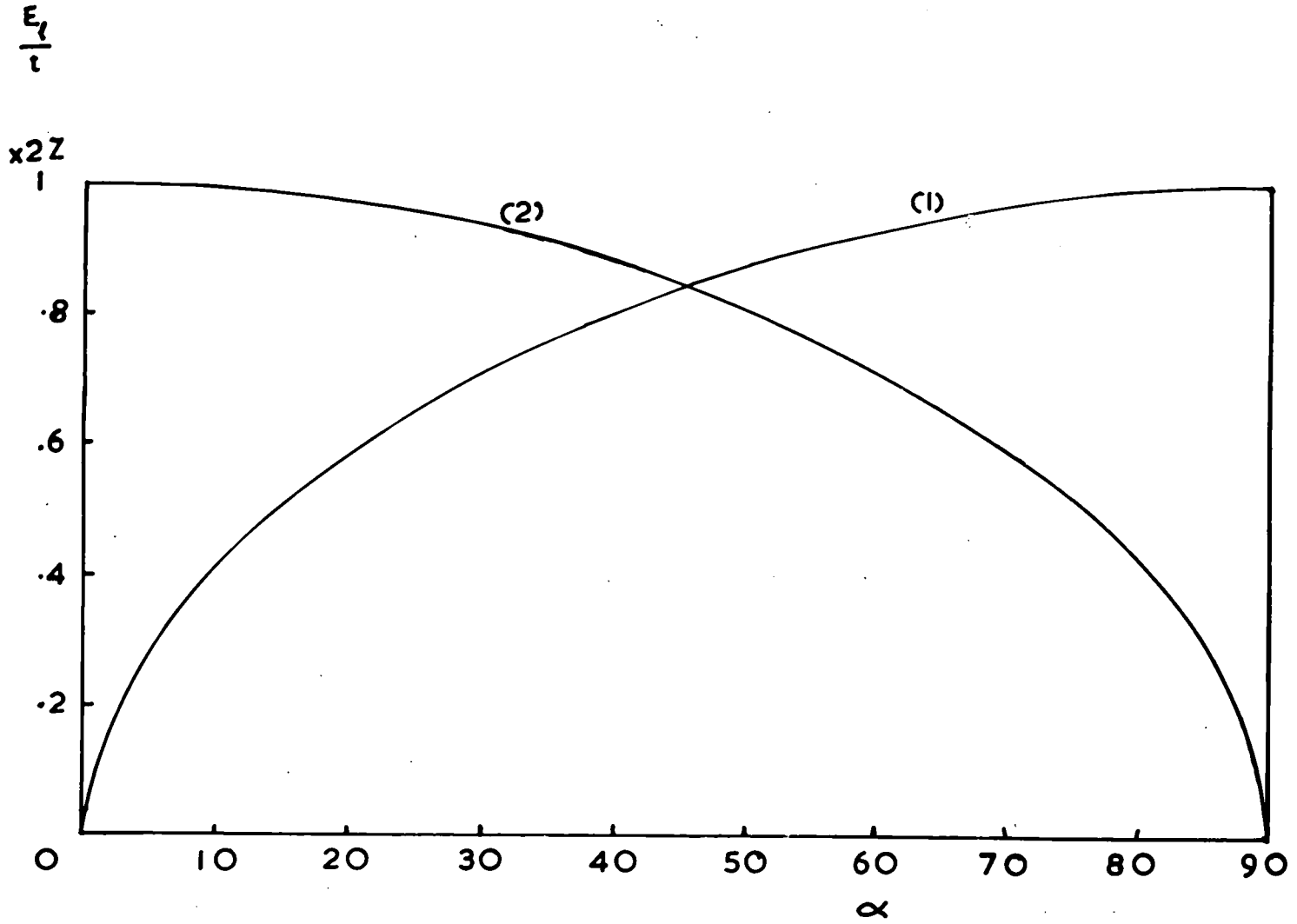

FIG 4.2b Energy per unit length as a funtion of orientation for simple domain structure at zero stress

the two cases are different. In the range $0<\alpha<45$, case (1) has the largest separation, and in the range $45<\alpha<90$, case (2) has the largest separation. The variation of d_o for both cases is shown in fig 4.2a, and as expected it can be seen that the domain spacings of (1) at an orientation α is the same as that for (2) at an orientation of $90-\alpha$.

If the above values for the pattern spacing are substituted back in the energy equation 4.4, we obtain:

Total energy per unit length

$$= 2t\left[\frac{3\cdot4\, I_s^2 \sin\alpha\, \gamma_{100}\, \omega}{1+\mu^2}\right]^{1/2} - \frac{3\sigma\omega t\lambda_{100}\cos^2\alpha}{2} \qquad \text{for (1)}$$

$$= 2Z\sin^{1/2}\alpha - \gamma\sigma\cos^2\alpha$$

Total energy per unit length

$$= 2t\left[\frac{3\cdot4\, I_s^2 \cos\alpha\, \gamma_{100}\, \omega}{1+\mu^2}\right]^{1/2} - 3\sigma\omega t\lambda_{100}\sin^2\alpha \qquad \text{for (2)}$$

$$= 2Z\cos^{1/2}\alpha - \gamma\sigma\sin^2\alpha \qquad \text{4.7}$$

For $\sigma = 0$; a) $0<\alpha<45$, (1) has the smallest energy,

b) $\alpha = 45$, (1) and (2) have equal energy, (fig 4.2b)

c) $45<\alpha<90$, (2) has the smallest energy.

Thus for all values of α, the case with the domains magnetised nearest to the axis of the whisker has the lowest energy, and should be the favoured one. However if the previous history is such that magnetisation in the direction farthest from the axis of the whisker has been produced, it should be a stable state as it is an energy minimum and there are no

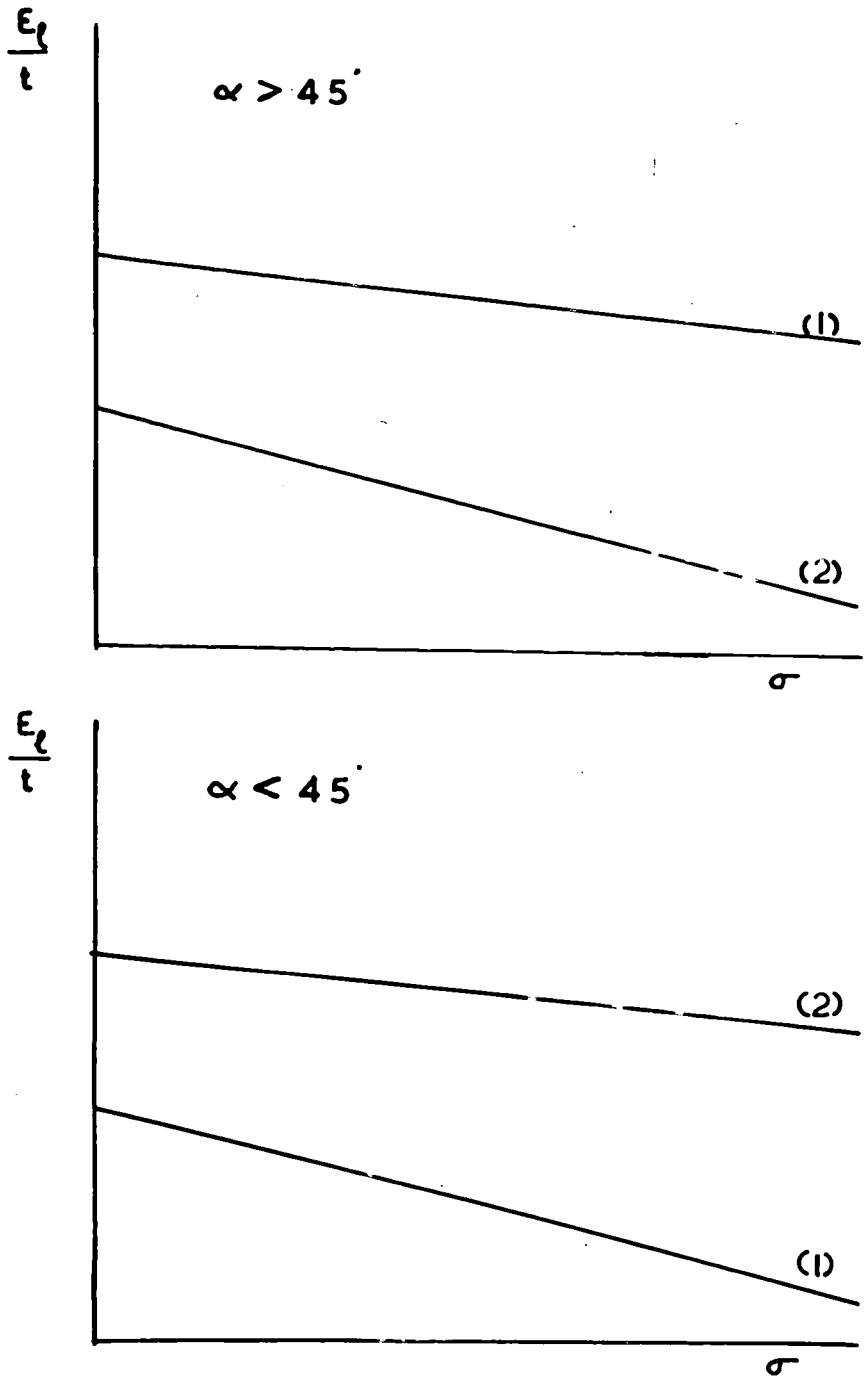

FIG 4.2c Variation of energy per unit length with stress at fixed orientations

suitably magnetised domains from which the other structure with the alternative orientation could grow.

There should be no effect on the spacing of either of these two patterns due to stress since the magnetoelastic energy term does not differ from one domain to the next. This appears to be true from equation 4.5 which does not include a contribution from the stress σ, since the magnetoelastic energy term does not depend on d. The effect of stress is simply to alter the energy difference between the two cases, making the favoured one more favourable, (fig 4.2c), without altering the domain spacing for minimum energy.

This type of structure is not usually obtained as the lack of closure domains leads to large amounts of magnetostatic energy, despite very narrow domains at the energy minimum. For the whisker shown in plate 4.1, with the following values:

$I_s = 1.7 \times 10^{3}$ e.m.u., $\gamma_{180} = 1.3$ dynes/cm^2, $(1+\mu^{\frac{1}{2}}) = 46.7$, $w = 12 \times 10^{-2}$ cm,

the equilibrium spacings calculated using equation are:

$d_o = 7.707 \times 10^{-4}$ cm for (1)

$d_o = 3.38 \times 10^{-4}$ cm for (2).

The measured value is 9.86×10^{-3} cm, which is a factor of 10 out, showing the large effect on the domain spacing of the closure strucure, which gives partial closure of the flux and a large reduction in the magnetostatic energy term.

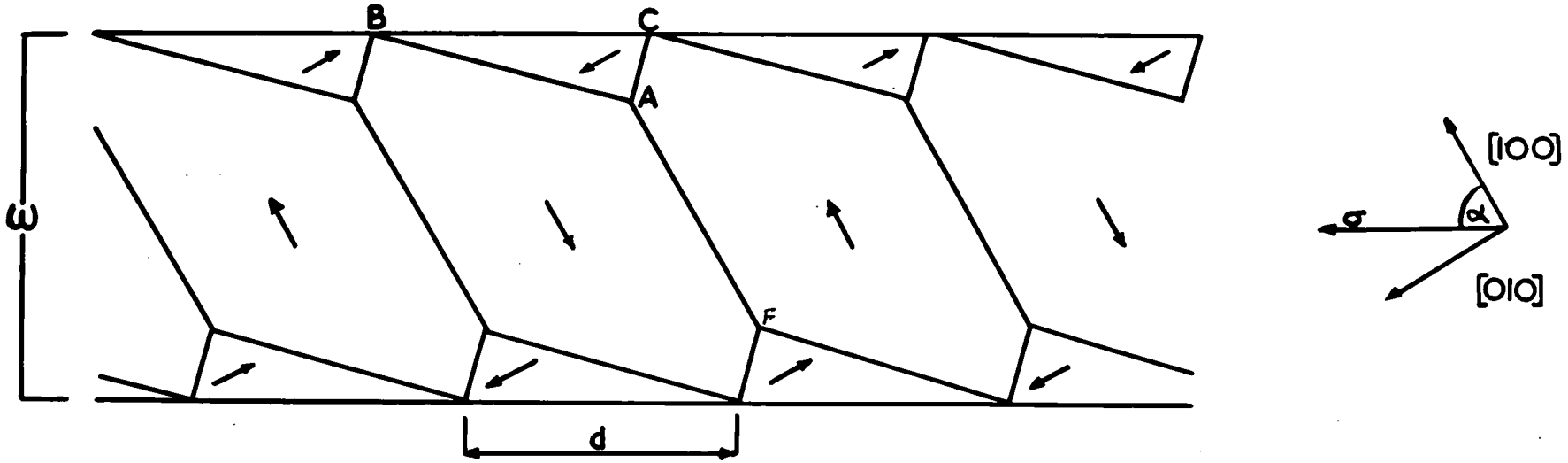

FIG 4·3 a

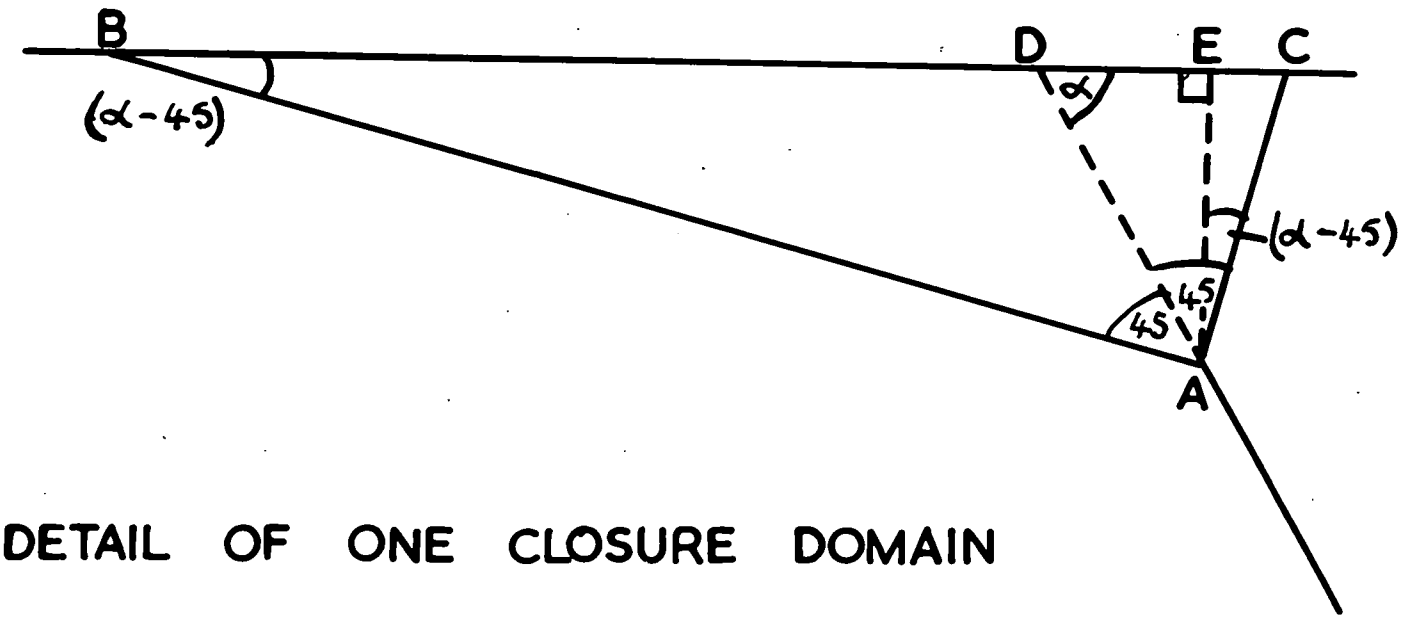

FIG 4·3b DETAIL OF ONE CLOSURE DOMAIN

4.2.2 Single Closure Domain Magnetised in the [010] Direction

In this pattern the flux path is closed by a single domain magnetised at right angles to the main domain, but the closure domain itself has some magnetostatic energy since the magnetation is not parallel to the whisker side but makes an angle of $90+\alpha$ with it. In this type there are a number of variations depending on the closure domain shape, and the three types shown in figs. 4.3, 4.4, 4.5, will be considered. The first one (type A) in fig 4.3a is the simplest with the closure domain walls being at 45° to the magnetisation directions. In the second (type B) and third (type C) configurations as in figs. 4.4a, and 4.5a, the walls of the closure domain are not at 45° to the magnetisation directions. The third type has closure domains at alternate ends of the main walls, whereas the other two have closure domains at each end of the main walls.

4.2.2.1 Type A with Closure Structure Walls at 45° to the Magnetisation directions

The energy contributions involved in this structure are wall, magnetostatic, magnetostrictive, and magnetoelastic energy.

In fig 4.3 wall AF is a 180° wall, walls AB and AC are 90° walls. The wall energy per main domain is therefore

$$2(AB+AC)t\gamma_{90} + AF\,t\,\gamma_{180}$$

$$= \gamma_{180}\,t\left\{d[\cos(\alpha-45)+\sin(\alpha-45)] + \frac{w}{\sin\alpha} - \frac{d\sin(2\alpha-90)}{\sin\alpha}\right\} \qquad 4.9$$

Assuming $2\gamma_{90} = \gamma_{180}$

The wall energy per unit length is:

$$\gamma_{180}\, t\left\{\cos(\alpha-45) + \sin(\alpha-45) + \frac{\omega}{d\sin\alpha} - \frac{\sin(2\alpha-90)}{\sin\alpha}\right\} \qquad 4.10$$

The magnetostatic energy per unit length is:

$$\frac{2}{1+\mu^2}\, 1.7\, I_s^2 \sin^2\vartheta\, dt \quad \text{where} \quad \vartheta = 90+\alpha \qquad 4.11$$

$$= \frac{2}{1+\mu^2}\, 1.7\, I_s^2 \cos^2\alpha\, dt.$$

The magnetostrictive energy due to the closure domains is given by

$$\frac{1}{2}\lambda_{100}^2 c_{11} \quad \text{/unit volume of closure domain.}$$

The volume of closure domain per unit length is:

$$2 \cdot \frac{\text{volume } ABC}{d} = \frac{dt}{2}\sin(2\alpha-90)$$

The magnetostrictive energy per unit length is therefore

$$\frac{\lambda_{100}^2 c_{11}\, dt}{4}\sin(2\alpha-90) \qquad 4.11$$

Magnetoelastic energy consists of two contributions, one from the main domainsof $-\frac{3}{2}\sigma\lambda_{100}\cos^2\alpha$ per unit volume, and one from the closure domains of $-\frac{3}{2}\sigma\lambda_{100}\sin^2\alpha$ per unit volume.

Magnetoelastic energy per unit length is:

$$-\frac{3}{2}\sigma\lambda_{100}\, t\left\{\omega\cos^2\alpha - \frac{1}{2}d\sin(2\alpha-90)\cos 2\alpha\right\} \qquad 4.12$$

Total energy per unit length is E_1

$$E_1 = \gamma_{180}\, t\left\{\cos(\alpha-45) + \sin(\alpha-45) - \frac{\sin(2\alpha-90)}{\sin\alpha} + \frac{\omega}{d\sin\alpha}\right\} + \frac{2\cdot 1\cdot 7\, I_s^2\cos^2\alpha\cdot dt}{1+\mu^2}$$

$$+ \frac{\lambda_{100}^2 c_{11} dt}{4}\sin(2\alpha-90) - \frac{3\sigma\lambda_{100}\, t}{2}\left\{\omega\cos^2\alpha - \frac{1}{2}d\sin(2\alpha-90)\cos 2\alpha\right\} \qquad 4.13$$

Differentiating this with respect to d and equating to zero gives:

$$\frac{\omega\gamma_{180}}{d^2\sin\alpha} = \frac{3\cdot 4\, I_s^2\cos^2\alpha}{1+\mu^2} + \frac{\lambda_{100}^2 c_{11}}{4}\sin(2\alpha-90) + \frac{3\lambda_{100}\sigma}{4}\sin(2\alpha-90)\cos 2\alpha$$

$$\therefore d^{-2} = \frac{3\cdot 4\, I_s^2\cos^2\alpha\sin\alpha}{(1+\mu^2)\omega\gamma_{180}} + \frac{\lambda_{100}\sin(2\alpha-90)\sin\alpha\,(\lambda_{100}c_{11} + 3\sigma\cos 2\alpha)}{4\omega\gamma_{180}} \qquad 4.14$$

From this we get the zero stress spacing

$$d_0 = \left\{\frac{3\cdot 4\, I_s^2\cos^2\alpha\sin\alpha}{(1+\mu^2)\omega\gamma_{180}} + \frac{\lambda_{100}^2 c_{11}\sin(2\alpha-90)\sin\alpha}{4\omega\gamma_{180}}\right\}^{-1/2} \qquad 4.15$$

and the variation with stress of $1/d^2$ as

$$\frac{1}{d^2} = \frac{1}{d_0^2} + \frac{3\sigma\lambda_{100}}{4\omega\gamma_{180}}\sin(2\alpha-90)\sin\alpha\cos 2\alpha \qquad 4.16$$

which is a straight line graph of slope

$$\frac{3\lambda_{100}}{4\omega\gamma_{180}}\sin(2\alpha-90)\sin\alpha\cos 2\alpha$$

This type of structure is limited to the range $45<\alpha<90$ because for orientations of $\alpha < 45$ the closure structures as drawn cannot exist. The domains magnetised in the directions in which the closure domains would be expected to be magnetised become the main domains, and vice versa for the expected main domain directions. In the range $45<\alpha<90$ for which this treatment is valid, the closure domains are magnetised in directions closer to the applied stress, i.e. the whisker axis, than are the main domains. The closure domains would

therefore be favoured by the application of a tensile stress along the whisker axis and should grow at the expense of the main domains. The spacing of the main domains should increase as the closure domains encroach upon the main domains. The value of $1/d^2$ should decrease as the stress increases, i.e. the slope of the graph of $1/d^2$ against σ should be negative. This is predicted by the above theory as the value of cos 2α for $45 < \alpha < 90$ is negative, while the other terms are all positive, making the total expression always negative.

This type of structure is not much different in energy for the same spacing as the stucture with no closure domains considered in the previous section, because the magnetostatic energy of the closure domains is the same as that for the main domains of the lower energy case when there are no closure domains. In fact the energy is higher as there is now a magnetostrictive energy contribution due to the closure structure together with some additional wall energy. The result of these extra terms is to reduce the domain spacing for minimum energy compared with the low energy pattern with no closure structure. The spacing should be greater however than that for the high energy case of section 4.2.1, as the magnetostatic energy is reduced compared with that case. This is borne out in the theory, the value of the zero stress pattern spacing for a whisker of the size and orientation of the one in plate 4.1 being 5.84×10^{-4} cm, compared with 7.71×10^{-4} cm and 3.38×10^{-4} cm

for the low and high energy cases of section 4.2.1 respectively.

This type of structure is less favoured than that of the previous section and is not present in the simple form presented above. It has to be modified in some form to explain the observations of plate 4.1, which has a zero stress spacing of 9.8×10^{-3} cm and a decrease in this spacing, fig 4.6, whereas the above predicts an increase.

In this whisker(plate 4.1) there is another factor to consider which could alter the equilibrium spacing. The whisker is not straight as the above treatment assumes, but has a number of kinks which cause the whisker to change its direction, while the orientation of the crystal relative to the axis stays the same. This must introduce an additional stress into the system and hence make the value of the magnetoelastic energy term not zero at zero applied tension. The domain spacing would then be characteristic of this internal stress and different from the value predicted above. In the system above, a tension perpendicular to the whisker axis of 147 Kgm/mm^2 would be necessary to produce the observed value of domain spacing. This is much above the yield point of iron so the domain spacing in this case cannot be due to this process. It will be seen later that the value of stress necessary in the system considered in section 4.2.2.3 is quite small and could produce the observed results.

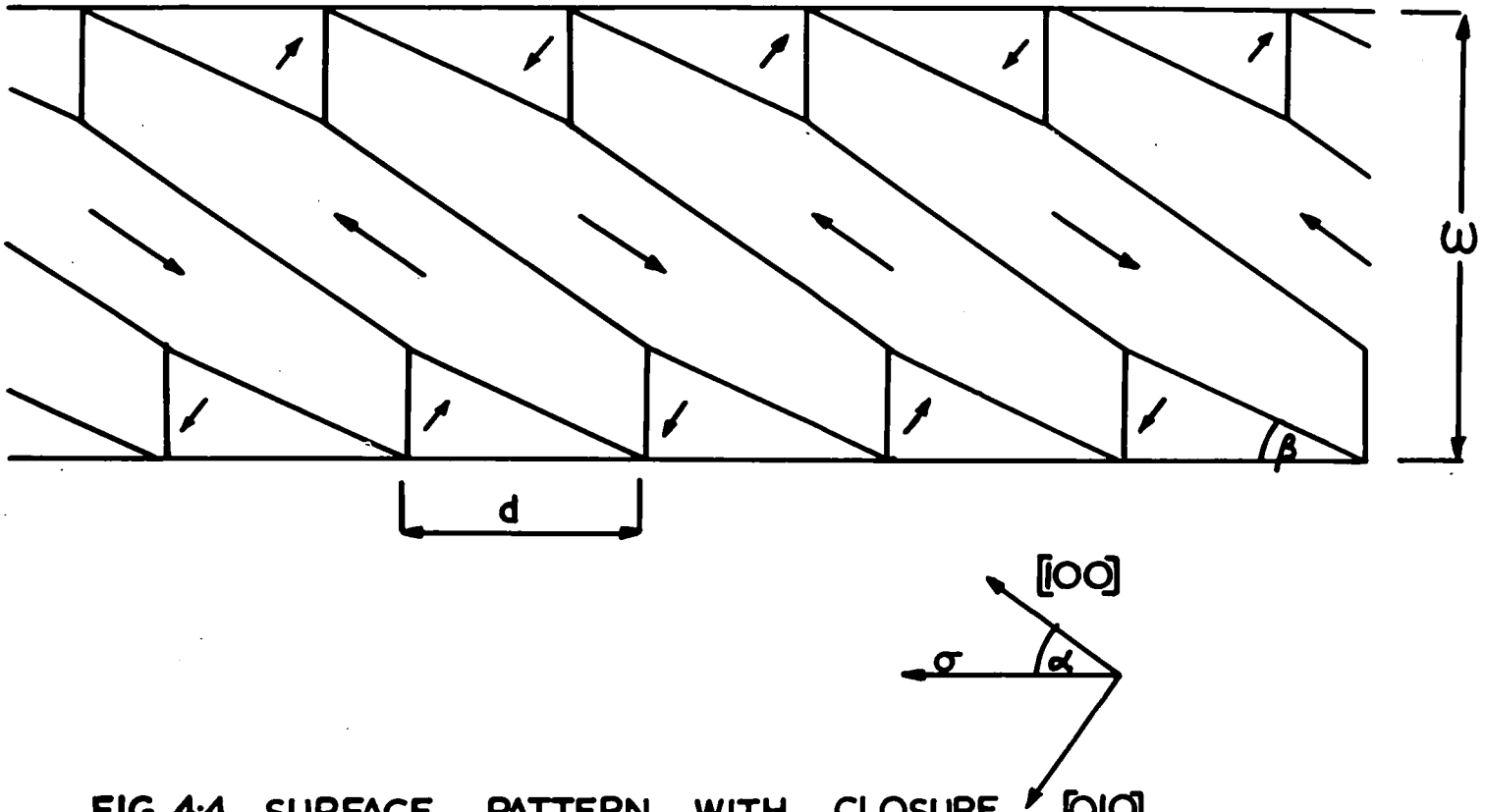

FIG. 4·4 SURFACE PATTERN WITH CLOSURE STRUCTURE AT EACH END OF MAIN WALLS.

4.2.2.2 Closure Structure with Walls not at 45° to the Magnetisation Directions

This structure is similar to that considered in the previous section, the difference being that the walls of the closure structures are not at 45° to the magnetisation directions, and it takes over from the above case in the range $0 < \alpha < 45$, where the other one could not exist since the walls AB in fig 4.4 would go towards the centre of the whisker rather than the edge. As the examples of these types of domain structures had orientations of approximately 30°, simplifications used in this and the following sections are that the shorter of the two sides of the closure domains is perpendicular to the whisker edge, and the wall energy is the same as for walls in a [110] direction.

The energy terms are wall, magnetostatic, magnetostrictive, and magnetoelastic energy, and the total energy per unit length E_1 is given by :

$$E_1 = \gamma_{100}\, t \left\{ \sin\beta \left[1 - \frac{2}{\sin\alpha} \right] + \frac{1}{\cos\beta} + \frac{\omega}{d \sin\alpha} \right\} + \frac{2}{1+\mu^2} \cdot 1.7 I_s^2 \cos^2\alpha\, t + \frac{1}{2} \lambda_{100}^2 c_{11}\, t\, d \sin\beta - \frac{3\sigma \lambda_{100}}{2} t \left\{ \omega \cos^2\alpha - d \sin\beta \cos 2\alpha \right\} \qquad 4.17$$

Differentiating with respect to d and equating to zero to obtain the equilibrium spacing gives:

$$\frac{1}{d^2} = \frac{3.4 I_s^2 \sin\alpha \cos^2\alpha}{(1+\mu^2)\, \gamma_{100}\, \omega} + \frac{\lambda_{100} \sin\alpha \sin\beta \left[\lambda_{100} c_{11} + 3\sigma \cos 2\alpha \right]}{2 \gamma_{100}\, \omega} \qquad 4.18$$

From this the zero stress spacing is given by

$$d_0 = \left\{ \frac{3.4 I_s^2 \sin\alpha \cos^2\alpha}{(1+\mu^2)\, \gamma_{100}\, \omega} + \frac{\lambda_{100}^2 c_{11} \sin\alpha \sin\beta}{2 \gamma_{100}\, \omega} \right\}^{-1/2} \qquad 4.19$$

and the variation with stress of $1/d^2$ as

$$\frac{1}{d^2} = \frac{1}{d_o^2} + \frac{3\sigma\lambda_{100}\sin\alpha\sin\beta\cos 2\alpha}{2\gamma_{180}\omega} \qquad 4.20$$

Using the value taken from plate 4.1 of $\alpha = 30^o$, $\beta = 30^o$, w $12\text{x}10^{-3}$cm, gives $d_o = 3.529\text{x}10^{-4}$cm and the slope of the $1/d^2/\sigma$ graph as $2.34\text{x}10^{-4}$ dyn^{-1}

The value of d_o is, as expected, close to that for the high energy case described in section 4.2.1, as the closure domains are at a high angle to the whisker edge i.e. 60^o the same as previously. If an internal stress due to the kinks in the whisker is the cause of the observed value for d_o of $9.8\text{x}10^{-3}$cm, it would be necessary to have a stress of 300 Kgm/mm.^{2} As in the previous case this is beyond the elastic limit of the iron so that it cannot be the explanation of the observed value, and a different structure is needed.

4.2.2.3 Closure Structure at Alternate Ends of Main Domains, with Closure Structure Walls not at 45^o to the Magnetisation Directions

The arrangement of this structure is shown in fig 4.5. From this it can be seen that the direction of magnetisation is the same along the whole of each side of the whisker, and opposite in sign on the two edges. The magnetostatic energy of the system is now independent of the separation of the main domains along the whisker, and a constant dependent only on the width and thickness of the whisker. In calculating the

domain separation the magnetostatic energy term can be neglected.

The energy terms are:

Wall energy per unit length

$$\gamma_{180}\, t \left\{ \frac{1}{2}\left(\sin\beta + \frac{1}{\cos\beta} - \frac{4\sin\beta}{\sin\alpha} \right) + \frac{w}{d\sin\alpha} \right\} \qquad 4.21$$

Magnetostatic energy is a constant = M

Magnetostrictive energy per unit length

$$\frac{\lambda_{100}^2\, c_{11}\, d\, t\, \sin\beta}{4} \qquad 4.22$$

Magnetoelastic energy per unit length

$$-\frac{3\sigma\lambda_{100}\, t}{2}\left\{ w\cos^2\alpha - \frac{d}{2}\sin\beta\cos 2\alpha \right\} \qquad 4.23$$

Minimising the value of the total energy per unit length to obtain the equilibrium spacing gives:

$$\frac{1}{d^2} = \frac{\lambda_{100}\sin\beta\sin\alpha}{4\gamma_{180}\, w}\left(\lambda_{100} c_{11} + 3\sigma\cos 2\alpha\right) \qquad 4.24$$

with a zero stress value of $d_o = \left\{ \frac{\lambda_{100}^2 c_{11}\sin\beta\sin\alpha}{4\gamma_{180}\, w} \right\}^{-1/2}$

and a slope of $\frac{3\lambda_{100}\sin\beta\sin\alpha\cos 2\alpha}{4\gamma_{180}\, w}$ for the $1/d^2$ against σ graph.

The values of these quantities, using the results from plate 4.1, are $d_o = 165\times10^{-3}$cm and the slope of the graph in dyn^{-1} is 1.178×10^{-4}. Again the zero stress value is greatly different from the observed value of 9.8×10^{-3}cm. In this case however the value of the internal stress necessary to produce this spacing is 9.02×10^{-1} Kgm/mm^2. This is not such a large value and it is possible that this could be the explanation. From

the actual photographs in plate 4.1 it seems however that there is not much of this structure present, there being a certain amount of an echelon type of pattern and not just the single closure domain considered here. In plate 4.2, which is a similarly orientated whisker, this pattern seems to predominate, especially towards the thinner end of the whisker. In the middle of plate 4.2c this type of structure is very evident. The values of α and β are 35° and 25° respectively, and the width w is 7.3×10^{-3} cm. Using these values the above theory gives $d_o = 131 \times 10^{-3}$ cm, and a slope of 1.29×10^{-4} for the $1/d^2$ against σ graph. The measured value of d_o in this case is 14.5×10^{-3} cm. There is a large discrepancy between these two values for the spacing, but if the value of internal stress necessary to produce the observed value from the predicted value is calculated it is only 3.7×10^{-1} Kgm/mm^2. This value is quite low, and in view of the amount of distortion present in the whisker it is very likely to be the cause of the above disagreement.

This result for the minimum energy domain spacing is a very high energy state due to the neglect of the magnetostatic energy, and although an energy minimum appears at the observed spacing when internal stresses are incorporated, the absolute value of the energy makes it an apparently unfavoured arrangement compared with the various other systems considered in the

remainder of this chapter. Despite this objection, the result for the whisker in plate 4.2, together with the actual photographs of the domain pattern, makes the structure considered above the most probable explanation of the observations.

Further proof of the type of closure structure actually present could have been obtained if it had been possible to observe the pattern on the sides of the whisker. Unfortunately this could not be done and a decision on the actual structure present has to be based on the above results leading to the conclusion outlined above.

4.2.3 Echelon Closure Structure

This type of structure is shown in fig 4.7. It consists of the main domains at an angle α to the whisker axis with a series of smaller domains magnetised alternately anti-parallel and perpendicular to the main domains. It is similar to that observed by Martin(1957) on (111) surfaces of a silicon iron crystal, and by Corner and Mason(1964) on (110) surfaces of silicon-iron subjected to stress. These workers considered different cases to the one shown here. Martin had the small closure domains further subdivided while Corner and Mason had additional structures at the surface with magnetisation in the plane of the surface to reduce the magnetostatic energy to zero. From the photographic results there is no evidence of any finer structure at the whisker edge. The

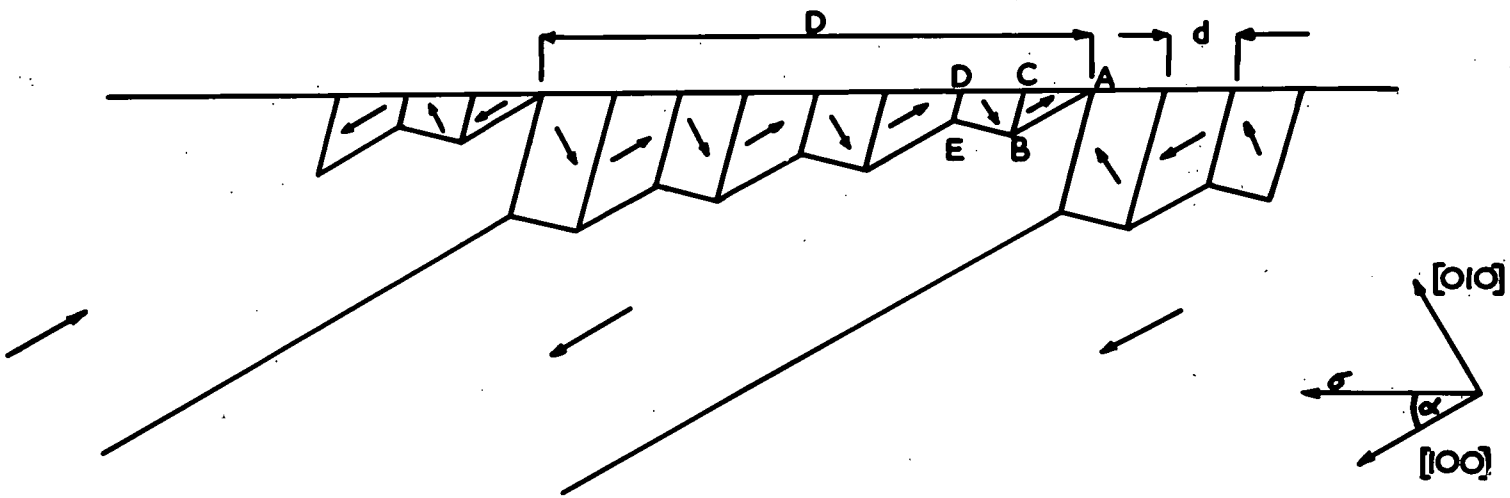

FIG 4·7 DETAIL OF ECHELON STRUCTURE ON ONE SURFACE OF A WHISKER.

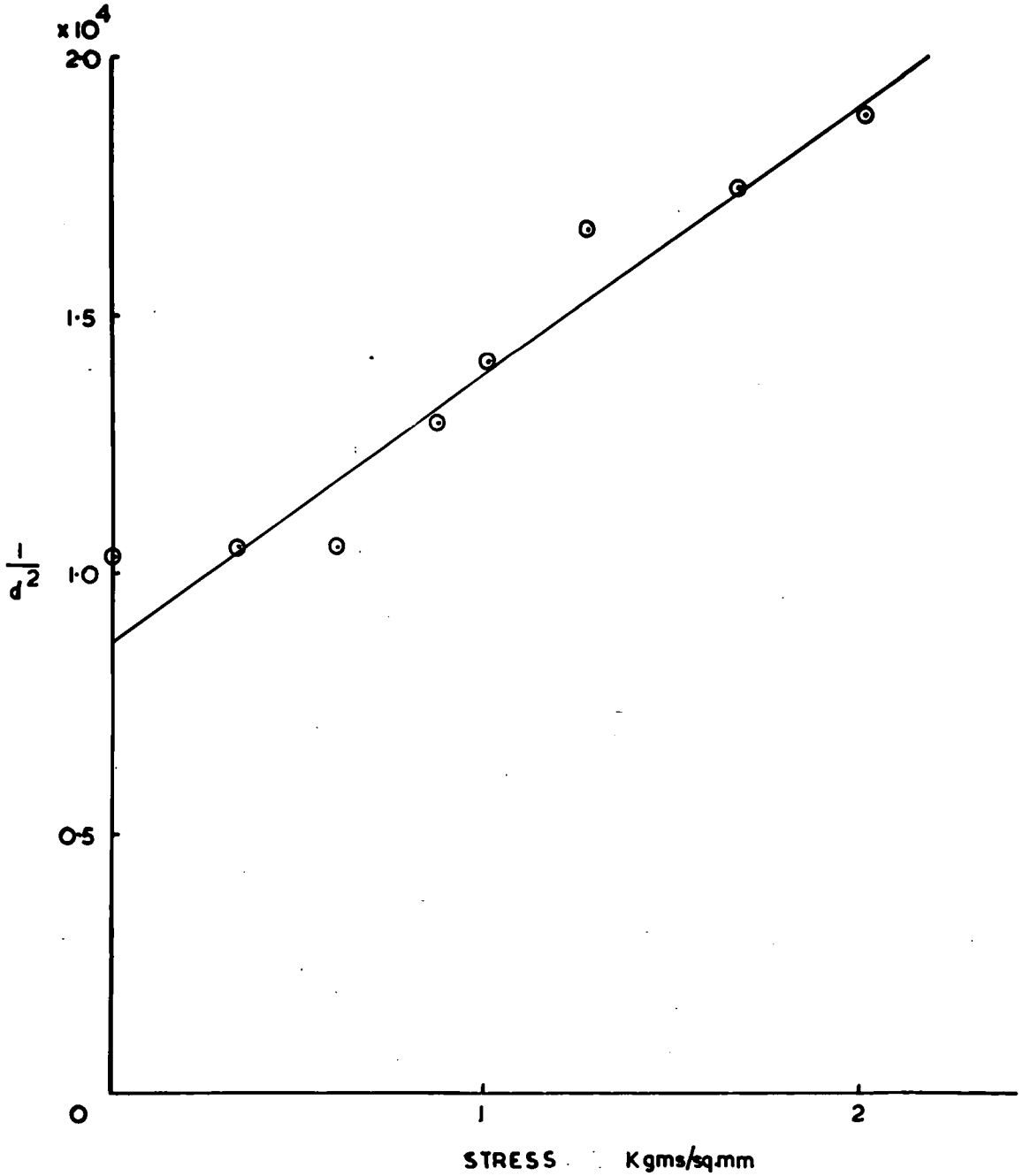

FIG 4·6 Result for whisker shown in plate 4.1

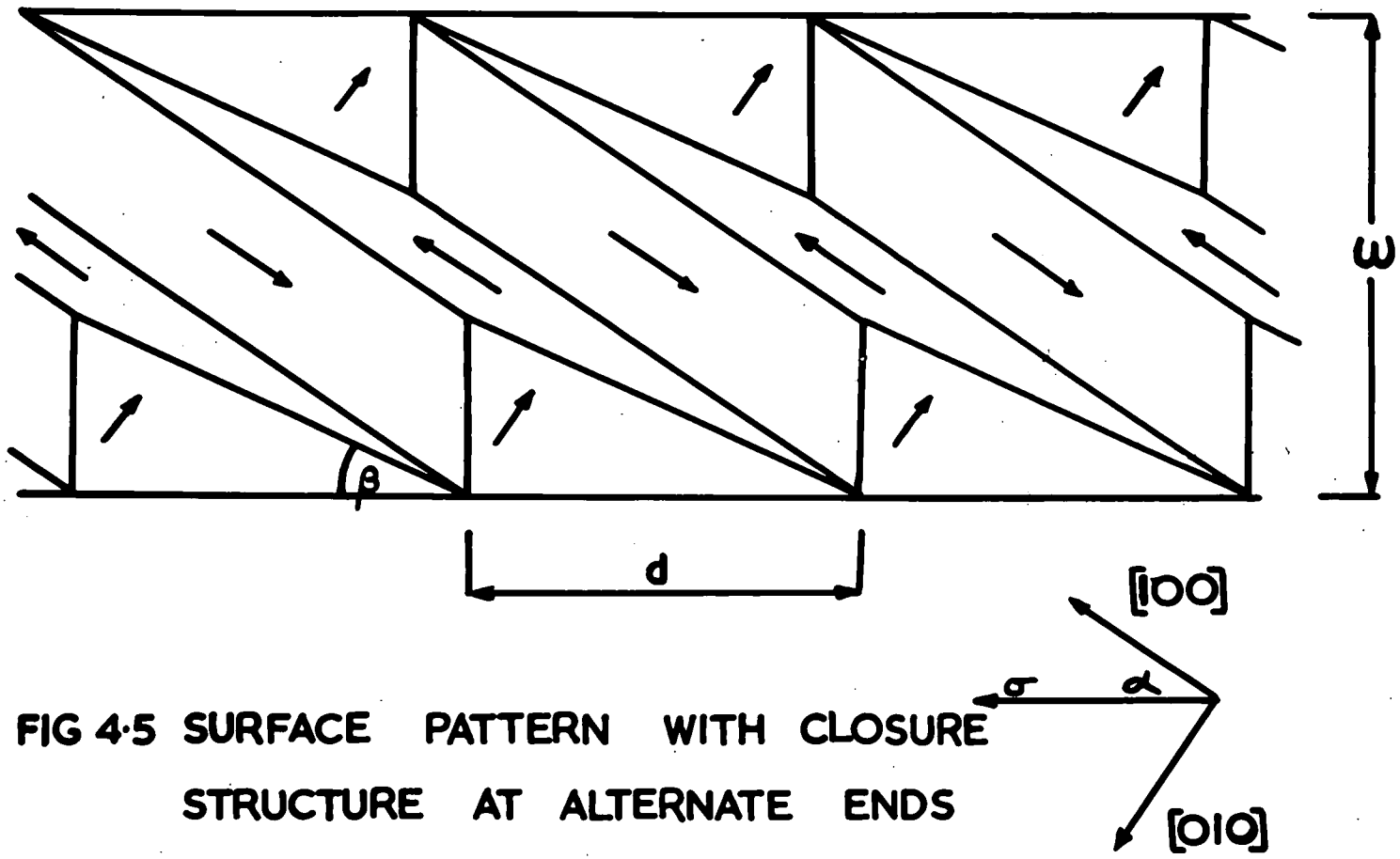

FIG 4·5 SURFACE PATTERN WITH CLOSURE STRUCTURE AT ALTERNATE ENDS OF MAIN WALLS

arrangement considered is therefore the one shown in fig 4.6, and a solution for the domain spacings obtained for all values in the range $0 < \alpha < 90$

The wall energy of ABCDEB is

$$\frac{\gamma_{180}\, d\, t}{2}\left\{\frac{2\sin(45+\alpha)+2\sin\alpha}{\sin 45} + \sin(45+\alpha) - \cos(45+\alpha)\right\} \qquad 4.25$$

Each subsequent pattern across the main domain increases the wall energy by an amount equal to twice the energy of DE compared with the previous pattern. For n complete patterns across the main domain the total wall energy of the echelon structure is

$$\frac{n}{2}\left(2\,(\text{energy of ABCDEB}) + (n-1)(\text{energy of }(2\times DE))\right)$$

The energy of wall DE is $\dfrac{d\sin\alpha}{\sin 45} - d\cos(45+\alpha)$

Total wall energy of one echelon structure is

$$\frac{n\,\gamma_{180}\, d\, t}{2}\left\{\frac{2\sin(45+\alpha)+\sin\alpha}{\sin 45} + \sin(45+\alpha)\right\} + \frac{n^2\gamma_{180}\, d\, t}{2}\left\{\frac{\sin\alpha}{\sin 45} - \cos(45+\alpha)\right\} \qquad 4.26$$

As there are two echelon structures per main domain, and 1/D main domains per unit length of the whisker, the total wall energy per unit length associated with the echelon structure is

$$\frac{n\,\gamma_{180}\, d\, t}{D}\left\{\frac{2\sin(45+\alpha)+\sin\alpha}{\sin 45} + \sin(45+\alpha)\right\} + \frac{n^2\gamma_{180}\, d\, t}{D}\left\{\frac{\sin\alpha}{\sin 45} - \cos(45+\alpha)\right\}$$

Substituting $n = D/2d$ in the above gives

$$\frac{\gamma_{180}\, t}{2}\left\{\frac{2\sin(45+\alpha)+\sin\alpha}{\sin 45} + \sin(45+\alpha)\right\} + \frac{\gamma_{180}\, D\, t}{4\, d}\left\{\frac{\sin\alpha}{\sin 45} - \cos(45+\alpha)\right\} \qquad 4.27$$

The energy of one main domain wall is

$$\frac{(\omega - 2PQ)}{\sin\alpha}\,\gamma_{180}\, t$$

$$= \frac{\gamma_{180}\, t}{\sin\alpha}\left\{\omega - b\left(\frac{\sin\alpha}{\sin 45} - \cos(45+\alpha)\right)\sin(45+\alpha)\right\} \qquad 4.28$$

This gives the energy of the main walls per unit length as

$$\frac{\gamma_{180}\, t}{2}\left\{\frac{\omega}{b\sin\alpha} - \frac{\sin(45+\alpha)}{\sin 45} + \frac{\cos 2\alpha}{2\sin\alpha}\right\}$$

The total wall energy per unit length is

$$\frac{\gamma_{180}\, t}{2}\left\{\frac{\sin\alpha}{\sin 45} + \sin(45+\alpha) + \frac{b}{2d}\left\{\frac{\sin\alpha}{\sin 45} - \cos(45+\alpha)\right\} + \frac{2\omega}{b\sin\alpha} + \frac{\cos 2\alpha}{\sin\alpha}\right\} \qquad 4.29$$

The magnetostatic energy per unit length is given by

$$\frac{2}{1+\mu^2}\, 1{\cdot}7\, I_s^2 \sin^2\delta\, d\, t$$

In this case however the value of δ is not the same for adjacent domains, but α and $(90+\alpha)$ alternately. As an approximation for the magnetostatic energy a value for $\sin\delta$ of $\frac{\sin\alpha + \sin(90+\alpha)}{2}$ will be used. The magnetostatic energy per unit length is now

$$\frac{2}{1+\mu^2}\cdot 1{\cdot}7\, I_s^2\,(\sin\alpha + \cos\alpha)^2\, d\, t$$

$$= \frac{1{\cdot}7\, I_s^2\, d\, t\,(1+\sin 2\alpha)}{2(1+\mu^2)} \qquad 4.30$$

Magnetostrictive energy is involved in the closure domains magnetised in [010] directions, i.e. at right angles to the main domains. The volumes involved are BCDE and equivalent parts of the other patterns.

The volume of BCDE is $d^2 t\left\{\frac{\sin\alpha}{\sin 45} - \frac{1}{2}\cos(45+\alpha)\right\}\sin(45+\alpha)$ 4.31

and the increase in volume of domains magnetised in [010] directions per pair of closure domains is volume CDEH which is equal to $d^2 t\left\{\frac{\sin\alpha}{\sin 45} - \cos(45+\alpha)\right\}\sin(45+\alpha)$ 4.32

The total volume magnetised in [010] directions per echelon pattern is

$$\frac{n}{2}\,(2.\ \text{volume BCDE} + (n-1)\ \text{volume CDEH})$$

$$= \frac{nd^2t}{2}\,\frac{\sin(45+\alpha)\sin\alpha}{\sin 45} + \frac{n^2d^2t}{2}\left\{\frac{\sin\alpha\sin(45+\alpha)}{\sin 45} - \frac{\cos 2\alpha}{2}\right\} \qquad 4.33$$

This must be multiplied by 2/D to obtain the volume per unit length. Then substituting n = D/2d and multiplying by $\frac{\lambda_{100}^2 c_{11}}{2}$ to obtain the magnetostrictive energy per unit length, we get

$$\frac{\lambda_{100}^2 c_{11} t}{8}\left\{\frac{2d\sin\alpha\sin(45+\alpha)}{\sin 45} + b\left\{\frac{\sin\alpha\sin(45+\alpha)}{\sin 45} - \frac{\cos 2\alpha}{2}\right\}\right\} \qquad 4.34$$

for this energy contribution.

The magnetoelastic energy per unit volume due to the applied stress is $-\frac{3\lambda_{100}\sigma\cos^2\alpha}{2}$ for the main domains and the part of the echelon structure magnetised in [100] directions, and $-\frac{3\lambda_{100}\sigma\sin^2\alpha}{2}$ for the remaining parts of the echelon structure magnetised in [010] directions. The volume per unit length of the closure domains magnetised in [010] directions is

$$\frac{dt\sin\alpha\sin(45+\alpha)}{2\sin 45} + \frac{bt}{4}\left\{\frac{\sin\alpha\sin(45+\alpha)}{\sin 45} - \frac{\cos 2\alpha}{2}\right\}$$

Therefore the magnetoelastic energy of these domains per unit length is

$$-\frac{3\sigma\lambda_{100}t}{8}\sin^2\alpha\left\{\frac{2d\sin\alpha\sin(45+\alpha)}{\sin 45} + b\left\{\frac{\sin\alpha\sin(45+\alpha)}{\sin 45} - \frac{\cos 2\alpha}{2}\right\}\right\} \qquad 4.35$$

The volume per unit length of domains magnetised in [100] directions is

$$vt - \left\{\frac{dt\sin\alpha\sin(45+\alpha)}{2\sin 45} + \frac{bt}{4}\left\{\frac{\sin\alpha\sin(45+\alpha)}{\sin 45} - \frac{\cos 2\alpha}{2}\right\}\right\}$$

Therefore the magnetoelastic energy of these domains per

unit length is

$$-\frac{3\sigma\lambda_{100}t}{8}\cos^2\alpha\left\{4\omega-\frac{2d\sin\alpha\sin(45+\alpha)}{\sin 45}+b\left\{\frac{\sin\alpha\sin(45+\alpha)}{\sin 45}-\frac{\cos 2\alpha}{2}\right\}\right\} \qquad 4.36$$

The total magnetoelastic energy per unit length is

$$-\frac{3\sigma\lambda_{100}t}{8}\left\{4\omega\cos^2\alpha-\cos 2\alpha\left\{2d\frac{\sin\alpha\sin(45+\alpha)}{\sin 45}+b\left\{\frac{\sin\alpha\sin(45+\alpha)}{\sin 45}-\frac{\cos 2\alpha}{2}\right\}\right\}\right\} \qquad 4.37$$

Summing all these energy terms gives the total energy per unit length as $E_t =$

$$\begin{aligned}
&\frac{\gamma_{100}t}{2}\left\{\frac{\sin\alpha}{\sin 45}+\sin(45+\alpha)+\frac{b}{2d}\left\{\frac{\sin\alpha}{\sin 45}-\cos(45+\alpha)\right\}+\frac{2\omega}{b\sin\alpha}+\frac{\cos 2\alpha}{2}\right\}\\
&+\frac{1\cdot7\,d\,t\,I_s^2}{2(1+\mu^2)}(1+\sin 2\alpha)\\
&+\frac{\lambda_{100}^2 c_{11}t}{8}\left\{\frac{2d\sin\alpha\sin(45+\alpha)}{\sin 45}+b\left\{\frac{\sin\alpha\sin(45+\alpha)}{\sin 45}-\frac{\cos 2\alpha}{2}\right\}\right\} \qquad 4.38\\
&-\frac{3\sigma\lambda_{100}t}{8}\left\{4\omega\cos^2\alpha-\cos 2\alpha\left\{\frac{2d\sin\alpha\sin(45+\alpha)}{\sin 45}+b\left\{\frac{\sin\alpha\sin(45+\alpha)}{\sin 45}-\frac{\cos 2\alpha}{2}\right\}\right\}\right\}
\end{aligned}$$

This equation contains both D, the main domain spacing, and d, the echelon domain spacing. To obtain the equilibrium spacing differentiate it with respect to each of these quantities separately and equate to zero to obtain the value of them at the energy minimum.

For D this gives:

$$\begin{aligned}
0=&\frac{\gamma_{100}t}{2}\left\{\frac{1}{2d}\left\{\frac{\sin\alpha}{\sin 45}-\cos(45+\alpha)\right\}-\frac{2\omega}{b_0^2\sin\alpha}\right\}+\frac{\lambda_{100}^2 c_{11}t}{8}\left\{\frac{\sin\alpha\sin(45+\alpha)}{\sin 45}-\frac{\cos 2\alpha}{2}\right\}\\
&+\frac{3\lambda_{100}\sigma t}{8}\cos 2\alpha\left\{\frac{\sin\alpha\sin(45+\alpha)}{\sin 45}-\frac{\cos 2\alpha}{2}\right\}
\end{aligned} \qquad 4.39$$

$$\begin{aligned}
\therefore\frac{1}{b_0^2}=&\frac{\sin\alpha}{\omega\gamma_{100}}\left\{\frac{\gamma_{100}}{4d}\left\{\frac{\sin\alpha}{\sin 45}-\cos(45+\alpha)\right\}\right.\\
&\left.+\frac{\lambda_{100}}{8}\left\{\frac{\sin\alpha\sin(45+\alpha)}{\sin 45}-\frac{\cos 2\alpha}{2}\right\}(\lambda_{100}c_{11}+3\sigma\cos 2\alpha)\right\}
\end{aligned} \qquad 4.40$$

$$\therefore \frac{1}{D_0^2} = \frac{A \sin\alpha}{4\omega d} + \frac{B \sin\alpha}{\omega \gamma_{150}} \qquad 4.41$$

where $A = \dfrac{\sin\alpha}{\sin 45} - \cos(45+\alpha)$

$$B = \frac{\lambda_{100}}{8}\left\{\frac{\sin\alpha \sin(45+\alpha)}{\sin 45} - \frac{\cos 2\alpha}{2}\right\}(\lambda_{100} c_{11} + 3\sigma\cos 2\alpha)$$

For d this gives:

$$0 = \frac{\gamma_{150} t}{2}\left\{-\frac{D}{2d_0^2}\left\{\frac{\sin\alpha}{\sin 45} - \cos(45+\alpha)\right\}\right\} + \frac{1.7\, t I_s^2 (1+\sin 2\alpha)}{2(1+\mu^2)} \qquad 4.42$$

$$+ \frac{\lambda_{100}^2 c_{11} t}{4}\frac{\sin\alpha \sin(45+\alpha)}{\sin 45} + \frac{3\sigma\lambda_{100} t}{4}\frac{\sin\alpha \sin(45+\alpha)\cos 2\alpha}{\sin 45}$$

$$\therefore \frac{1}{d_0^2} = \frac{4}{D\gamma_{150}}\left\{\frac{\sin\alpha}{\sin 45} - \cos(45+\alpha)\right\}^{-1/2}\left\{\frac{1.7 I_s^2 (1+\sin 2\alpha)}{2(1+\mu^2)}\right. \qquad 4.43$$

$$\left. + \frac{\lambda_{100}\sin\alpha \sin(45+\alpha)(\lambda_{100} c_{11} + 3\sigma\cos 2\alpha)}{4\sin 45}\right\}$$

$$\therefore \frac{1}{d_0^2} = \frac{4}{D\gamma_{150}} \cdot \frac{C}{\sqrt{A}} \qquad 4.44$$

where $C = \dfrac{1.7 I_s^2 (1+\sin 2\alpha)}{2(1+\mu^2)} + \dfrac{\lambda_{100}\sin\alpha \sin(45+\alpha)(\lambda_{100} c_{11} + 3\sigma\cos 2\alpha)}{4\sin 45}$

Solving equations 4.41 and 4.44 for D and d gives

$$\frac{D_0^4 B \sin^2\alpha}{\omega^2 \gamma_{150}} - \frac{D^3 C A^{3/2} \sin^2\alpha}{4\omega^2 \gamma_{150}} - \frac{2 D_0^2 B \sin\alpha}{\omega \gamma_{150}} + 1 = 0 \qquad 4.45$$

$$\frac{d_0^4 B \sin\alpha}{\gamma_{150}} + \frac{d_0^3 A \sin\alpha}{4} - \frac{A\omega\gamma_{150}^2}{16 c^2} = 0 \qquad 4.46$$

Solving these equations for the whisker in plate 4.1 with the previously given values for the orientation and width gives

$D_0 = 4.6\times10^{-3}$cm ; $d_0 = 4.55\times10^{-4}$cm.

The measured value of D_0 is 9.8×10^{-3}cm and the predicted value above agrees quite well with this, compared with the previously described systems. The value of d_0 is also quite

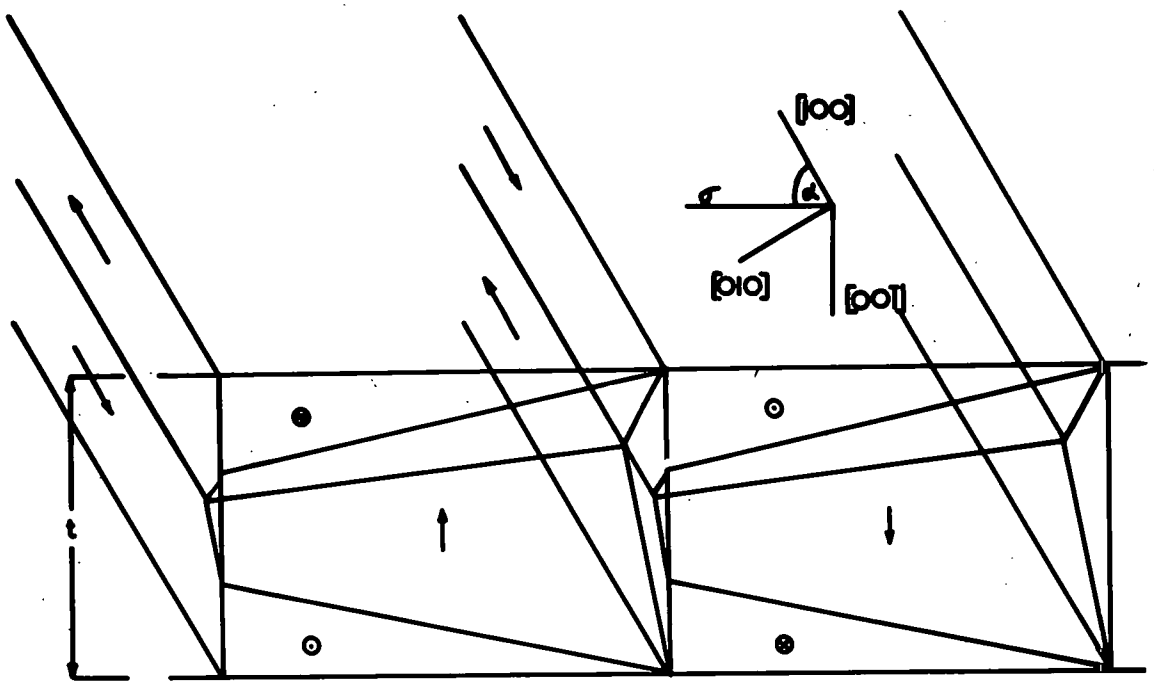

a) CLOSURE STRUCTURE AT ONE EDGE OF A WHISKER

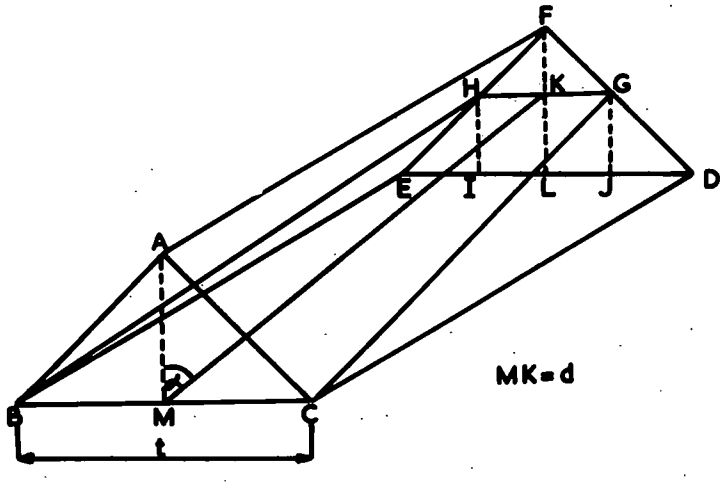

b) DETAIL OF ONE CLOSURE DOMAIN

FIG 4·8

good, being a factor of 2 out. This calculated value means there are five complete echelons across each main domain. Observations on the actual whisker however do not give this number, four being the maximum observed. The photographs show that the echelon strucure does not in fact extend right across the main domains, and in view of this the theory cannot be accurate for the whisker considered. The value of D_o for the whisker in plate 4.2a as calculated is 1.9×10^{-3}cm. The actual value is 4.1×10^{-3}cm, so there is again the factor of 2 between theory and observation. This is possibly due to the magnetostatic energy term. This has a large effect on the energy of the system and a small change in this can alter considerably the position of the energy minimum, so that the approximation made in this term could give this discrepancy.

This structure then appears to explain the structure in the whisker shown in plate 4.1, despite the fact that the structure is not a perfect echelon structure.

4.2.4 Single Closure Domain Magnetised in the [001] Direction

Instead of the closure structure being magnetised in a direction parallel to the top of the whisker, as in the previous type of structure considered, it is, in this section, magnetised in a direction perpendicular to the top and bottom surfaces of the whisker. The structure is as shown in fig 4.8, assuming that the whisker has a rectangular cross-section. This type

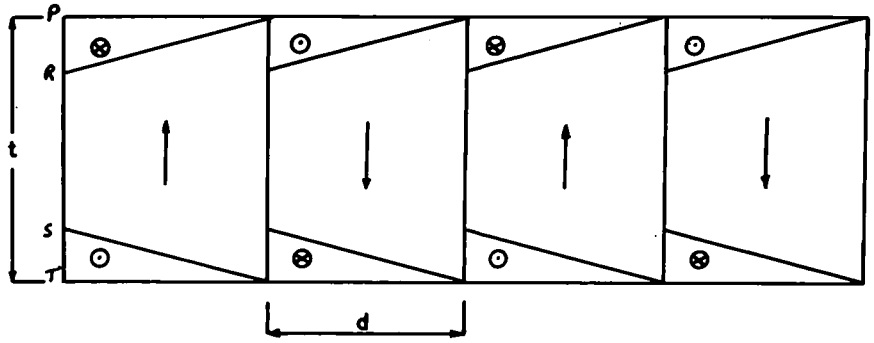

a)

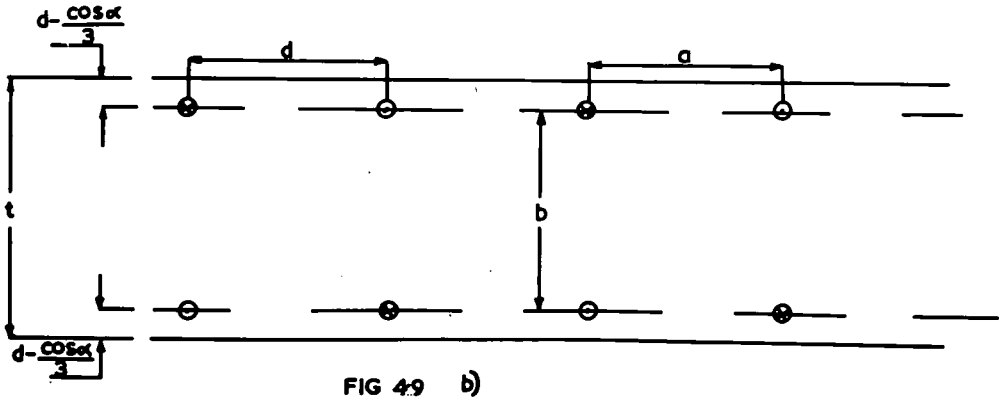

FIG 4·9 b)

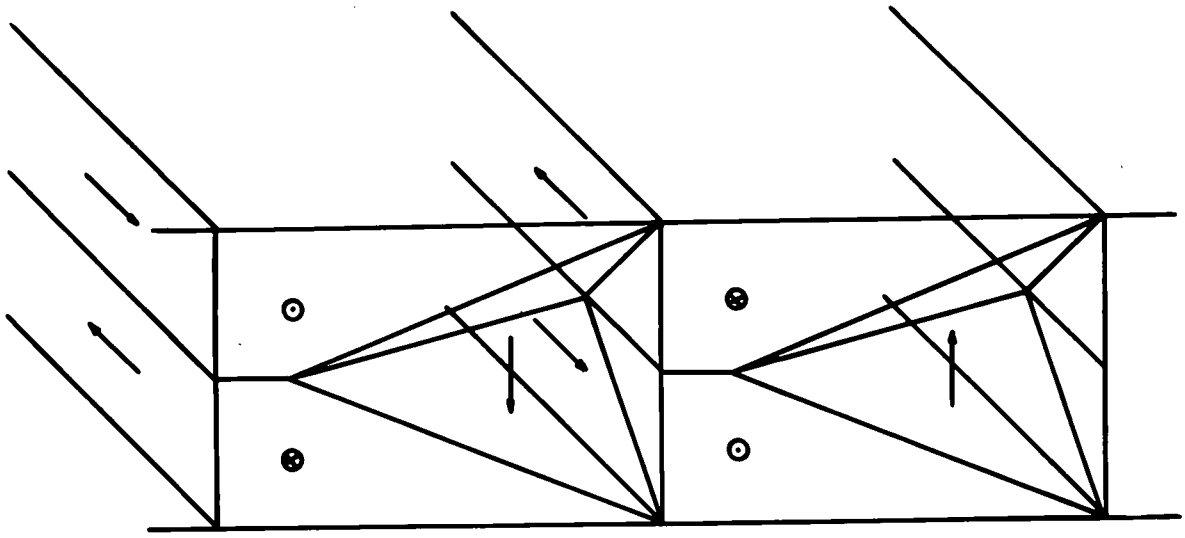

a)

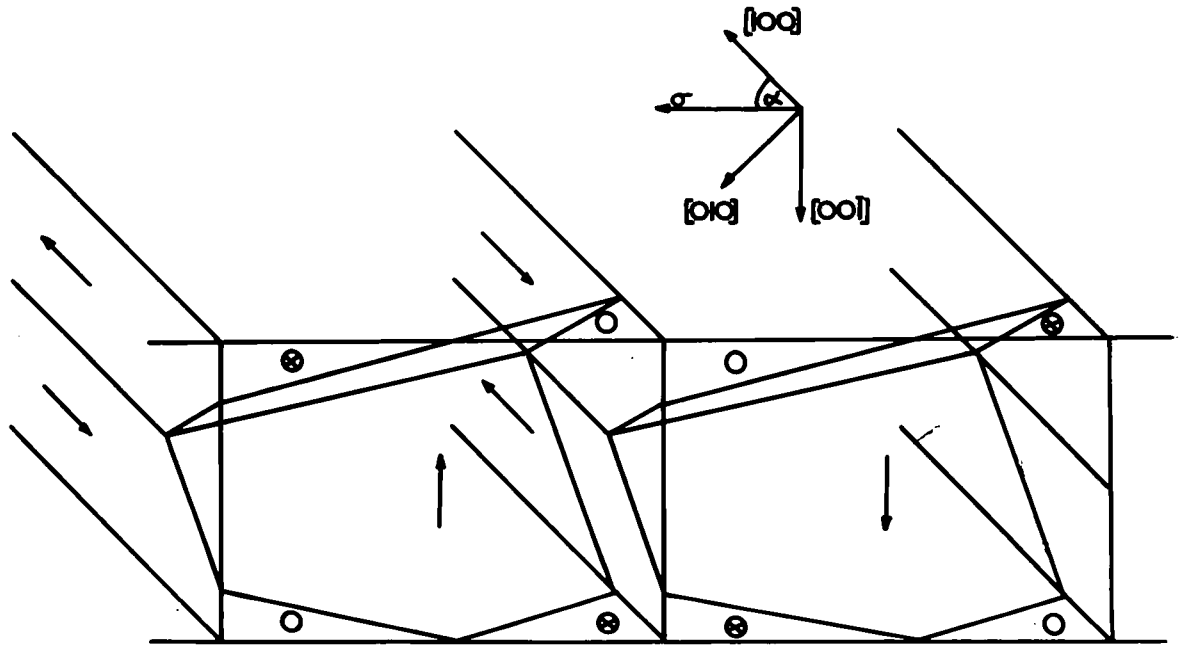

b)

FIG 4·10 CLOSURE STRUCTURES AT WHISKER EDGE

of pattern has a limiting size when the two triangular areas of free pole on the whisker sides just touch, i.e. R and S in fig 4.9a are the same point. The length PR is given by $PQ\cos\alpha$, and the limit is when $2PR = PT$, i.e. $2d\cos\alpha = t$. Above this limit the pattern must be altered to either of the structures shown in fig 4.10, and it is not obvious which of thesestwo types will occur. The interaction of areas of free pole on the side with similarly situated areas is greater than the interaction between areas on the side with areas on the top for equal values of the component of magnetisation on these areas. However the magnetisation vector for the top areas of free pole is normal to the surface, while that for the sides is at an angle α to the surface. There will,in any given case, be a minimum energy configuration, but this can only be determined in each case by detailed calculation and not by simple inspection.

In a practical case it should be possible to determine which of these two patterns is present from the colloid deposits. As there will be free poles at the surface, the colloid collects over these regions and areas of heavy deposit will appear enabling the two types of structure to be detected and distinguished.

In the following section only the simple case of fig 4.8 which does not exceed the limit will be considered, as this

structure is the most amenable to calculation for the general case.

To obtain the equilibrium pattern size it is necessary to find the total energy and then minimise this. The energy contributions are wall, magnetostatic, magnetostrictive, and magnetoelastic energy.

The wall structure consists of 90° walls in the closure structure and 180° walls between the main domains.

The area of 90° wall per main domain is

$$2(ABC - FGH + ACGF + ABHF)$$

$$= \frac{t^2}{2} - \left\{\frac{t^2}{2} - 2dt\cos\alpha + 2d^2\cos^2\alpha\right\} + \frac{t}{\cos 45}\left\{1 + \frac{t - 2d\cos\alpha}{t}\right\} d\sin\alpha$$

$$= 2dt\cos\alpha - 2d^2\cos^2\alpha + \frac{2dt\sin\alpha}{\cos 45} - \frac{d^2\sin 2\alpha}{\cos 45} \qquad 4.47$$

The area of 180° wall per main domain is

(main domain side wall $-$ 90° part of side wall + main domain middle wall)

$$= \frac{\omega t}{\sin\alpha} - 2dt\cos\alpha + 2d^2\cos^2\alpha + d\sin\alpha\left\{\frac{\omega}{\sin\alpha} - t + d\cos\alpha\right\}$$

$$= \frac{\omega t}{\sin\alpha} - 2dt\cos\alpha + 2d^2\cos^2\alpha + d\omega - dt\sin\alpha + d^2\sin\alpha\cos\alpha \qquad 4.48$$

Taking $2\gamma_{90} = \gamma_{180}$ then :

Total wall energy per main domain is

$$\gamma_{180}\left\{\omega d + \frac{\omega t}{\sin\alpha} + d^2\cos^2\alpha - dt\cos\alpha + (\sqrt{2}-1)\left\{dt\sin\alpha - \frac{d^2\sin 2\alpha}{2}\right\}\right\} \qquad 4.49$$

Then wall energy per unit length is

$$\gamma_{180}\left\{\omega + \frac{\omega t}{d\sin\alpha} + d\cos^2\alpha - t\cos\alpha + (\sqrt{2}-1)\left\{t\sin\alpha - \frac{d\sin 2\alpha}{2}\right\}\right\} \qquad 4.50$$

The magnetostrictive energy appears in the closure domains. The volume of the closure domains per unit length is

$$\frac{2}{d}\left\{\frac{ABC-FGH}{2}\right\}CD = \left\{\frac{t^2}{2} - dt\cos\alpha + d^2\cos^2\alpha\right\}\sin\alpha$$

The magnetostrictive energy per unit length is

$$\frac{\lambda_{100}^2 C_{11}}{2}\left\{\frac{t^2\sin\alpha}{2} - \frac{dt\sin 2\alpha}{2} + \frac{d^2\cos\alpha\sin 2\alpha}{2}\right\} \qquad 4.51$$

The magnetoelastic energy is given in chapter one as

$$-\frac{3\sigma}{2}\left[\lambda_{100}(\alpha_1^2\gamma_1^2 + \alpha_2^2\gamma_2^2 + \alpha_3^2\gamma_3^2) + 2\lambda_{111}(\alpha_1\alpha_2\gamma_1\gamma_2 + \alpha_2\alpha_3\gamma_2\gamma_3 + \alpha_3\alpha_1\gamma_3\gamma_1)\right]$$

where $[\alpha_1\alpha_2\alpha_3]$ are the direction cosines of the magnetisation and $[\gamma_1\gamma_2\gamma_3]$ are the direction cosines of the applied stress. In this case the main domains have [100], the closure domains [001] as the direction cosines fot the magnetisation, while the stress has direction cosines $[\cos\alpha, \sin\alpha, 0]$.
The magnetoelastic energy of the main domains per unit volume is therefore $-\frac{3}{2}\sigma\lambda_{100}\cos^2\alpha$

and the magnetoelastic energy of the closure domains is zero. The volume of the main domains per unit length is

$$\omega t - \left\{\frac{t^2\sin\alpha}{2} - \frac{dt\sin 2\alpha}{2} + \frac{d^2\cos\alpha\sin 2\alpha}{2}\right\}$$

Therefore the magnetoelastic energy per unit length is

$$-\frac{3}{2}\sigma\lambda_{100}\cos^2\alpha\left\{\omega t - \left\{\frac{t^2\sin\alpha}{2} - \frac{dt\sin 2\alpha}{2} + \frac{d^2\cos\alpha\sin 2\alpha}{2}\right\}\right\} \qquad 4.52$$

The exact calculation of the magnetostatic energy is difficult and tedious in this case, and so an approximation

replacing each triangular area of free pole by a point pole equal in magnitude to the total pole in the triangle will be used. The point pole is regarded as being at the centre of gravity of the triangle it replaces. We therefore have the situation illustrated in fig 4.9b of a collection of point poles on a regular lattice. To obtain the energy of this system, the potential at one pole due to all the others is calculated and then multiplied by the pole strength under consideration. This result is then multiplied by $\frac{4}{a(1+\psi^2)}$ to obtain the energy per unit length for a rectangular crystal.

Ignoring the self energy, the potential at Z due to all the other poles is

$$-2\left\{\frac{P}{a}-\frac{P}{2a}+\frac{P}{3a}\cdots\cdots\frac{(-1)^{n+1}P}{na}+\frac{P}{2b}-\frac{P}{\sqrt{a^2+b^2}}+\frac{P}{\sqrt{(2a)^2+b^2}}-\frac{P}{\sqrt{(3a)^2+b^2}}\cdots\frac{(-1)^n P}{\sqrt{(na)^2+b^2}}\right\}$$

where P is the pole strength at each point, and a and b are the lattice constants as shown in fig 4.9b.

Therefore the potential at Z is

$$-\left\{\frac{2P}{a}\sum_{1}^{\infty}\frac{(-1)^{n+1}}{n}+\frac{P}{b}\cdot 2P\sum_{1}^{\infty}\frac{(-1)^n}{\sqrt{(na)^2+b^2}}\right\} \qquad 4.53$$

The first term, $\frac{2P}{a}\sum_{1}^{\infty}\frac{(-1)^{n+1}}{n}=\frac{2P}{a}\log_e 2$

To evaluate the third term it is written as

$$2P\sum\frac{(-1)^n}{na}\left\{1+\frac{b^2}{n^2a^2}\right\}^{-1/2}$$

and then expanded to

$$2P\sum_{1}^{\infty}\frac{(-1)^n}{na}\left\{1-\frac{1}{2}\frac{b^2}{(na)^2}+\frac{1}{2}\cdot\frac{3}{2}\cdot\frac{1}{2!}\frac{b^4}{(na)^4}-\frac{1}{2}\cdot\frac{3}{2}\cdot\frac{5}{2}\cdot\frac{1}{3!}\frac{b^6}{(na)^6}\cdots\right\}$$

$$= 2\rho \sum_{1}^{\infty} \left\{ \frac{(-1)^n}{na} - \frac{1}{2}\frac{(-1)^n b^2}{(na)^3} + \frac{3}{8}\frac{(-1)^n b^4}{(na)^5} - \frac{5}{16}\frac{(-1)^n b^6}{(na)^7} \cdots \right\}$$

Since a > b, terms of higher order than the fifth can be neglected.

The expansion then becomes

$$2\rho \sum_{1}^{\infty} \left\{ \frac{1}{a}\frac{(-1)^n}{n} - \frac{1}{2}\frac{b^2}{a^3}\frac{(-1)^n}{n^3} + \frac{3}{8}\frac{b^4}{a^5}\frac{(-1)^n}{n^5} - \frac{5}{16}\frac{b^6}{a^7}\frac{(-1)^n}{n^7} + \frac{35}{128}\frac{b^8}{a^9}\frac{(-1)^n}{n^9} \cdots \right\}$$

$$\sum_{1}^{\infty} \frac{(-1)^n}{n} = -\log_e 2 \quad ; \quad \sum_{1}^{\infty} \frac{(-1)^n}{n^p} = \left(1 - \frac{2}{2^p}\right) \zeta(p)$$

where $\zeta(p)$ is the Reimmann Zeta function. Obtaining values for this Zeta function from tables gives the value of the third term in equation 4,53 as

$$2\rho \left\{ -\frac{1}{a}\log_e 2 + \frac{1}{a}\left\{ 0{\cdot}4508\frac{b^2}{a^2} - 0{\cdot}3645\frac{b^4}{a^4} + 0{\cdot}3102\frac{b^6}{a^6} - 0{\cdot}2729\frac{b^8}{a^8} \cdots \right\} \right\}$$

Substituting back in equation 4.53 gives the potential at Z as

$$-\rho \left\{ \frac{1}{b} + \frac{2}{a}\left\{ 0{\cdot}4508\frac{b^2}{a^2} - 0{\cdot}3645\frac{b^4}{a^4} + 0{\cdot}3102\frac{b^6}{a^6} - 0{\cdot}2729\frac{b^8}{a^8} \right\} \right\} \qquad 4.54$$

We have $a = d$, $b = t - \frac{2d\cos\alpha}{3} = t - kd$, and $P = \frac{Id^2 \sin 2\alpha}{4}$.

Substituting for a and b gives the potential at Z as

$$-\rho \left\{ \frac{1}{t-kd} + \frac{2}{d}\left\{ 0{\cdot}4508\left(\frac{t}{d}-k\right)^2 - 0{\cdot}3645\left(\frac{t}{d}-k\right)^4 + 0{\cdot}3102\left(\frac{t}{d}-k\right)^6 - 0{\cdot}2729\left(\frac{t}{d}-k\right)^8 \right\} \right\}$$

$$= -\rho \left\{ \frac{1}{t-kd} + \frac{2}{d}\left\{ Q_0 + Q_1\frac{t}{d} + Q_2\frac{t^2}{d^2} + Q_3\frac{t^3}{d^3} + Q_4\frac{t^4}{d^4} + Q_5\frac{t^5}{d^5} + Q_6\frac{t^6}{d^6} + Q_7\frac{t^7}{d^7} + Q_8\frac{t^8}{d^8} \right\} \right\} \qquad 4.55$$

where Q_0 etc. are appropriate coefficients as given below.

$$Q_0 = 0.4508k^2 - 0.3645k^4 + 0.3102k^6 - 0.2729k^8$$

$$Q_1 = -0.9016k + 1.4580k^3 - 1.86k^5 + 2.18k^7$$

$$Q_2 = 0.4508 - 2.187k^2 + 4.653k^4 - 7.65k^6$$

$$Q_3 = 1.458k - 6.204k^3 + 15.3k^5$$

$$Q_4 = -0.3645. + 4.653k^2 - 19.1k^4$$

$$Q_5 = -1.8612k + 15.3k^3$$

$$Q_6 = 0.3102 + 7.65k^2$$

$$Q_7 = 2.18k$$

$$Q_8 = -0.2729$$

The magnetostatic energy per unit length is now

$$-\frac{4\rho}{d(1+\mu^2)}\cdot\rho\left\{\frac{1}{t-kd}+\frac{2}{d}\left\{Q_0+Q_1\frac{t}{d}+Q_2\frac{t^2}{d^2}+Q_3\frac{t^3}{d^3}+Q_4\frac{t^4}{d^4}+Q_5\frac{t^5}{d^5}+Q_6\frac{t^6}{d^6}+Q_7\frac{t^7}{d^7}+Q_8\frac{t^8}{d^8}\right\}\right\}$$

$$=-\frac{I_s^2 sin^2 2\alpha}{4(1+\mu^2)}\left\{\frac{d^3}{t-kd}+2\left\{Q_0d^2+Q_1dt+Q_2t^2+Q_3\frac{t^3}{d}+Q_4\frac{t^4}{d^2}+Q_5\frac{t^5}{d^3}+Q_6\frac{t^6}{d^4}+Q_7\frac{t^7}{d^5}+Q_8\frac{t^8}{d^6}\right\}\right\} \qquad 4.56$$

$$=-\frac{I_s^2 sin^2 2\alpha}{4(1+\mu^2)}\left\{\frac{d^3}{t-kd}+2f(d)\right\} \qquad 4.57$$

The self energy of each area is given by

$$\frac{1}{2}\cdot\frac{4\pi\rho^2}{(1+\mu^2)}\cdot 2$$

In the above derivation of the magnetostatic energy, the potential at the reference point has been taken as negative for opposite poles and positive for like poles. In calculating a value for the self energy we are concerned with the interaction of like poles, so the potential is positive, i.e. the field

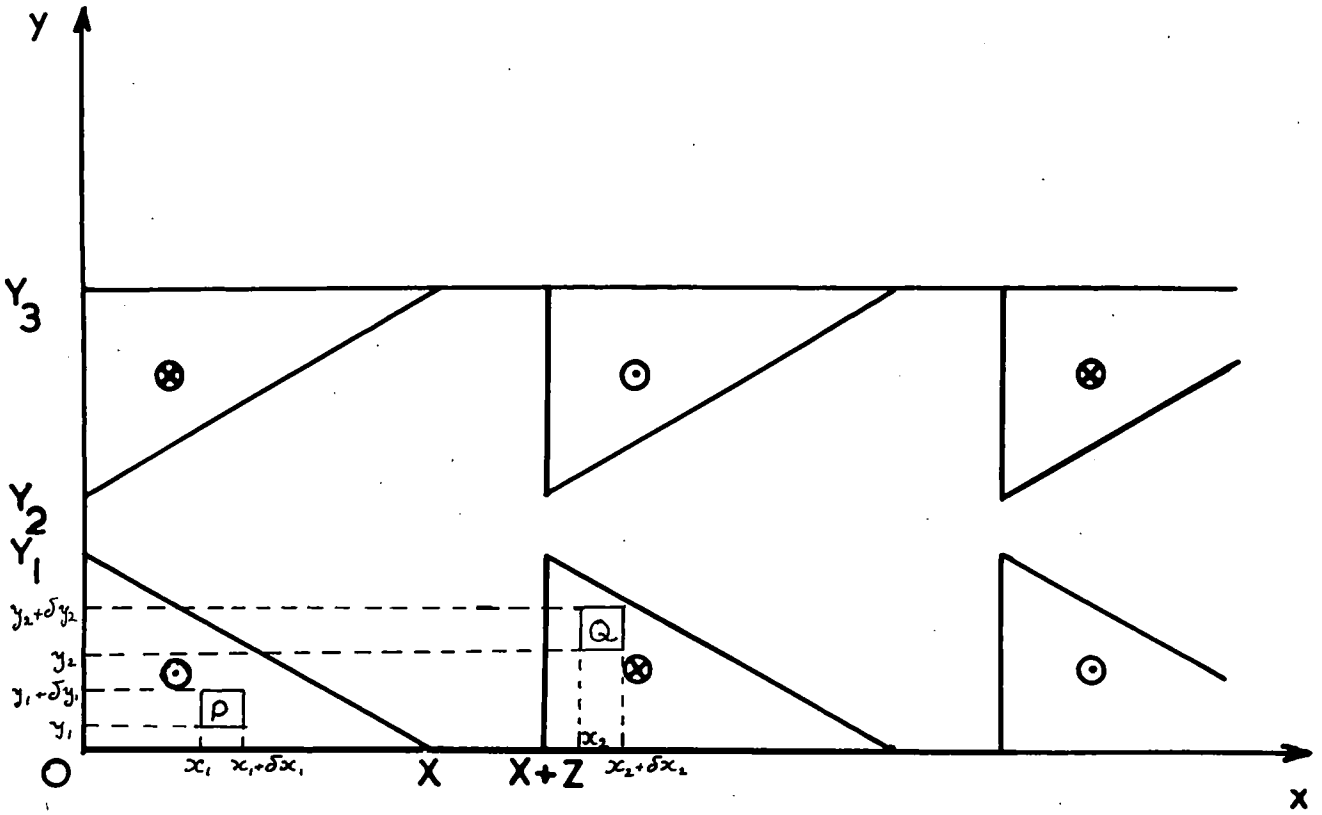

FIG 4.11 Surface domain pattern used in computer calculation of magnetostatic energy

direction at Z due to its own field is opposite to the field due to the neighbouring poles. Using this sign convention employed in equation 4.53 onwards, the self energy per unit length becomes $+\frac{2\pi I_s^2 d^3 \sin^2 2\alpha}{(1+\mu^2)}$

The total magnetostatic energy per unit length is

$$\frac{I_s^2 \sin^2 2\alpha}{4(1+\mu^2)} \left\{ d^3 \left\{ 8\pi - \frac{1}{1-kd} \right\} - 2\beta(d) \right\} \qquad 4.58$$

Despite the fact that the above treatment is crude it gives quite an accurate value for the magnetostatic energy. To check its accuracy, intrgrations to find an accurate value for magnetostatic energy were carried out on a computer. This allows the interactions between any two of the areas of pole to be calculated. The individual interactions then have to be summed to get a value for the total energy of the system.

The computer was used to obtain an arithmetical solution for the magnetostatic energy contribution of a whisker of known size and orientation. The interaction between the two elemental areas of pole, P and Q, along the whisker side, shown in fig 4.11, is given by

$$\frac{I_s^2 \, dx_1 \, dx_2 \, dy_1 \, dy_2}{\left[(x_2-x_1)^2 + (y_2-y_1)^2\right]^{1/2}}$$

The total interaction between the areas of free pole is

$$\pm I_s^2 \int_0^{x} \int_{x+z_1}^{2x+z_1} \int_0^{y_1-Mx_1} \int_0^{y_1-Mx_2} \frac{dx_1 \, dx_2 \, dy_1 \, dy_2}{\left[(x_2-x_1)^2 + (y_2-y_1)^2\right]^{1/2}} \qquad 4.59$$

where X_2 Y_2 Z_2 are as shown in fig 4.11, and $M = Y_1/X$, the expression having either a positive or negative sign depending on whether the areas have like or unlike polarity.

For the interaction between areas of free pole along the top edge with areas along the bottom edge, the expression to be integrated is the same as that in equation 4.59, but the limits of integration have to be changed, and the interaction for these is

$$\pm I_s^2 \int_0^X \int_{x+2_1}^{2x+2_1} \int_0^{Y_1 - Mx_1} \int_{Y_2+Mx_2}^{Y_3} \frac{dx_1\,dx_2\,dy_1\,dy_2}{\left[(x_2-x_1)^2+(y_2-y_1)^2\right]^{1/2}} \qquad 4.60$$

These two expressions for the interactions can be generallised to take account of all areas along the whisker edge to give the following

$$\pm I_s^2 \int_0^X \int_{\rho(x+2_1)}^{\rho(x+2_1)+X} \int_0^{Y_1 - Mx_1} \int_0^{Y_1 - Mx_2} \frac{dx_1\,dx_2\,dy_1\,dy_2}{\left[(x_2-x_1)^2+(y_2-y_1)^2\right]^{1/2}} \qquad 4.61a$$

$$\pm I_s^2 \int_0^X \int_{\rho(x+2_1)}^{\rho(x+2_1)+X} \int_0^{Y_1 - Mx_2} \int_{Y_2+Mx_2}^{Y_3} \frac{dx_1\,dx_2\,dy_1\,dy_2}{\left[(x_2-x_1)^2+(y_2-y_1)^2\right]^{1/2}} \qquad 4.61b$$

where $p = 0,1,2$, etc. to specify which two areas are being considered. The case of $p = 0$ in equation 4.61a corresponds to the interaction of an area of free pole with itself, and provided the case where $x_1 = x_2$ and $y_1 = y_2$ is ignored by the computer, i.e. the interaction of one elemental area with itself but not with the rest of the main area is discounted, provides a value for the self energy of one of the areas of free pole.

These expressions were then solved numerically using

Simpsons Rule for a particular set of values of X, Y_1 Y_2 Y_3 and Z_1, and a range of values for p from zero upwards, until, considering subsequent areas, the contribution was reduced to about 1% of its value at p = 1. This was found to occur at p = 10, so in future calculations a range of p from 0 to 10 was used. These results for these areas were then summed taking account of the alternating sign of the interaction as the sign of the free pole changed (fig 4.9). The result of this was then multiplied by

$$\frac{1}{d} \cdot 4\mu^2\beta \cdot \frac{2 \cdot 2}{2} \cdot \frac{2}{(1+\mu^2)} = \frac{4\mu^2\beta}{d(1+\mu^2)}$$

where d is the domain separation, β is the angle the magnetisation makes with the surface normal, and the other factors of two are to account for two layers of pole along each edge, two sides to the whisker, and to prevent use of an area as both source and affected area. This then gives a value for the magnetostatic energy per unit length of the whisker which can be compared with values obtained from other methods.

In the evaluation of the individual integrals, the use of Simpsons rule necessitates the division of the integral into a number of equal regions. For the subsequent calculations the integral has been divided into five parts. Trial evaluations of the integral were made using a larger number of parts, but the effect of doubling the number was only seen in the third or later sigificant figure for integrals with p = 1.

For the integral with $p = 0$ the change was about 10%. In view of these results and the amount of computer time needed to evaluate the integrals, it was decided to limit the division of the range over which the integral was performed into five parts.

For a particular system with $d = 10^{-2}$cm, $t = 6\times10^{-3}$cm, and β given by $\cos\beta = \frac{\cos 30}{3}$ i.e. $\beta = 73^{\circ}12'$, the value of magnetostatic energy obtained from equation 4.58 is 0.378 ergs/cm. Using a computer to calculate the energy for all areas up to a distance of 10d from the reference area gives a value of 0.4 ergs/cm. The difference between these two results is 5.5% and shows that the approximation using the centre of gravity of the areas is quite good in this case. The particular values used in this comparison are very near to the limit of the model, the separation between the apieces of the two triangles, i.e. the distance RS in fig 4.9a, is 2.26×10^{-4}cm. This result would be expected to show the largest discrepancy between the approximation and the computed result since the areas of pole are as close as possible giving a large interaction from the areas of free pole that are close together.

The expression for the total energy of the system is now

$$\gamma_{100}\left\{\omega + \frac{\omega t}{d\sin\alpha} + d\cos^2\alpha - t\cos\alpha + (J_2-1)\left\{t\sin\alpha - \frac{d\sin 2\alpha}{2}\right\}\right\}$$

$$+ \frac{I^2\sin^2 2\alpha}{4(1+\mu^2)}\left\{d^3\left\{8\pi - \frac{1}{(t-kd)}\right\} - 2f(d)\right\}$$

$$+ \frac{1}{2}\lambda_{100}^2 c_{11}\left\{\frac{t^2\sin\alpha}{2} - \frac{dt\sin\alpha}{2} + \frac{d^2\cos\alpha\sin 2\alpha}{2}\right\} \qquad 4.62$$

$$- \frac{3\sigma\lambda_{100}\cos^2\alpha}{2}\left\{\omega t - \left\{\frac{t^2\sin\alpha}{2} - \frac{dt\sin\alpha}{2} + \frac{d^2\cos\alpha\sin 2\alpha}{2}\right\}\right\}$$

This expression is then differentiated with respect to d and put equal to zero to obtain the energy minimum postion. If d_o is the equilibrium spacing then

$$0 = \gamma_{100}\left\{\cos^2\alpha - \frac{\omega t}{d_o^2\sin\alpha} - (J_2-1)\frac{\sin 2\alpha}{2}\right\}$$

$$+ \frac{I^2\sin^2 2\alpha}{4(1+\mu^2)}\left\{24\pi d_o^2 - \frac{3td_o^2 - 2kd_o^3}{(t-kd_o)^2} - \left\{4Q_0 d_o + 2tQ_1 - 2Q_2\frac{t^3}{d_o^2}\right.\right.$$

$$\left.\left. - 4Q_4\frac{t^4}{d_o^3} - 6Q_5\frac{t^5}{d_o^4} - 8Q_6\frac{t^6}{d_o^5} - 10Q_7\frac{t^7}{d_o^6} - 12Q_8\frac{t^8}{d_o^7}\right\}\right\} \qquad 4.63$$

$$+ \frac{1}{4}\lambda_{100}(2d_o\cos\alpha\sin 2\alpha - t\sin 2\alpha)(\lambda_{100}c_{11} + 3\sigma\cos^2\alpha)$$

Solving this equation for d_o gives the pattern spacing at equilibrium.

In view of the high orders of d_o that are present in equation 4.63, it is impossible to solve the equation directly. To obtain a value for d_o that corresponds to a minimum in the energy of the system, values for the left hand side of

equation 4.63were obtained for different values of d_o using a computer. The value for d_o necessary to satisfy the equation was found by plotting the results obtained from the computer against the value of d_o used, and reading of the value where the graph crossed the d_o axis going from negative to positive in the computer results, i.e. corresponding to a minimum in the expression for the total energy of the system.

No actual results on this structure were calculated however as it did not appear in any of the whiskers observed, and consequently there was no possibility of checking the theory against experimental results.

Calculations based on the above treatment to obtain a value for the equilibrium spacing have to be treated with a little care however to check whether the results obtained are consistent with the model used, With the obtained value for d_o, the depth of the triangular area on the whisker side should be calculated. The maximum value this can have for the above model to hold is t/2, i.e. half the thickness of the whisker. If it is found that this value is exceeded then the simple model is no longer applicable and further calculations should be carried out using a modification of this method, taking account of the possible patterns shown in fig 4.10.

4.3 Interpretation of Structures with Apparant Gaps in the Domain Wall Pattern

The structure under consideration in this section is shown

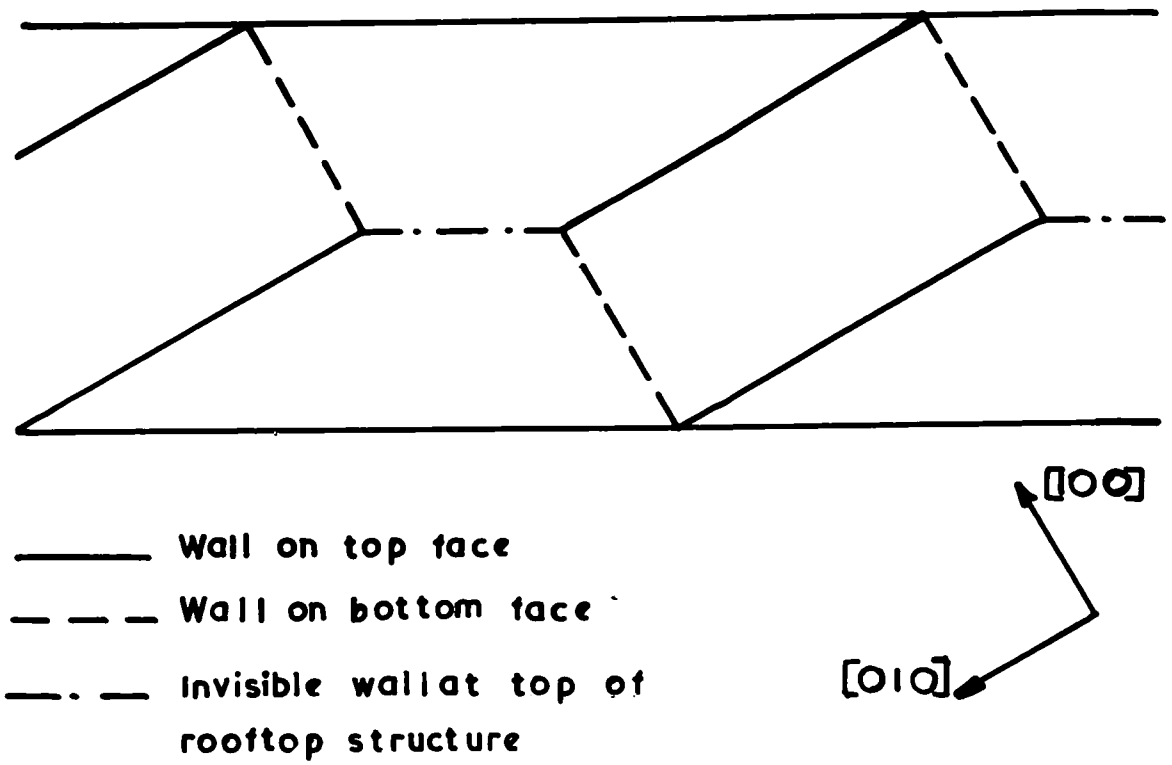

FIG 4·12 Register between walls on top and bottom faces of the whisker shown in plate 4·3

in plates 4.3 and 4.4. In plate 4.3 the structure on the top and bottom surfaces of a whisker under no applied stress are seen. On each of the surfaces the walls are along one of the easy directions of magnetisation. The walls appear to break and suffer a displacement along the whisker axis approximately at the centre of the whisker with no observable wall between, the two halves remaining parallel to each other and the other walls on their own face. If the top and bottom surfaces are compared, the walls are found to be at right angles to each other, i.e. in different easy directions of magnetisation, and also to be in register, the walls ending at the same point in the centre of the whisker and linking the start of one wall at the whisker edge to the break at the centre of the whisker of the next wall along (fig 4.12).

In plate 4.4 the same general type of structure can be seen on one surface of a different whisker. In this case however, the breaks in the walls do show up by a wall which collects colloid to a lesser extent than the rest of the walls, and there also appear to be sections of wall that are curved, instead of walls meeting at a sharp angle. For this whisker only the top surface was photographed as the effect upon this structure of appling a magnetic field along the axis was studied. The sequence of events as the magnetic field was applied is shown in plate 4.4.

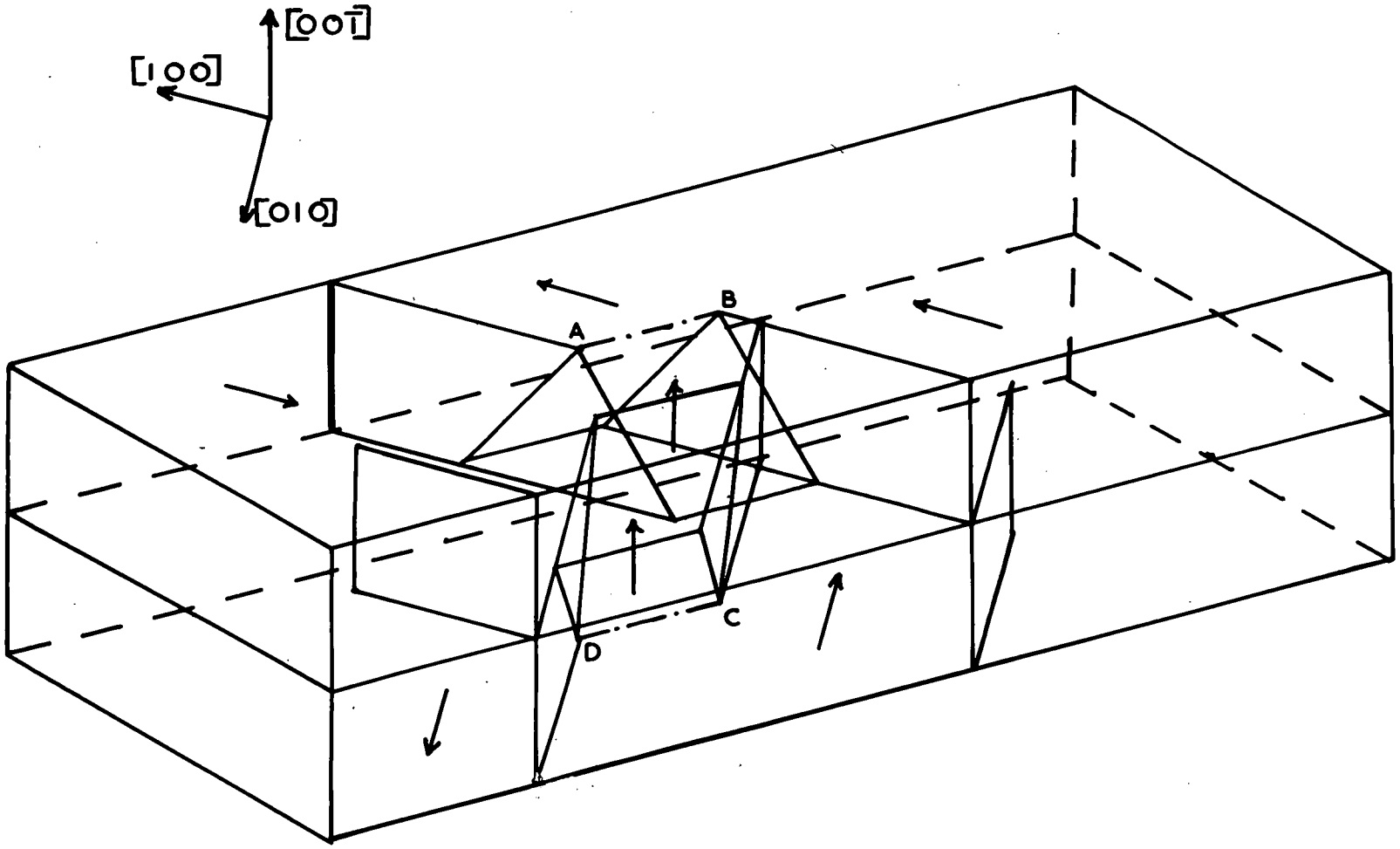

FIG 4-13 Internal domain arrangement showing simplified rooftop structures

The proposed structure to explain these observations on the two whiskers is shown in simplified form in fig 4.13. There is a main 190° wall running through the centre of the whisker in a plane parallel to the top and bottom faces of the whiskers dividing the whisker into two halves. The structures in the top and bottom halves are similar consisting of anti-parallel domains separated by 180° walls, the domains in the bottom being magnetised in the easy direction at right angles to the magnetisation direction occupied by the top domains. Providing a link between adjacent antiparallel main domains at the top and bottom, and also the structure at the top and bottom, are closure domains magnetised alternately up and down. These closure structures are essentially two roof-top shaped domains placed with their bases together, and the two sloping 90° walls between them and the main domains meet in a 'V' line structure in the whisker surface linking together the opposite halves of main domain wall. These are labelled AB and CD in fig 4.13. As these two 90° walls are of opposite rotation they give a much reduced field gradient at the surface and hence have only low rates of colloid deposition. In plate 4.3 they are invisible and in plate 4.4 show up as faint lines.

In the simplified structure shown in fig 4.13 there are areas of the bases of these rooftop structures where the normal component of magnetisation is not continuous and so one would

expect there to be free pole produced in these regions with an appropriate amount of magnetostatic energy. To counterbalance this energy increase and reduce the amount of free pole produced the walls in these regions become curved to improve the register between the two rooftop structures. Evidence for this curvature of the walls can be seen in plate 4.4 where the walls exhibit quite considerable bending in the region at the ends of the rooftop structures, where the free pole would be expected to appear. The increase in wall energy due to the wall being distorted is counteracted by the reduction in the magnetostatic energy due to the disappearance of most of the free pole.

The effect of an axial magnetic field on this structure, as seen in plate 4.4, follows from the above model if the movement of the walls is such that the closure structure moves at right angles to the whisker axis. Motion in this direction enables the main domains with a component in the same direction as the applied field along the whisker axis in both top and bottom halves of the whisker to grow at the expense of the others. The expected motion of the pattern is therefore the increase of alternate domains along the whisker axis with the movement of the 'V' line towards the whisker edge. This is initially observed in plate 4.4 before the structure is destroyed by the closure structures reaching the whisker edge and so this model seems to fit the observations quite well.

It was not possible to observe the effect of stress on these two whiskers, the one shown in plate 4.4 was too short and the pattern seen in plate 4.3 was accidently destroyed by bending the whisker during the operation of fixing the whisker into the stress apparattus. The expected result of applying a tensile stress along the axis to this structure is the gradual elimination of the closure structures and the re-alignment of the separated sectionsof the main domain walls. If a sufficiently high stress could be applied then a further change involving the disappearance of the main domain system, either the top or the bottom, that was magnetised in the easy direction making the largest angle with the whisker axis. This change would however lead to a large increase in the magnetostatic energy of the system as the whisker side would only be split into two areas of opposite polarity instead of four. This occurs because this change is brought about by the movement in a direction normal to its plane of the 180^{o} wall originally along the whisker axis parallel to the top and bottom surfaces. One would therefore expect that a considerable reduction in the ddmain spacing would accompany this transition in an attempt to reduce the magnetostatic energy. The first change described above does not involve much change in magneto-static energy as the 180^{o} wall remains, but a reduction in the amount of of energy associated with the rooftop structure

for the other types of energy present, so that a slight increase in magnetostatic energy and hence domain spacing could occur.

FIG. 5.1 Basic Domain Structure

Dashed out line shows {110} faces only

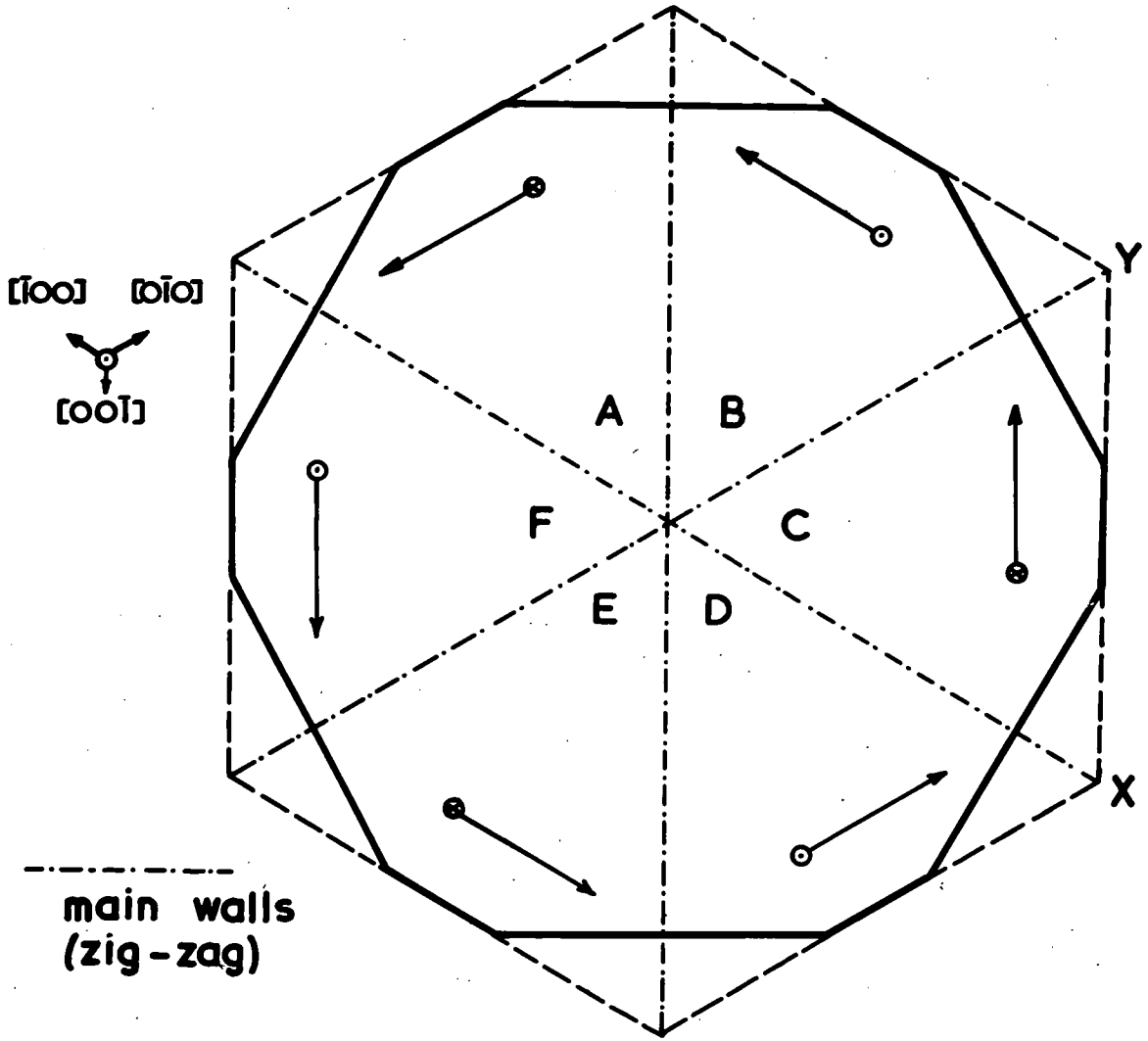

CHAPTER FIVE

WHISKERS WITH AXIS [111] DIRECTIONS

5.1 Introduction

Whiskers with this orientation have a basic structure consisting of main domains running the whole length of the whisker. The difference between this structure however and that in whiskers with an axial direction of [100], as described in chapter three, is that each main domain is magnetised at an angle of 90° to its neighbours and hence there are usually six main domains instead of only two domains magnetised anti-parallel in the case of the [100] axis whiskers.

The general form of this type of structure has been described and observed by Coleman and Scott (1958) and Kaczér and Gemperle (1959). In a whisker with the axis [111] and side faces (110), there are six main domains along the whisker length bounded by three 90° walls in (110) planes which intersect along the whisker axis. The domains are magnetised in the appropriate easy direction that lies in each of the (110) faces ofthe whisker, i.e. the magnetisation is at an angle of 55° to the axis of the whisker and parallel to the whisker face bounding the domains. This is shown in fig 5.1. The domain walls meet the surface of the whisker at the junction of the whisker faces, thus there is no component of magnetisation normal to the whisker face and hence no closure structure is needed along the length of the whisker. At the ends of the

whisker however, there would be a normal component where the six axial domains terminate. Here a closure strucure is needed and a suggested structure is given by Coleman and Scott (1958). This structure is completed and analysed quantitatively by Kaczér and Gemperle (1959) to provide a satisfactory explanation. This consists of pairs of 90° walls meeting in the surface and hence not attracting colloid to any noticeable extent, in agreement with the experimental observations of Coleman and Scott.

The main domain walls are 90° walls lying in (110) planes. I t has been found that for this type of domain wall the minimum energy state occurs when the wall takes a zig–zag structure.(Chikazumi and Suzuki 1955). This happens because the wall has no free poles along it provided its normal lies in a (110) plane. The wall energy however depends upon its orientation, thus there is an equilibrium position where the decrease in wall energy due to the wall orientation is balanced by an increase in total area of the wall. The wall therefore forms a zig–zag stucture with alternate pieces of it being rotated right and left about the mean (110) plane of the wall. The minimum energy orientation has been calculated for the wall segments by Chikazumi and Suzuki (1955) using an approximate method, and by Kaczer and Gemperle (1959) using an analytical approach. These give the angle the zig–zag wall segments make

with the (110) plane as 62°, i.e. the angle between the adjacent parts of the zig–zags is 124°. This gives the energy density of the zig–zag walls as $1.425\gamma_o$, where γ_o is the energy of a 90° wall with its normal in a [001] direction (Kaczér and Gemperle 1959), compared with $1.7274\gamma_o$ for the undisturbed 90° wall in a (110) plane (Lilley 1950).

5.2 Experimental Results

In the present work, the whiskers also had (211) faces appearing. These are faces that occur midway between (110) faces, so effectively cutting off the corners where the (110) faces meet. The cross–section of such a whisker is shown in fig 5.1. If the main structure is the same as that described above, then on these new faces the main domain boundaries should meet the surface and be plainly visible, instead of meeting the surface at the junction of two faces and hence not being easily seen, as in the simple case described above. This is in fact observed and examples of this can be seen in plates 5.1–4. Also there is no visible stucture present on the intervening (110) faces, showing that the magnetisation direction is in the easy direction present in the surface(plate5.1)

5.2.1 Main Structure

The main walls seen in these whiskers are obviously zig–zag walls, as would be expected. The angle observed on the whisker surface however differs from the equilibrium angle of 124° as

FIG. 5.3 Intersection of zig-zag wall with {112} and {110} surfaces

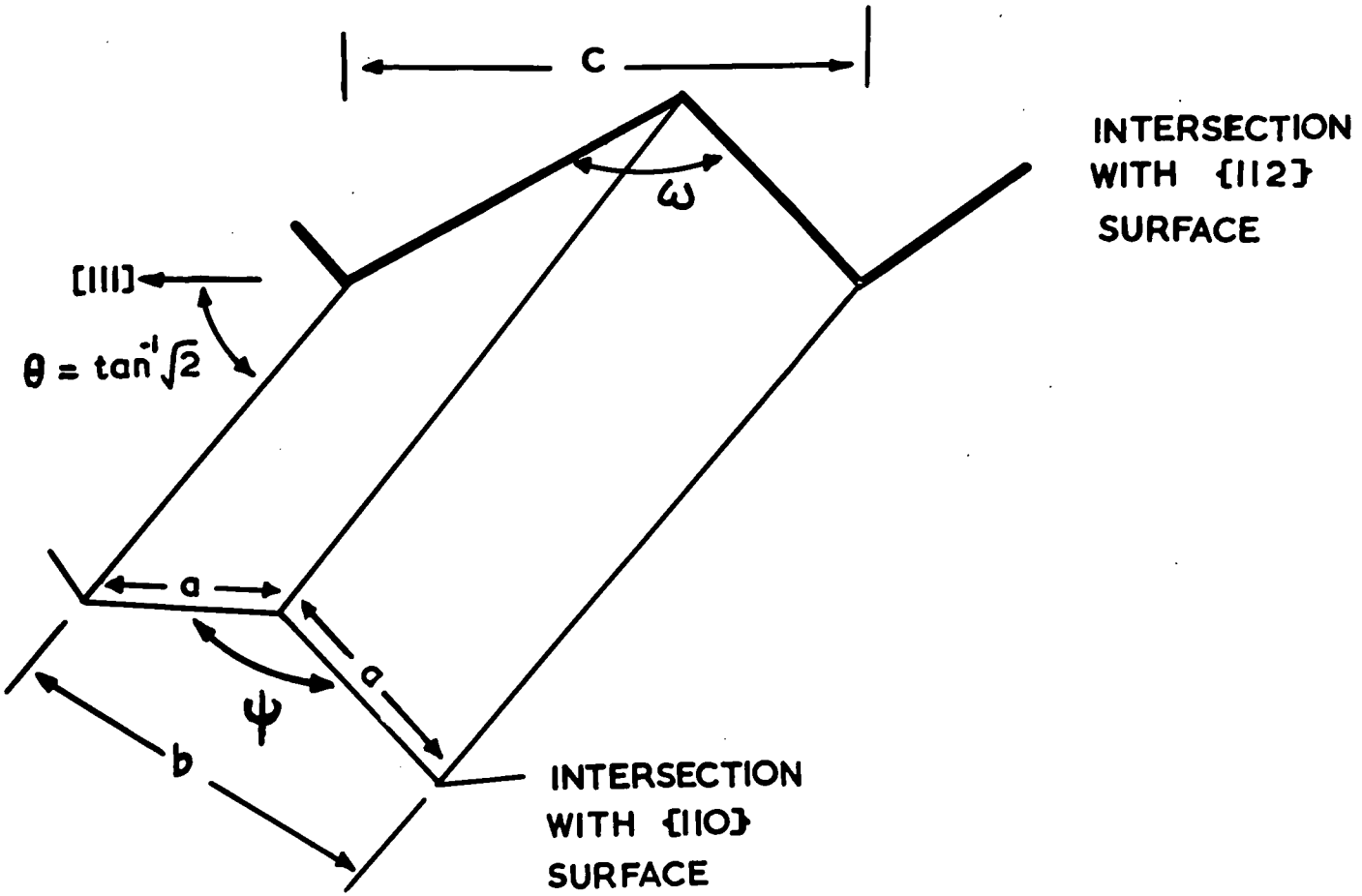

the included angle of the zig–zag since the surface cuts the zig–zag structure obliquely.

The calculation of the zig–zag angle observed on a crystal plane is performed using the following method. Refering to fig 5.3, the actual zig–zag angle is ψ and the observed angle is ω.

$$b^2 = 2a^2 + 2a^2\cos\psi = 2a^2(1-\cos\psi)$$

$$c = \frac{b}{\sin\theta} = \frac{a[2(1-\cos\psi)]^{1/2}}{\sin\theta}$$

$$\tan\frac{\omega}{2} = c/2 \Big/ \left(a^2 - \frac{b^2}{4}\right)^{1/2}$$

$$= \frac{a[2(1-\cos\psi)]^{1/2}}{2\sin\theta} \cdot \frac{1}{\left[a^2 - \frac{a^2}{2}(1-\cos\psi)\right]^{1/2}}$$

$$\tan\frac{\omega}{2} = \frac{(1-\cos\psi)^{1/2}}{\sin\theta(1+\cos\psi)^{1/2}} \qquad 5.1$$

This can be rearranged to give

$$\cos\psi = \frac{1-\sin^2\theta\tan^2\frac{\omega}{2}}{1+\sin^2\theta\tan^2\frac{\omega}{2}} \qquad 5.2$$

For the case being considered here,

$$\cos\theta = \sqrt{\frac{2}{3}} \; ; \text{ i.e. } \sin^2\theta = \frac{1}{3}$$

The observed value of zig–zag angle from plate 5.2 is $147\pm1^\circ$.

$$\therefore \frac{\omega}{2} = 73.5\pm0.5^\circ$$

Substituting these values in equation 5.2 gives a value of $125.5\pm1^\circ$ for ψ, the actual zig–zag angle. This compares very well with the calculated angle of 124°, showing that the main domain walls are the normal type of zig–zag wall as previously observed.

In some of the experimental results small magnetic fields were applied to the whiskers. The effects of these fields on the domain structure is to favour domains with a component of magnetisation in the direction of the applied field, the movement of the walls enabling these domains to grow. The observations of the movement of the main domain walls agree with this as suitably orientated main domains grow at the expense of the others.

The simplest way in which walls could move under the influence of an axial magnetic field is by rotation of the walls about the axis of the whisker, adjacent main walls rotating in opposite directions. This would however alter the plane of the domain walls and increase their energy. Hence this rotation should lead to a change in angle of the zig–zag as the mean plane of the wall changes. Measurements of variation of the zig–zag angle with wall position in plate 5.3 however, show no observable change. The spread of results from this whisker is about $\pm 5^{\circ}$ so that a change of angle of less than 5° might not be detectable against this spread. If the walls do rotate from the (110) plane, then the zig–zag segments of the wall would no longer have their normals in (110) planes. Free poles would therefore develop as the walls rotated with the consequent introduction of magnetostatic energy along the walls. This process further increases the wall energy and makes it more unlikely that the wall movement

FIG. 5.4 Effect of magnetic field applied along axis

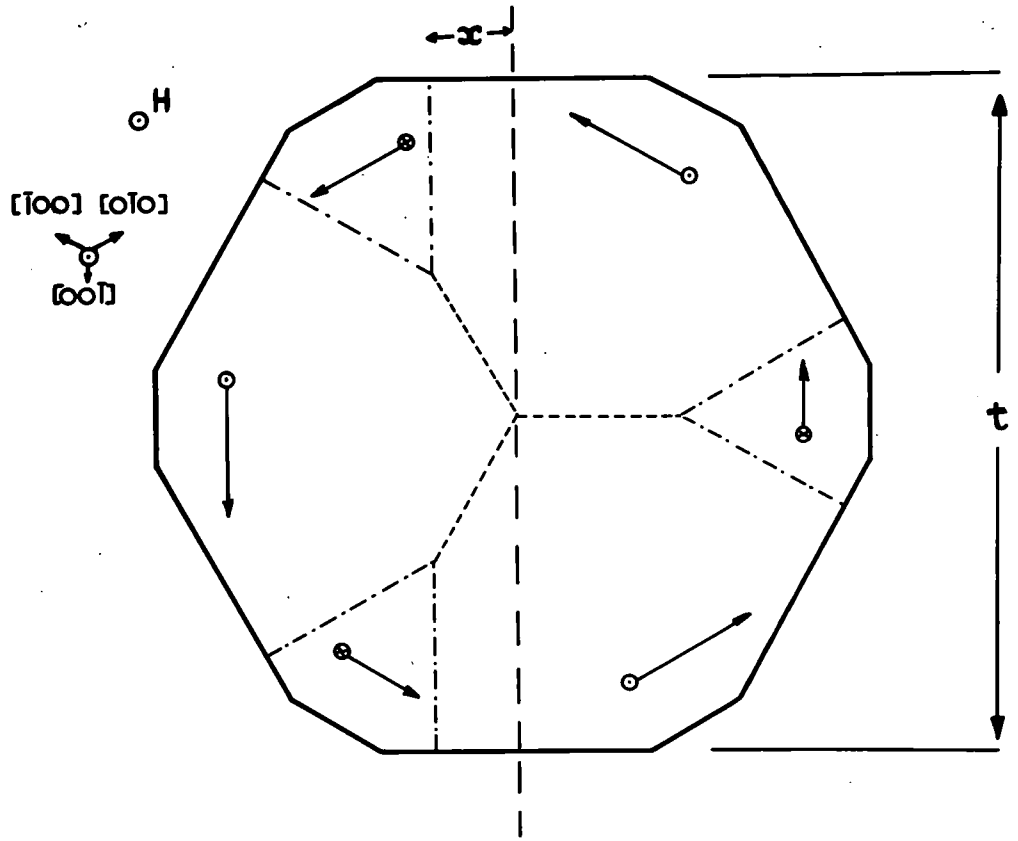

occurs by simple rotation.

If there is no rotation of the main walls, the the motion is probably as shown in fig 5.4. The two main walls of the unfavoured domains move together in such a way that the mean plane of the zig–zags stays constant, and the centre of the whisker is joined by a single new wall radiating out from the centre of the whisker in a (211) plane to the new junction of the two zig–zag walls. This configuration is a lower energy state for the walls compared with either the initial state or the simple rotation of the domain walls. If rotation occured then both the energy of the main walls and their area would increase as the walls moved out of the (110) plane. With the structure suggested above (fig 5.4) then the energy per unit area of the zig–zag walls remains constant, while their area decreases. The new section of wall in a (211) plane has an area less than that part of the zig–zag walls that have disappeared and also a lower energy per unit area so that the total wall energy is reduced in this type of change.

For this type of structure the change in the wall energy can be calculated. Refering to fig 5.4, for the zero field state the wall energy per unit length f_w is

$$3.t\ 1.4275\ \gamma_o$$

$$\therefore\ f_w = 4.275\ t\ \gamma_o \qquad 5.3$$

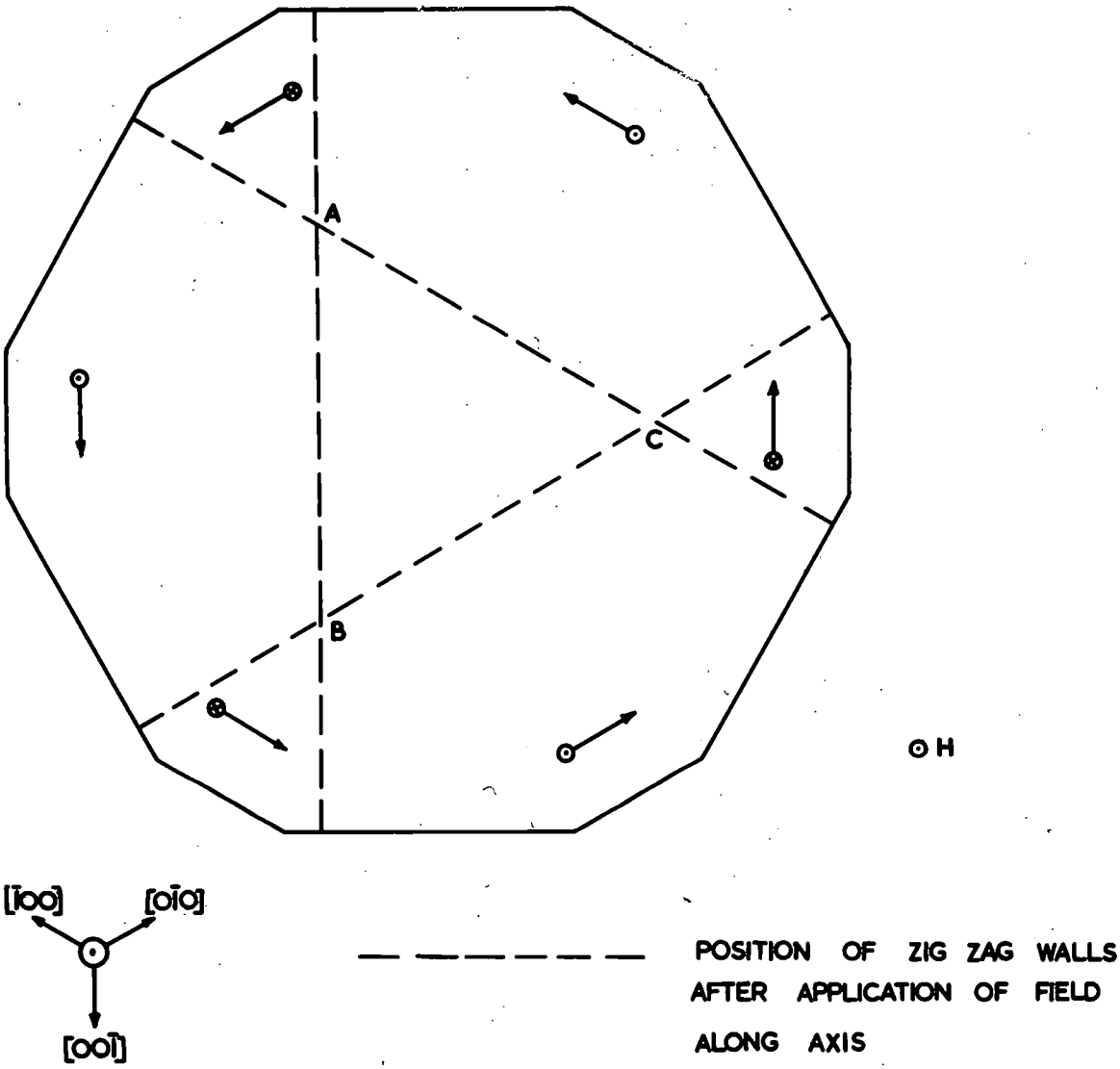

FIG. 5.5 MOTION OF MAIN WALLS NORMAL TO THEIR PLANE WHEN MAGNETIC FIELD APPLIED ALONG AXIS. DIRECTION OF MAGNETISATION OF THE REGION ABC IS UNDETERMINED FROM ORIGINAL STRUCTURE BY THIS TYPE OF CHANGE.

For the field induced structure, the wall energy per unit length $f_{w'}$ is

$$3\left[\frac{2\alpha}{\sin 30}\gamma_{211} + \left(t - \frac{2\alpha}{\tan\theta}\right)\gamma_{3\bar{1}\bar{3}}\right] \qquad 5.4$$

From equation 1.18

$$\gamma_{211} = \gamma_0(1.7274 - 1.2289\cos 19°30' + 0.5015\cos^2 19°30')$$

$$\therefore \gamma_{211} = 1.015\,\gamma_0 \qquad 5.5$$

$$\therefore f_{w'} = \frac{2\alpha}{t}\left[6.09 + 4.275\left(\frac{t}{2\alpha} - 2\sqrt{3}\right)\right] t\gamma_0 \qquad 5.6$$

The ratio of the energy of the field induced pattern to that of the zero field pattern is

$$\frac{f_{w'}}{f_w} = \frac{2\alpha}{4.275t}\left[6.09 + 4.275\left(\frac{t}{2\alpha} - 2\sqrt{3}\right)\right]$$

$$\frac{f_{w'}}{f_w} = 1 - 2.05\frac{2\alpha}{t} \qquad 5.7$$

The wall energy is therefore reduced for the field induced pattern compared to the field free pattern. Comparing this type of change with the change by wall rotation this is obviously energetically preferable since the energy of the walls is actually reduced, while rotation produces an increase in energy. This reduction in wall energy must be balanced by an increase of the magnetostatic energy of the disturbed surface patterns in the applied magnetic field.

The other possibility shown in fig 5.5 is that the walls move bodily through the whisker so that the domains magnetised in the field direction grow. This however leads to a volume in the centre where the direction of magnetisation is unknown,

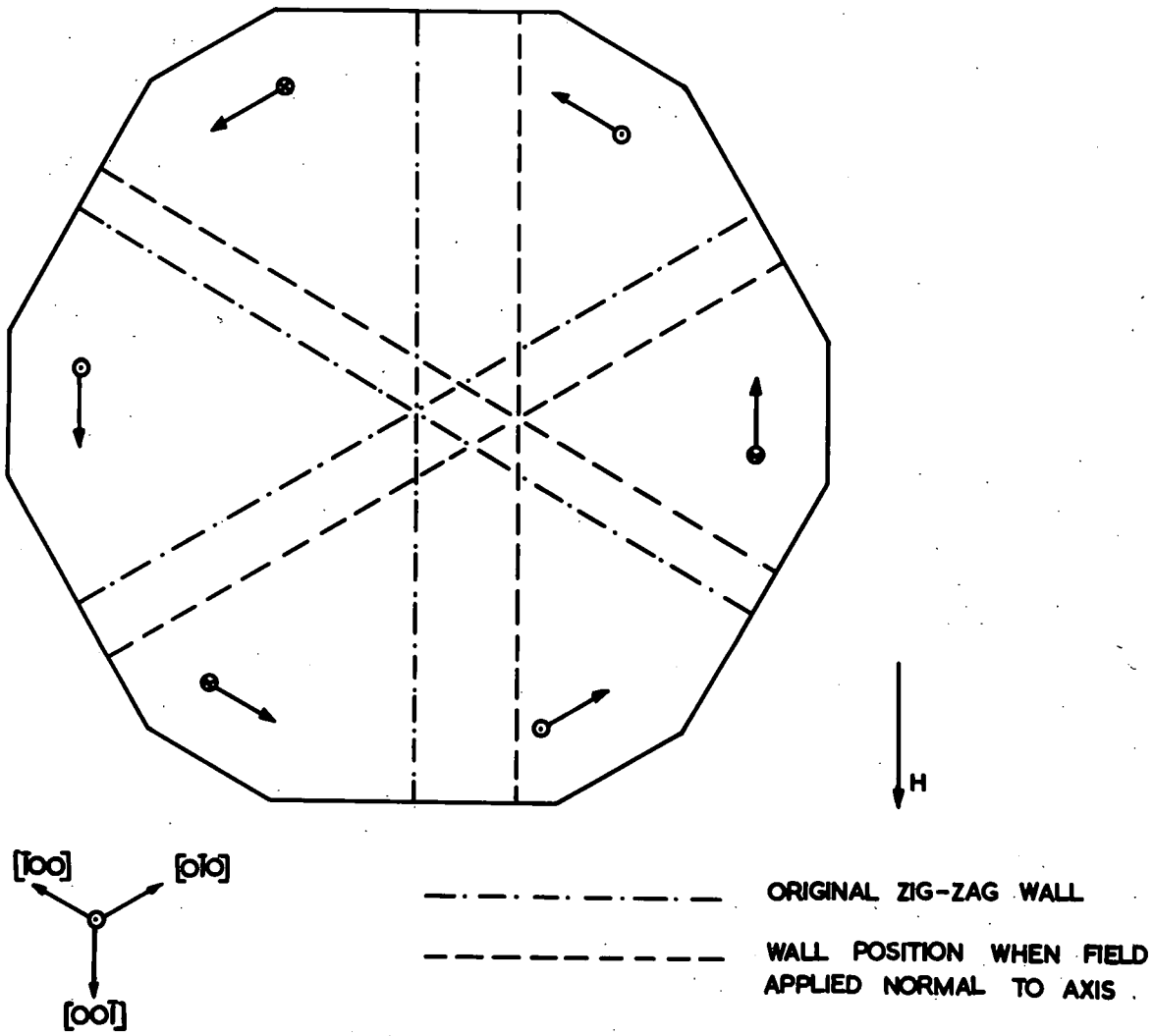

FIG. 5-6 EFFECT OF APPLYING A MAGNETIC FIELD NORMAL TO WHISKER AXIS.

and the possibility here is that one of the three directions of magnetisation nearest to the field direction for a field along the axis grows preferentially. Unless one particular domain has some local anomaly so that it is prefered to the other two, there seems no reason why the changes should occur by this method since the wall energy here stays constant.

In the case of a field applied perpendicular to the whisker axis, the field favours three adjacent domains on one side of the whisker to the three om the other side, and the centre one of the three favoured ones is even more favourable than the other two. The changes occuring in this system then, are probably due to the movement of the three main walls bodily through the whisker to make the domains in one half of the whisker grow at the expense of the others. This is shown in fig 5.6.

5.2.2 Closure Structure

The magnetisation directions of the main domain s are in the (110) planes at an angle of $55^{\circ}$to the whisker axis. Thus on the (211) faces of these whiskers there is a component of magnetisation from the main domains normal to the surface, and there is no easy direction of magnetisation in the surface. There would be therefore quite an appreciable amount of free pole appearing on these (211) faces giving a large magnetostatic energy contribution to the energy of the whisker, if the pattern described above occured in its simple state with no

surface closure structure.

To reduce this magnetostatic energy a complex closure structure is formed on the (211) faces. Since there is no easy direction of magnetisation in the surface a network of small closure domains is formed magnetised in some of the other easy directions. There must still be a large amount of free pole on the surface, but the total magnetostatic energy is reduced by subdividing the surface into very small areas of different polarity. The actual closure structures are very complex and it is not possible to analyse the pattern into its individual components. Because of this only the general features of this structure will be discussed here.

From the photographs it can be seen that there are two different types of closure occuring, and they occur on opposite sides of a main zig-zag wall on each face. Also adjacent halves of neighbouring (211) faces have the same type of closure structure, i.e. each main domain has the same type of closure structure where it meets the whisker surface, and adjacent main domains have different closure structures, so that each closure structure appears on alternate main domains. If we look at the magnetisation directions of the main domains in fig 5.2, we can see that the components of magnetisation along the whisker axis of adjacent domains are antiparallel, but of alternate domains are parallel. Thus the same closure

structure occurs on domains with components of magnetisation along the whisker axis in the same direction. The reason for the appearance of the two types of closure structure is probably due to the relative directions of magnetisation present in the closure structure, that are needed to reduce the magneto-static energy of the system. The direction and orientation of the walls of the closure structure between the magnetisation directions present in the individual closure patterns are different depending on the magnetisation direction of the main domain, and so lead to the different types of closure structure observed. Alternate domains have their magnetisations in the same directions relative to their surfaces, so the closure structures alternate as well.

5.2.3 The Effect of Stress

As the whisker axis is a [111] direction, the directions of easy magnetisation are all equally inclined about the whisker axis, so the main domains and the closure domains are all magnetised at an angle of $\pm 55^{\circ}$ to the whisker axis. If a tensile stress is applied along the whisker axis, the magnetisation directions will all be equally inclined to it so that there should be no effect on the pattern due to the stress. The total energy of the system will change due to the magnetoelastic energy introduced, but each domain should change by an equal amount per unit volume and therefore the

pattern should remain unchanged if the only mechanism is the effect of stress on the magnetisation in the domains. This ignores the effect of the stress on the domain walls, which depends on the relative orientation of the wall and the stress. There will thus be some wall directions which correspond to higher energies than others when the stress is applied and it might be expected that the structure would change so as to reduce the area of wall of higher energy.

.. The zig-zag setions of the main walls are equally inclined to the stress directions so the effect on these will be equal and opposite and simply an increase in the energy density of these walls. As the angle of the zig-zag is a result of an equilibrium between wall energy and wall area (see section 5.1), the increase in wall energy with applied stress would be expected to affect this and lead to a change in the zig-zag angle. This effect has been calculated previously by Chikazumi and Suzuki (1955) using an approximate solution and by Corner and Mason (1963) taking account of the effect of stress on the 90° walls. Corner and Mason found that the zig-zag angle was approximately constant in the range 0-50 $Kgm.mm^{-2}$. As the maximum stress used for the present work was less than 10 $kgm.mm^{-2}$, the expected variation of the zig-zag angle is zero. From the results in plate 5.4 no change in the angle of the zig-zag wall was observed up to the point where the

structure changed, agreeing with the above mentioned theoretical treatment. Any effect of stress on this structure cannot be due to the main zig–zag walls.

In the case of the closure structure there are two differing types, each with different wall arrangements. It is unlikely that these two types would have the same response to the application of a tensile stress, one of them is going to have a lower energy when the stress is taken into account than the other. The result of this is that the main domains with the lower energy closure structure will increase at the expense of the others, so the main walls will move to allow this to happen, the main walls probably moving in a manner similar to that observed when a magnetic field is applied along the whisker axis since this reduces the energy associated with the main domain walls.

The experimental results in plate 5.4 agree with this explanation, but more complex changes also occur at low stress values. The closure structure also changes its form somewhat and at the higher stress values the main domain boundaries seem to split for part of their length and a closure structure associated with the zig–zags appears. At the highest stresses, the main walls are moved completely from the (211) planes and a very irregular closure structure

appears. this new structure is field dependent and remains when the stress is removed in a slightly changed form, but the main zig–zag walls do not reappear upon removal of the stress, so that a completely new and more complex structure has been formed.

After the results shown in plate 5.4 had been obtained the whisker was subjected to random magnetic fields and applied stresses and the original type of pattern was regained, but this was probably by a complete switch of the domain structure back to the original state, and not a simple reversal of the changes that occured when the whisker was originally stressed.

CHAPTER SIX

SUMMARY OF RESULTS

This work covers domain patterns in iron whiskers with a variety of orientations. In the simplest case with the axis a [100] direction and the surfaces (100) planes, a number of different types of pattern, including cross magnetised domains of various shapes, were observed and the explanations for the observed surface patterns obtained from the postulated internal domain arrangements. In most of these a complete explanation was possible, but one pattern defied explanation and only the general features were understood. In this case the surface magnetisation directions were obtained but an appropriate internal domain structure could not be derived.

For whiskers with the axis at a small angle to the [100] direction the structural changes caused by the application of a stress along the axis agreed well with the theory for the initial changes, but the lack of agreement concerning the second major pattern change is unsatisfactory and the domain patterns on the whisker sides need investigating before a complete calculation of the energies can be made. This would involve a more complex apparatus to enable some or all of the other faces to be observed at the same time as the top surface. A piece of apparatus to do this would

prove very useful and enable a large number of difficulties to be overcome in the analysis and explanation of domain structures.

When the whisker is orientated at a large angle to the [100] direction with the faces still (100) planes, various different structures are possible differing in the type of closure structure present. To obtain reasonable agreement between the observed patterns and the theory an internal stress must be assumed to be present in the whiskers. In view of the irregular growth habit of whiskers with this type of orientation, the stresses present from the deformation of the crystal structure could probably produce the observed pattern since in the suggested structure the required stresses are quite low. ($\sim$1Kgm.mm^{-2}). The configuration suggested as the explanation for these results has a large magnetostatic energy as the magnetisation is in the same direction along the full length of each of the whisker sides. If this occured then there would be a very heavy colloid deposit along the whisker sides. From the photographs on this structure it is impossible to tell whether this deposit occurs, and so here again observation of the whisker edges at the same time as the observations on the top would give invaluable additional information.

A theoretical analysis of the echelon structure was also

carried out to obtain the equilibrium domain spacing and although a certain amount of echelon structure occurs in some patterns, complete agreement is impossible as the amount occuring seems to vary from one domain to the next. The theory includes an approximate estimate for the magnetostatic energy of the small domains of the echelon structure and it could be further refined if an accurate value for the magnetostatic energy could be found. It is expected however that the change resulting from a more accurate determination would be small in view of the small size of the echelon domains.

Where the closure structure is magnetised in [001] directions, free pole appears in separated regions and the approximate value for the magnetostatic energy obtained by considering them as point poles on a regular lattice at the centre of gravity of their respective areas seems to have reasonable validity. The check performed using a computer to calculate an accurate value for the magnetostatic energy in a particular case almost on the limit of the model seemed to be very satisfactory. This technique would seem to be of more general application to complex patterns provided the regions of free pole are not too close together.

The final orientation of whisker used i.e. axis [111] direction, is not completely understood. The main features

of the pattern agree with previous observations on whiskers with only (110) surfaces instead of the (110) and (211) surfaces as observed here. This enables the main walls to be observed easily and the zig–zag nature of the walls to be seen. The zig–zag angle calculation shows that the main walls are the normal type previously reported. The effects of applying magnetic fields parallel and perpendicular to the whisker axis were studied, and the explanation given showing the reduction of the total wall energy of the main walls by the introduction of new wall sections in (211) planes. The two distinct types of closure pattern observed on these whiskers were too fine and complex to be examined in detail. Further work using the Kerr magneto–optical method to study them needs to be carried out to determine the directions of magnetisation present in the surface to enable the detailed structure to be determined and to show how the different magnetisation directions that are needed in alternate domains to reduce the magnetostatic energy interact to give the final closure structures. This work would also enable a quantitative explanation of the effect of stress on the domain pattern to be given, since it is the interaction of the stress with the closure structure walls rather than with the magnetisation in the domains that produces the pattern changes.

ACKNOWLEDGEMENTS

I would like to thank my supervisor, Dr. W. D. Corner for the help and guidance given during the period of research.

Thanks are also due to Professor G. D. Rochester for the facilities granted.

To the Physics Department Technical Staff for their help.

To the Department of Scientific And Industrial Research for a Research Studentship from 1961 to 1964.

G. L. 1966.

REFERENCES

Becker R. and Doring W. 1939 Ferromagnetismus (Springer Berlin)

Bhide V.G. and Shenoy G.K. 1963 J. Appl. Phys. 34 1778

Bitter F. 1931 Phys. Rev. 38 1903

Brenner S.S. 1956 Acta Met. 4 62

Brown W. F. 1957 Phys. Rev. 105 1479

Chikazumi S. and Suzuki K. 1955 J. Phys Soc. Jap. 10 523

Coleman R.V. and Scott G.G. 1957 Phys Rev. 107 1276

1958 J. Appl. Phys. 29 526

Corner W.D. and Mason J.J. 1963 Proc. Phys. Soc. 81 925

1964 Brit. J. Appl. Phys. 15 709

Craik D.J. 1956 Proc. Phys. Soc. B69 647

Craik D.J. and Tebble R.S. 1961 Rep. Prog. Phys. 24 116

1965 Ferromagnetism and Ferromagnetic Domains,(North Holland)

De Blois R.W. and Graham C.D.Jr. 1957 G.E. Reseach Report No.57-RL1862

1958 J. Appl. Phys. 29 931

Dijkstra L.J. and Martius U.M. 1953 Rev. Mod. Phys. 25 146

Elmore W.C. 1938 Phys. Rev. 54 310

Fowler C.A. and Fryer E.M. 1954 Phys. Rev. 94 310

Graham C.D.Jr. 1957 A.I.E.E. Conf. on Magnetism, 410

Herring C. 1960 J. Appl. Phys. 31S 3S

Heisenberg W. 1928 Z. Phys. 49 619

Isin A. and Coleman R.V. 1965 137 Phys Rev. A1609

Kaczér J. and Gemperle R. 1959 Czech. J. Phys. 9 306

Kirenski L. V., Dylgerov V. D. and Savchenko M. K. 1957 Bull. Acad. Sci. U. S. S. R. 21 1157

Kittel C. 1949 Rev. Mod. Phys. 21 541

Kranz J. 1956 Naturwissenshaften 43 370

Lilley B. A. 1950 Phil. Mag. 41 792

Martin D. H. 1957 Proc. Phys. Soc. B70 77

Néel L. 1944a J. Phys. Rad. 5 241

b Cah. de Phys. 25 1

Prutton M. 1964 Thin Magnetic Films. (Butterworths. London)

Shockley W. 1948 Phys. Rev. 73 1246

Shtrikman S. and Treves D. 1960 J. Appl. Phys. 31S 147S

Stewart K. H. 1954 Ferromagnetic Domains. (Cambridge University Press)

Van Vleck J. H. 1952 Rev. Mod. Phys. 23 213

Wayman C. M. 1961 J. Appl. Phys. 32 1844

Weiss P. 1907 J. Phys. Theo. Appl. 6 661

Williams H. J., Bozorth R. M. and Shockley W. 1948 Phys. Rev. 75 155

Majima M. and Togino S. 1927 Sci. Reports of the Institute of Physical and Chemical Research, Tokyo, 7 260

a)

b)

c)

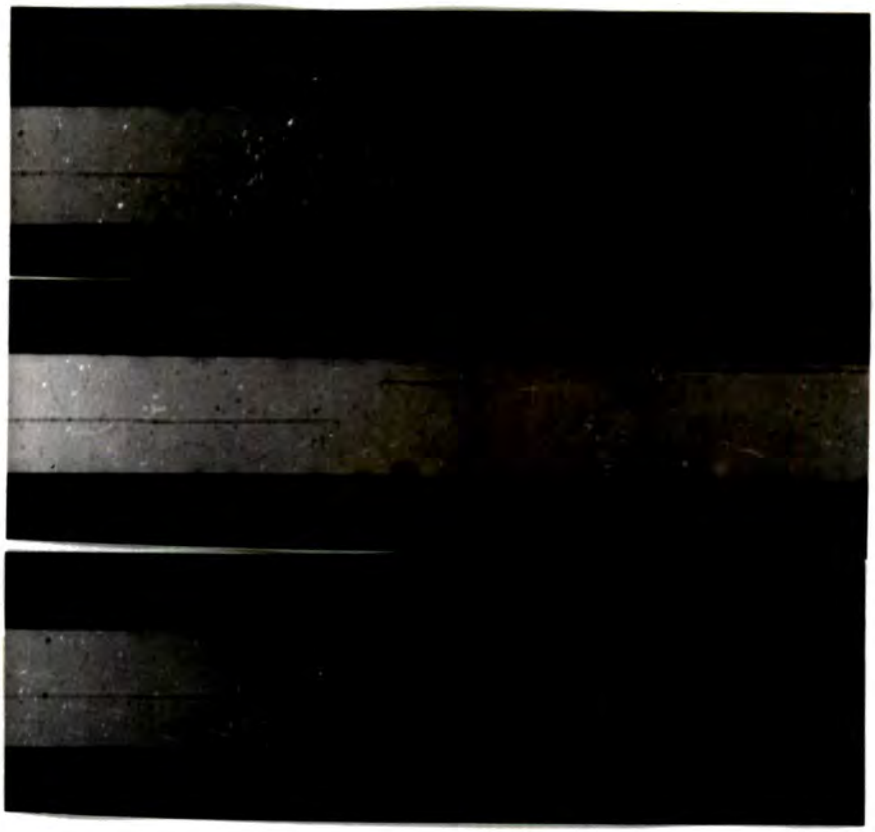

a) Zero stress

b) 1.45 Kgm/sq.mm.

c) 2.17 Kgm/sq.mm.

Width of whisker is 0.096mm.

PLATE 3.1

[001]
[010]

a)

Whisker width is 0.12mm
Composite photograph of all four faces of a whisker.

Explanation of the patterns is given in figure 3.1

PLATE 3.2

Whisker width is 0.1mm

Photographs of the four faces of a whisker in the region where the main 180° walls change position and orientation.

Explanation of the patterns is given in figure 3.2

PLATE 3.3

Whisker width is 0.08mm

Single cross-magnetised domain. The position, shape, and size was unaltered by the application of stress.

PLATE 3.4

a)

b)

c)

d)

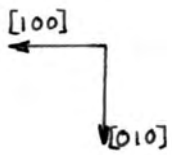

a) Zero stress

b) 0.257 Kgm/sq.mm.

c) 0.514 Kgm/sq.mm.

d) 0.642 Kgm/sq.mm.

PLATE 3.5

e)

f)

g)

h)

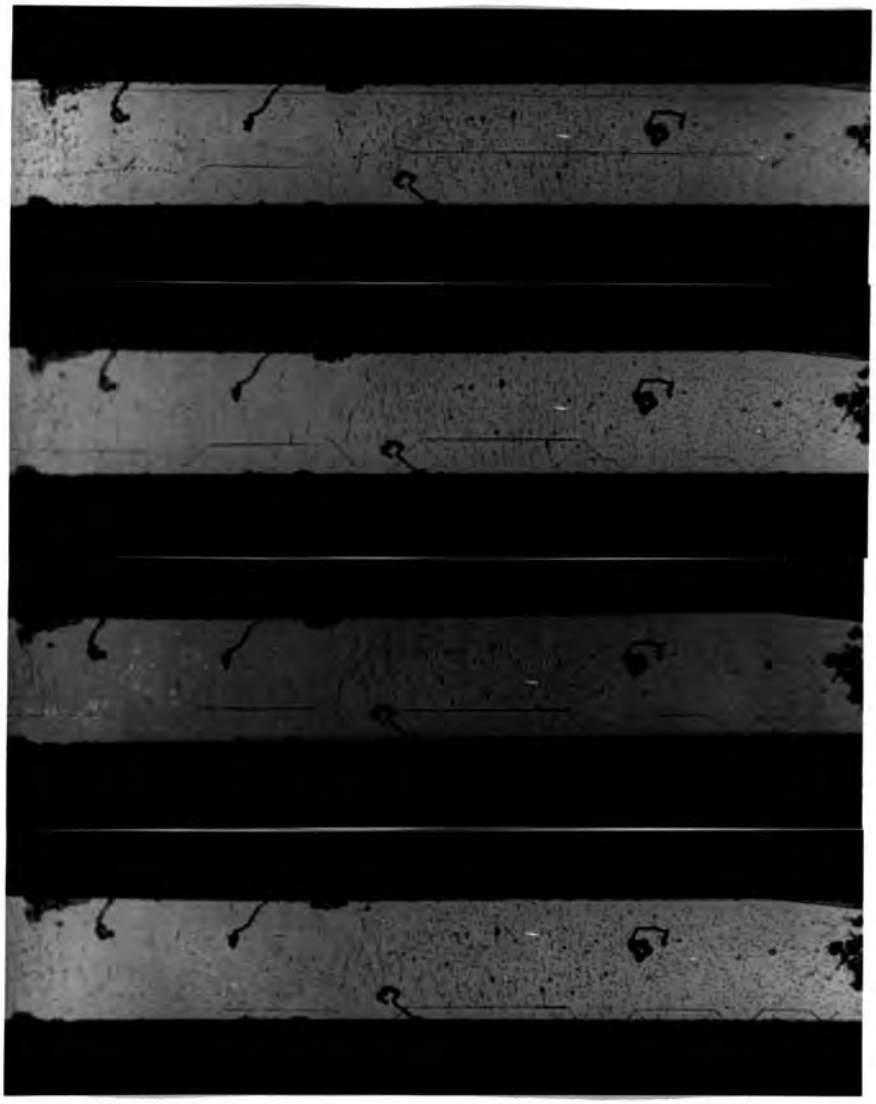

e) 0.902 Kgm/sq.mm.

f) 2.32 Kgm/sq.mm.

g) 1.28 Kgm/sq.mm.

h) Zero stress

Whisker width is 0.15 mm.

The cross –magnetised domains gradually reduce in volume

PLATE 3.5

a)

b)

c)

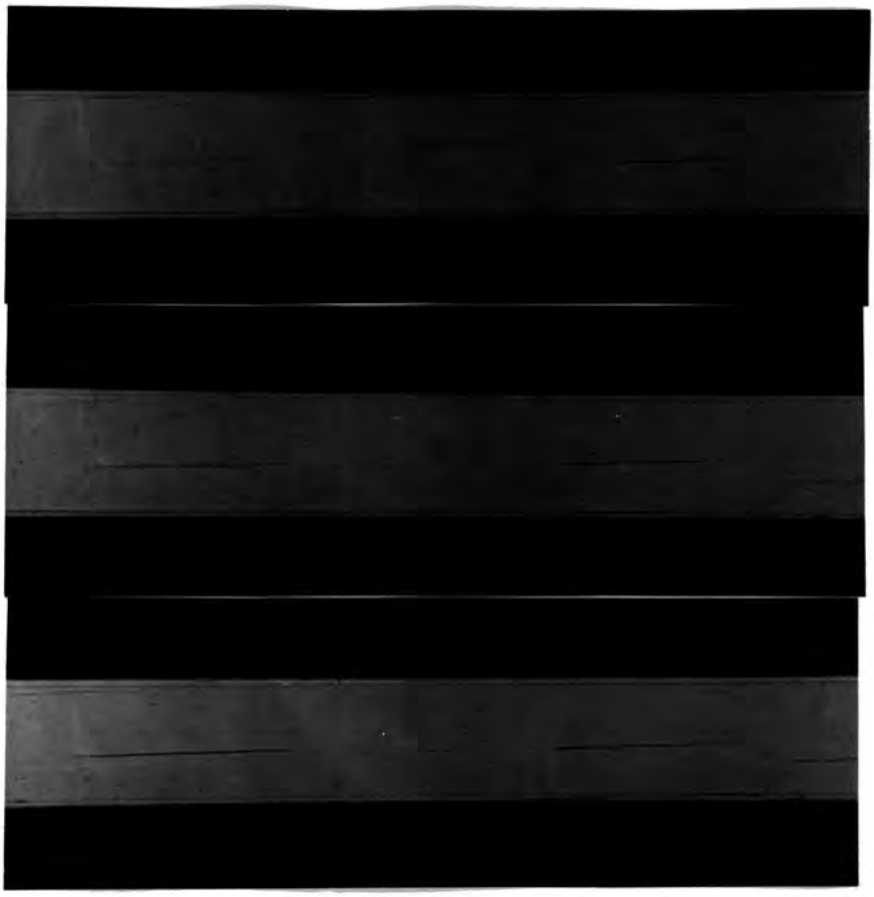

a) Zero stress

b) 0.5 Kgm/sq.mm. Centre pair of cross domains have disappeared.

c) 0.9 Kgm/sq.mm.

PLATE 3.6

d)

e)

f)

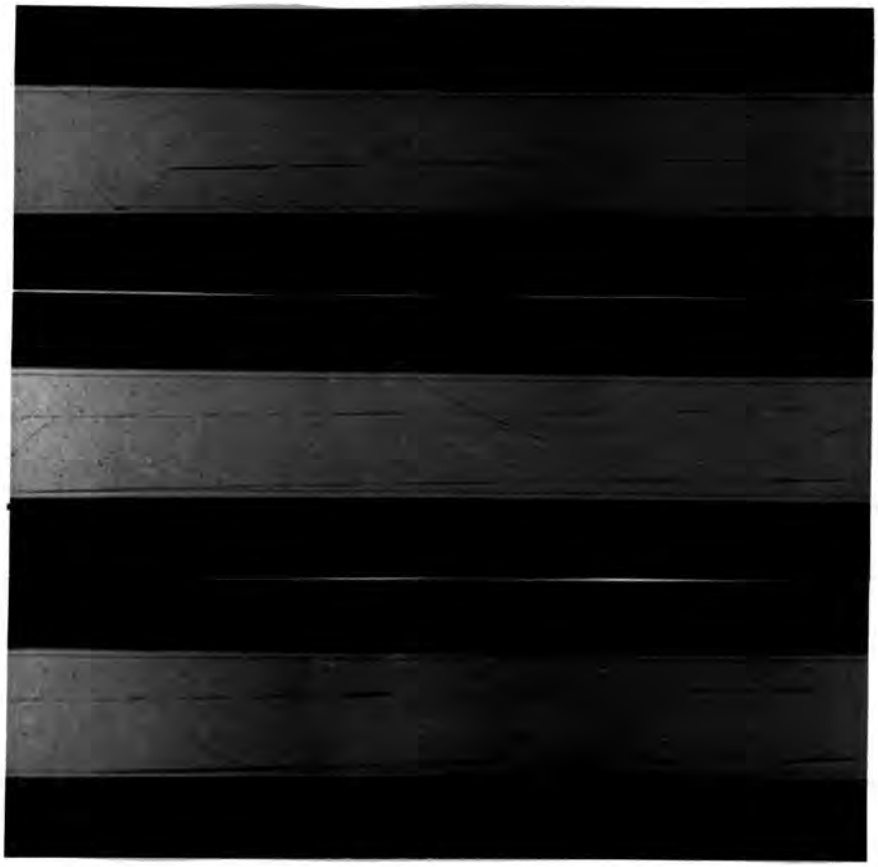

d) 1.1 Kgm/sq.mm. Outer pair of cross domains have moved together slightly and altered their shape.

e) 1.5 Kgm/sq.mm. Second pattern change occurs as all the cross magnetised domains disappear.

f) Zero stress. Stress induced pattern remains the same with alternate left and right hand Bloch wall sections.

Whisker width is 0.15mm

PLATE 3.6

a)

b)

c)

d)

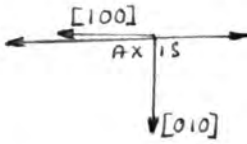

Whisker is 0.1mm wide at the centre.

a) Zero stress

b) 3 Kgm/sq.mm.

c) 3.38 Kgm/sq.mm.

d) 3.62 Kgm/sq,mm.

The cross-magnetised domain at the left of the whisker gradually moves along until it suddenly disappeares completely.

PLATE 3.7

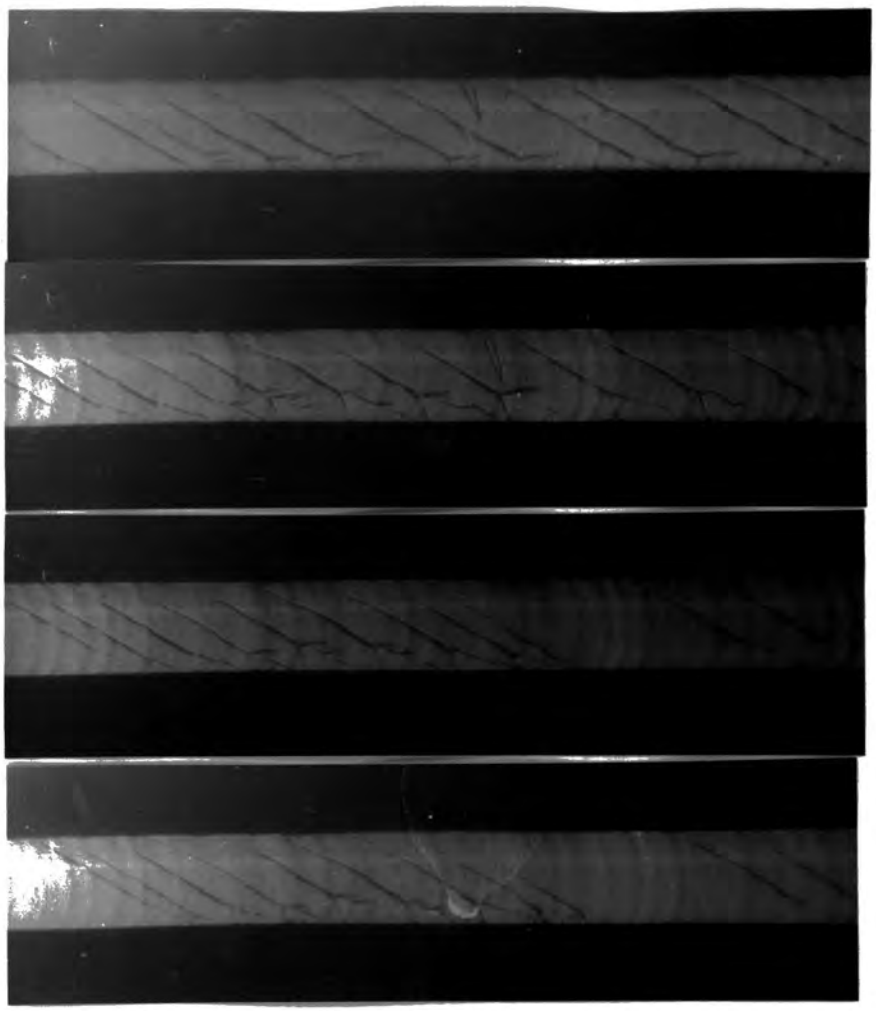

a) Zero stress

b) 0.9 Kgms/sq.mm.

c) 1.74 Kgm/sq,mm.

d) 2.1 Kgm/sq.mm.

As the stress increases the spacing of the domains decreases.

See figure 4.6. Whisker width is 0.12 mm.

PLATE 4.1

Sequence of photographs at zero stress along the same (100) face of a whisker as its width gradually increases. The domain pattern spacing and form vary as the width changes.

Width at centre of a) is 0.054mm.

Width at centre of d) is 0.075mm.

PLATE 4.2

e)

e) Higher magnification photograph of a detail from the domain structure of section a).

PLATE 4.2

a)

b)

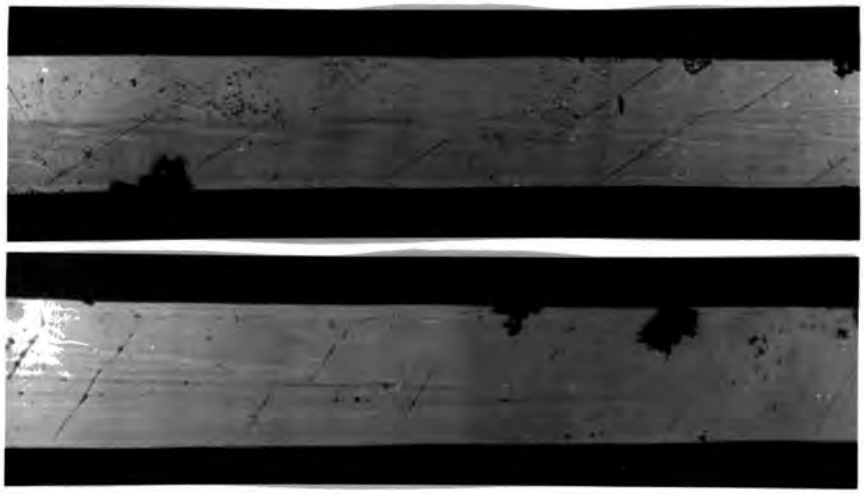

Domain patterns on the top and bottom surfaces of a whisker with faces (001) and $(00\bar{1})$, and axis at approximately 30° to the [100] direction. Whisker width is 0.19 mm.

PLATE 4.3

a)

b)

c)

a) Zero field

b) 0.71 Oersteds

c) 0.81 Oersteds

PLATE 4.4

d)

e)

f)

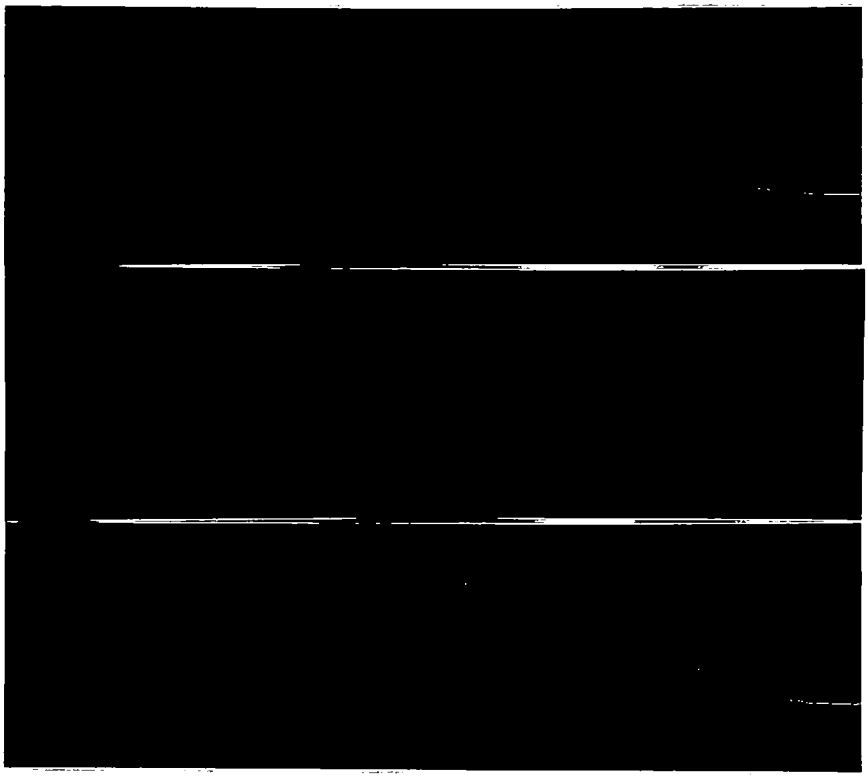

d) 1.08 Oersteds

e) 1.35 Oersteds

f) Zero field

Effect of applying a magnetic field along the axis of a whisker with orientation and domain structure similar to the whisker shown in plate 4.3.

Whisker width is 0.1 mm.

PLATE 4.4

{211} {110} {211} {110} {211}

Adjacent faces on the circumference of a whisker with axis [111] and {211} and {110} faces present, showing the complex closure structures present, similar on adjacent halves of neighbouring {211} faces, but disimilar on opposite sides of each {211} face.
{211} faces are 0.076 mm. wide.
{110} faces are 0.036 mm. wide

PLATE 5.1

Detail from one {211} face of plate 5.1 at higher magnification showing complex closure structure.

PLATE 5.2

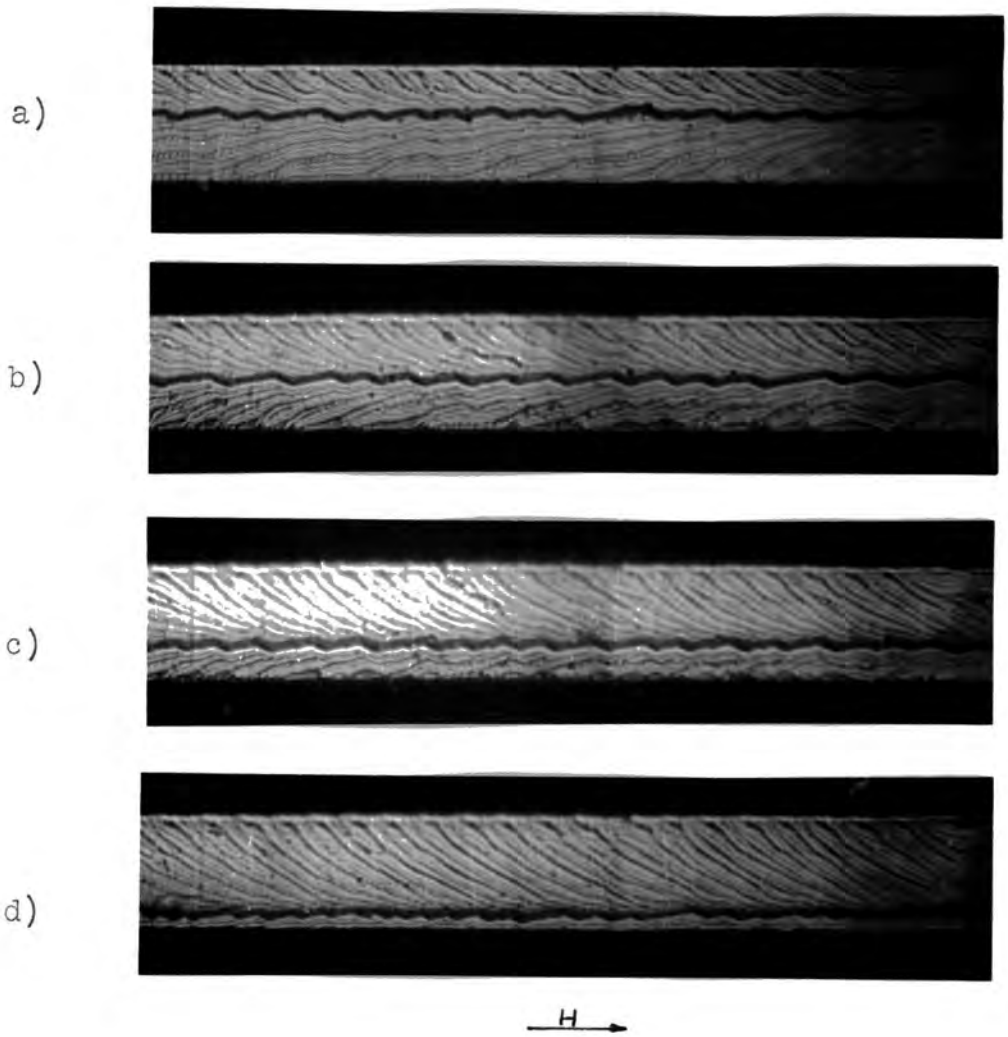

Whisker width is 0.08mm.

Effect of applying small magnetic field along the whisker axis

PLATE 5.3

a)

b)

c)

d)

Whisker width is 0.05mm.

a) Zero stress

b) 1.12 Kgm/sq.mm.

c) 1.21 Kgm/sq.mm.

d) 3.56 Kgm/sq.mm.

PLATE 5.4

e) 

e) Zero stress after release of tension.

Destruction of zig–zag wall structure on the {211} faces by the application and removal of stress along the [111] axis

PLATE 5.4